

**The Role of Brain Derived Neurotrophic Factor in Multiple
Sclerosis and The Role of Fractalkine in Multiple Sclerosis
induced Neuropathic Pain**

by

Wenjun Zhu

A Thesis submitted to the Faculty of Graduate Studies of

The University of Manitoba

in partial fulfilment of the requirements of the degree of

DOCTOR OF PHILOSOPHY

Faculty of Pharmacy
University of Manitoba

Winnipeg

Copyright © 2013 by Wenjun Zhu

ACKNOWLEDGEMENTS

I would never have been able to finish my doctoral thesis without the guidance of my committee members, help from friends, and support from my family.

Above all, I would like to thank family for their support and great patience at all times. My parents have given me their unequivocal support throughout, as always, for which my mere expression of thanks likewise does not suffice.

I would like to express my deepest gratitude to my principal advisor, Dr. Mike Namaka, for his excellent guidance, caring, patience, providing me with an excellent atmosphere for doing research and financially supporting my research. The good advice and support of Dr. Emma Frost has been invaluable on both an academic and a personal level, for which I am extremely grateful.

I would also like to thank Dr. Yuewen Gong, Dr. Xiaochen Gu, and Dr. Maria Vrontakis for guiding my research for the past several years and helping me to develop my background in research.

Many thanks to Dr. Prakash Pillai, Kim Madec, Jeremy Paterson, Kelvin Au, Farhana Begum, Parvez Vora, Elizabeth Tran, Jan Mustapha, Magda Pawlak, Crystal Acosta, and other colleagues in the laboratory of Dr. Namaka for helping me in my study. My research would not have been possible without their help.

Finally, I would like to acknowledge the financial, academic and technical support of the University of Manitoba, particularly in the award of a research assistantship that provided the necessary financial support for this research. I also thank the Faculty of Pharmacy for their support and assistance since the start of my studies in 2002.

Abstract:

Multiple sclerosis (MS) is a chronic inflammatory autoimmune disease, characterised by demyelination in the central nervous system (CNS). The exact pathophysiology of MS is still unknown but it is believed to be associated with infiltration of T cells and activation of microglia that result in myelin damage leading to neurological deficits including neuropathic pain. Current treatment strategies such as glatiramer acetate have recognized the importance of BDNF in myelin repair. In addition, the proposed role of the chemokine CX3CL1 and its receptor CX3CR1 in the control of microglia activation and leukocyte infiltration place this chemokine in an important position in regulation of MS-induced neuropathic pain. In this research study, the experimental autoimmune encephalomyelitis (EAE) rat model of MS was used to examine the role of BDNF in myelin repair as well as CX3CL1's role in neuropathic pain. *Methods:* A total of 66 adult female Lewis rats are divided into 3 experimental groups: naïve control, active control and active EAE. Naïve control animals do not receive any injections. Active control animals receive 2 intraperitoneal injections of pertussis toxin and injections of Freund's adjuvant and Mycobacterium Tuberculosis. Active EAE animals receive the same regimen administered to active controls plus full inoculation with fatty acid and Guinea pig myelin basic protein. Expressions of BDNF, CX3CL1 and CX3CR1 in a time dependent manner (day 0, 3, 6, 9, 12 & 15) were examined using immunohistochemistry (IHC), ELISA, Western blot, RT-PCR and real time-PCR. *Results:* There was a significant increase in BDNF, CX3CL1 and CX3CR1 expression of protein and mRNA in DRG at day 12 after induction of MS. The neurons and glial cells were identified to express BDNF, CX3CL1 and CX3CR1 in the spinal cord of EAE animal. *Conclusion:* The antigenic-induced expression of BDNF within the DRG may represent a key

element involved in facilitating central myelin repair. In addition, the chemokine CX3CL1 and its receptor CX3CR1 represent key mediators involved in the development of MS-induced pain.

Keywords: Multiple sclerosis, MS, experimental autoimmune encephalomyelitis, EAE, CX3CL1, CX3CR1, neuropathic pain, myelin repair

TABLE OF CONTENTS

ACKNOWLEDGEMENTS	2
Abstract.....	3
List of abbreviations	13
Chapter 1- GENERAL INTRODUCTION.....	16
1.1 Multiple Sclerosis (MS)	16
1.1.1 Forms of MS	18
1.1.2 Symptoms of MS	18
1.1.3 Treatments for MS	19
1.2. Oligodendrocytes	19
1.2.1 Myelination.....	19
1.2.2 Demyelination	20
1.2.3 Remyelination.....	21
1.3 Brain Derived Neurotrophic Factor (BDNF)	22
1.3.1 Neurotrophin Receptors.....	22
1.3.2 BDNF and Oligodendrocytes	23
1.4 Neuropathic Pain	25
1.4.1 Pain Processing Loop	26
1.5 Fractalkine.....	27
1.5.1 Fractalkine and Pain	28

1.6 Dorsal Root Ganglia (DRG).....	29
1.7 Experimental Autoimmune Encephalomyelitis (EAE).....	31
1.8 Project Description.....	32
1.9 References.....	33
 Chapter 2 – AN OVERVIEW OF RELAPSING REMITTING MULTIPLE SCLEROSIS AND CURRENT TREATMENT OPTIONS.....	 41
2.1 Statement of contribution.....	41
2.2 Introduction.....	42
2.2.1 Etiology and Pathophysiology.....	43
2.2.2 Categorization and Diagnosis of MS.....	44
2.3 Treatment Options for RRMS.....	46
2.3.1 Symptom Management in MS.....	51
2.3.2 Nonpharmacological Treatments.....	54
2.4 Pharmacist’s Role.....	54
2.5 Summary.....	55
2.6 References.....	56
 Chapter 3 – THE ROLE OF DORSAL ROOT GANGLIA ACTIVATION AND BRAIN DERIVED NEUROTROPHIC FACTOR IN MULTIPLE SCLEROSIS.....	 63
3.1 Statement of Contribution.....	63
3.2 Abstract.....	64

3.3 Introduction	65
3.4 Materials and Methods	66
3.4.1 EAE Model	66
3.4.2 Tissue Harvesting and Sectioning	67
3.4.3 Western Blot	67
3.4.4 Immunohistochemistry	68
3.4.5 Reverse Transcription Polymerase Chain Reaction (RT-PCR) and Real Time PCR...	69
3.4.7 Enzyme Linked Immunosorbent Assay	69
3.4.8 Statistical Analysis	70
3.5 Results	70
3.5.1 Neurological Disability Scores	70
3.5.2 Immunohistochemical Analysis of BDNF Protein Expression in DRG.....	70
3.5.3 Enzyme Linked Immunosorbent Assay Analysis of BDNF Protein Expression in the DRG.....	72
3.5.6 BDNF Gene Expression Analysis in the DRG.....	73
3.5.7 BDNF Protein and Gene Expression in the Spinal Cord.....	73
3.5.8 BDNF Protein Expression in the Dorsal Roots	74
3.6 Discussion	74
3.7 Summary	78
3.8 References	80

3.9 Figures.....	86
Chapter 4 – THE IDENTIFICATION OF BDNF RESPONSIVE CELLS IN SPINAL CORD FROM AN EAE ANIMAL MODEL OF MS.....	
4.1 Statement of Contribution.....	96
4.2 Abstract.....	96
4.3 Introduction.....	97
4.4 Experimental Section.....	100
4.4.1 EAE Model.....	100
4.4.2 Real Time Reverse Transcription Polymerase Chain Reaction.....	100
4.4.3 Western Blot.....	101
4.4.4 Immunohistochemistry (IHC).....	101
4.4.5 Statistical analysis.....	102
4.5 Results and Discussion.....	102
4.5.1 Establishment of an MBP-Induced EAE Model.....	102
4.5.2 Expression of TrkB mRNA in the EAE Spinal Cord.....	103
4.5.3 Up-regulation of TrkB Protein in the EAE Spinal Cord.....	104
4.5.4 IHC analysis of BDNF Responsive Cells in the Spinal cord.....	107
4.6 Discussion.....	116
4.7 Conclusions.....	118
4.8 References and Notes.....	120

Chapter 5 – FRACTALKINE (CX3CL1) AND FRACTALKINE RECEPTOR (CX3CR1) EXPRESSION IN THE SPINAL CORD ASSOCIATED WITH EXPERIMENTAL AUTOIMMUNE ENCEPHALOMYELITIS (EAE) INDUCED NEUROPATHIC PAIN 125

5.1 Statement of Contribution 125

5.2 Abstract 126

5.3 Introduction 127

5.4 Objective 129

5.5 Methods 129

5.5.1 Experimental Autoimmune Encephalomyelitis (EAE) Model 129

5.5.2 Tissue Harvesting and Sectioning 130

5.5.3 Thermal Sensory Testing 130

5.5.4 Immunohistochemistry 131

5.5.5 Real Time Reverse Transcription Polymerase Chain Reaction 131

5.5.6 Enzyme Linked Immunosorbent Assay (ELISA) 132

5.5.7 Statistical Analysis 132

5.6 Results 133

5.6.1 Neurological Disability Scores 133

5.6.2 Thermal Sensory Testing 133

5.6.3 CX3CL1 Gene Expression Analysis in the DRG 134

5.6.4 CX3CL1 Protein Expression Analysis in the DRG by ELISA 135

5.6.5 CX3CR1 Gene Expression Analysis in the DRG.....	136
5.6.6 CX3CR1 Protein Expression Analysis in the DRG by ELISA	137
5.6.7 CX3CL1 Gene Expression Analysis in the Spinal Cord	137
5.6.8 CX3CL1 Protein Expression Analysis in the Spinal Cord by ELISA.....	138
5.6.9 CX3CR1 Gene Expression Analysis in the Spinal Cord.....	139
5.6.10 CX3CR1 Protein Expression Analysis in the Spinal Cord by ELISA	140
5.6.11 Immunohistochemical Analysis of CX3CL1 Protein Expression in the Spinal Cord	140
5.6.12 Immunohistochemical Analysis of CX3CR1 Protein Expression in the Spinal Cord	141
5.7 Conclusions	141
5.8 Discussion	142
5.8.1 Acknowledgements	146
5.9 References	146
5.10 Figures.....	151
5.11 Figure legends	160
Chapter 6 - A NOVEL DECALCIFICATION METHOD FOR ADULT RODENT BONE FOR HISTOLOGICAL ANALYSIS OF PERIPHERAL-CENTRAL NERVOUS SYSTEM CONNECTIONS.	165
6.1 Statement of Contribution.....	165
6.2 Abstract	166

6.3 Keywords	166
6.4 Introduction	167
6.5 Materials and Methods	169
6.5.1. Tissue Preparation	169
6.5.2. Decalcification.....	170
6.5.3. Chemical Testing of Calcium Extraction	172
6.5.4. Tissue Processing for Cryosectioning	172
6.5.5. Evaluation	173
6.5.6. Immunohistochemistry for Myelin Basic Protein (MBP)	173
6.5.7. In situ Hybridization	174
6.5.8. Imaging.....	174
6.6 Results	175
6.1. Morphological Assessment.....	175
6.2. RDO-G.....	176
6.3. Krajian solution	179
6.4. EDTA-G	181
6.5. 6% TCA.....	182
6.6. In Situ Hybridization	184
6.7 Discussion	185
6.8 Conclusion.....	187

6.9 References	188
Chapter 7 - OVERALL CONCLUSIONS AND DISCUSSION.....	193
7.1 Overview	193
7.2 BDNF	195
7.3 TrkB	197
7.4 Fractalkine.....	200
7.5 Summary	203
7.6 Future Research Direction.....	205
7.7 References	207

LIST OF ABBREVIATIONS

AC - Active Control

ANOVA - Analysis of Variance

BBB - Blood Brain Barrier

BDNF - Brain Derived Neurotrophic Factor

CGH - Comparative Genomic Hybridization

CGRP - Calcitonin Gene Related Peptide

CLIC1- Chloride Intracellular Channel 1

CNS - Central Nervous System

CSF - cerebral spinal fluid

DAPI - 4',6-Diamidino-2-Phenylindole

DIG - Digoxigenin

DR - Dorsal Roots

DRG - Dorsal Root Ganglion

EAE - Experimental Autoimmune Encephalomyelitis

EDSS - Expanded Disability Status Scale

EDTA- Ethylenediaminetetraacetic Acid

EEG - Electroencephalogram

ELISA - Enzyme Linked Immunosorbent Assay

FGF2 - Fibroblast Growth Factor 2

GA - Glatiramer Acetate

GAPDH - Glyceraldehyde-3-phosphate dehydrogenase

GFAP - Glial Fibrillary Acidic Protein

H&E – Hematoxylin and Eosin

IFN γ - Interferon Gamma

Ig-C2- Immunoglobulin-Like C2 Type Domains

IHC - Immunohistochemical

IL - Interleukins

IL-12 - Interleukin-12

ISH - *In situ* Hybridization

MAG - Myelin Associated glycoprotein

MBP - Myelin Basic Protein

MOG - Myelin Oligodendrocyte Glycoprotein

MS - Multiple Sclerosis

NC - Naïve Control

NDS - Neurological Disability Score

NGF - Nerve Growth Factor

NT - Neurotrophin

OL - Oligodendrocytes

ON - Optic Neuritis

PDGFA - Platelet Derived Growth Factor A

PDGFR- α – Platelet-derived Growth Factor Receptor alpha

pdi - Days Post-disease Induction

PLP - Proteolipid Protein

PML - Progressive Multifocal Leukoencephalopathy

PPMS - Primary Progressive MS

qRT-PCR - Real time reverse transcription polymerase chain reaction

RRMS - Relapsing/Remitting MS

RT-PCR - Reverse Transcription Polymerase Chain Reaction

SPMS - Secondary Progressive MS

TACE - TNF Converting Enzyme

TCA - Trichloroacetic Acid

Th1 - T-helper Type 1 cell

TNF - Tumor Necrosis Factor

Trk - Tropomyosin-Related Kinase Receptors

CHAPTER 1- GENERAL INTRODUCTION

1.1 MULTIPLE SCLEROSIS (MS)

Multiple sclerosis (MS) was first described by Charcot and Vulpian in 1866 [1]. It is an inflammatory disease of the central nervous system (CNS). The inflammation causes patches of damage called plaques or lesions, which are predominantly located in the white matter of the CNS. At present, the autoimmune theory represents the most plausible and widely accepted explanation of disease pathology. According to this theory, circulating Th1-cells in the blood were activated upon exposure to specific CNS antigenic determinants such as: myelin basic protein (MBP), proteolipid protein (PLP) and/or myelin oligodendrocyte glycoprotein (MOG). Once activated Th1-cells begin to secrete inflammatory cytokines such as interleukin-12 (IL-12), interferon gamma ($IFN\gamma$) and tumor necrosis factor (TNF) which are pivotal in the pathogenic immune response directed against CNS myelin. IL-12 facilitates the conversion of naïve T-cells to the Th1 lineage [2] and induces cell-mediated cytotoxicity [3]. In addition, it is a powerful inducer of $IFN\gamma$ production by T-cells and natural killer cells [4]. The $IFN\gamma$ induces the expression of major histocompatibility complex II on antigen presenting cells [5], enhances production of IL-12 [6] and exerts toxic effects on CNS oligodendrocytes. The damage to CNS myelin interrupts electrical nerve impulse transmission, which results clinically in a variety of disease-induced symptoms such as weakness, fatigue, cognitive dysfunction and neuropathic pain [7] [see **Figure 1**].

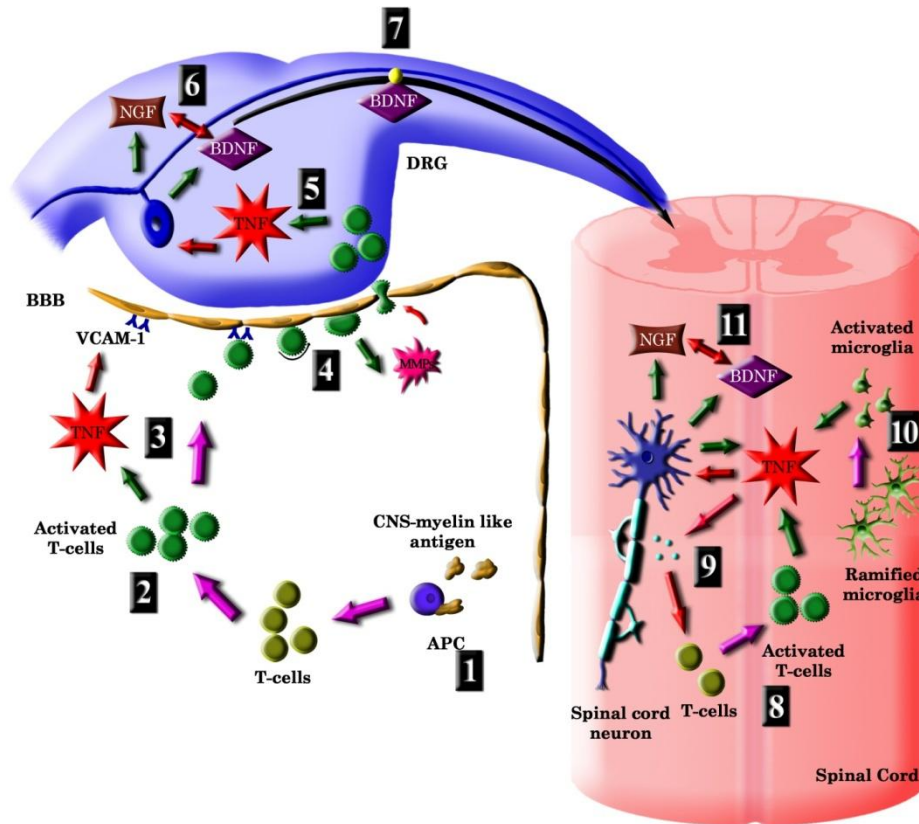


Figure 1: Model of MS

(Permission from Dr Emma Frost, Faculty of Pharmacy, University of Manitoba)

Investigation into the specific structure of MS lesions reveals a diverse antibody-mediated primary oligodendroglia apoptosis. Autoantibodies against myelin constituents including MBP and MOG have been implicated in tissue damage in some MS patients [8]. It has been reported that IgM antibodies specific to MOG and MBP can be found in the serum of patients with initial attacks of demyelination. The presence of these antibodies predicts progression of demyelination to chronic MS. They also support the concept that therapies targeting humoral immune pathway might prove useful in the treatment of MS.

1.1.1 FORMS OF MS

There are three internationally recognized forms of MS: relapsing/remitting MS (RRMS), primary progressive MS (PPMS) and secondary progressive MS (SPMS). Most people presenting with MS (about 80%) are first diagnosed with RRMS. In this form, patients experience a series of relapses (also known as exacerbations) followed by complete or partial disappearance of the symptoms (remissions) until another relapse occurs. There are 10-20% of people with MS suffer from PPMS. This form is characterized by a gradual progression of disease involving a decline in the patient's abilities without any periods of remission. About 50% of MS patients who are first diagnosed as having RRMS will develop SPMS within 10 years. The SPMS form is characterized by a steady progression of clinical neurological damage with or without superimposed relapses and minor remissions.

1.1.2 SYMPTOMS OF MS

People diagnosed with MS usually experience partial or complete loss of any bodily function controlled by the CNS. The symptoms can vary greatly in type and severity depending on the areas of the CNS affected and damaged. The RRMS form typically starts with sensory disturbances, unilateral optic neuritis, diplopia, Lhermitte's sign (trunk and limb paresthesia evoked by neck flexion), limb weakness, clumsiness, gait ataxia, and neurological bladder and bowel symptoms [9]. Patients who have PPMS often present with a slowly evolving upper-motor-neuron syndrome of the legs (chronic progressive myelopathy). This form of MS usually worsens gradually. Visual loss, brain-stem syndromes, and cerebellar, bowel and sexual dysfunction can develop [10].

1.1.3 TREATMENTS FOR MS

Presently, there is no cure for MS. In addition, there are currently no effective treatment strategies for PPMS or SPMS. However, there are treatments to slow down the course of the disease and treat the symptoms associated with RRMS. Several drugs that modify the course of the disease have been approved for clinical treatment of RRMS such as interferon beta-1a (Avonex[®]), interferon beta-1a (Rebif[®]), interferon beta-1b (Betaseron[®]), glatiramer acetate (Copaxone[®]) and Mitoxantrone [11].

1.2. OLIGODENDROCYTES

Oligodendrocytes (OL) are the myelinating cells of the CNS [12]. They produce extensive sheets of lipid rich membrane that wrap around the axon to form a multi-layered sheath [12]. During early embryogenesis, OL pre-progenitors originate in the telencephalon [13], and migrate across the sub-pallial layer to the ganglionic eminences and germinal matrix of the sub-ventricular zone [14].

1.2.1 MYELINATION

Myelination is a critical for normal mammalian function. An intact myelin system facilitates efficient salutatory conductance of nerve impulses through the CNS. Some of the proteins that make up myelin are MBP, MOG, myelin associated glycoprotein (MAG) and PLP [15]. These proteins have both structural and functional significance to the myelin sheath. For example, MBP binds the cytoplasmic faces of the myelin membrane, and forms the major dense line of the myelin sheath [16]. PLP and MAG are also adhesion molecules. PLP binds the extracellular

faces of the myelin sheath together, to ensure compaction [17]. MAG binds the myelin membrane to the axonal membrane, specifically at the nodes of Ranvier [18]. Each OL can interact with up to 50 different neurons and myelinates each axon in 1-2 mm lengths. These short lengths of myelin insulate the axon against membrane depolarization between the nodes of Ranvier. The clustering of sodium channels at the nodes of Ranvier accelerates impulse conduction along the axon [19]. Nerve impulse conduction is severely impeded by the absence of myelin, resulting in weakened or lost function [20]. The myelin sheath is a highly dynamic structure that regulates axonal diameter, controls the ionic content of the periaxonal space, and insulates the axon against loss of signal transmission [21]. The regulation of myelin formation is very tightly regulated via a series of extracellular cues including growth factors; substrate bound molecules, and transcription factors [22].

1.2.2 DEMYELINATION

Immune-mediated damage to oligodendrocytes and the myelin sheath is probably orchestrated through T-cell mediated cytotoxicity. The concept that “myelin-like antigen activated T-cells recruit further T-cells into the CNS, followed by a secondary, antibody-mediated response by B-cells activated by the same or different myelin antigen, is required to effect demyelination via antibody-dependent cell-mediated cytotoxicity” was originally proposed in 1983 [23]. The role of T-cell mediated lesion formation has been extensively studied in the past 3 decades culminating in the widely accepted hypothesis that myelin degeneration occurs as a direct result of macrophage and T-cell derived cytokines causing the initial damage to myelin, which is further damaged by a subsequent antibody/complement mediated process [24]. It is likely that multiple events occur at different time points during the evolution of the lesion. The damaged

myelin is then transformed into extracellular membranous droplets and networks, which are taken up by macrophages. As MS progresses, oligodendrocytes and the axons themselves are destroyed leading to a worsening of disease-induced symptoms.

1.2.3 REMYELINATION

In demyelinating diseases, such as MS, myelin damage results in impaired conduction and progressive axonal degeneration. Limited spontaneous remyelination occurs in acute MS lesions, yet recurring myelin damage is not repaired. The cellular and molecular mechanisms of remyelination are not clear; however a key feature is the generation of remyelinating cells from local precursor cells. Several studies have identified immature oligodendrocyte lineage cells in the normal adult human CNS and the density of these immature oligodendrocytes is increased in acute MS lesions. These precursor cells may serve as targets for developing therapeutic strategies to improve oligodendrocyte regeneration and the extent of remyelination in human demyelinating diseases.

Regulatory mechanisms involved in remyelination can be readily analyzed in adult rodent CNS models that achieve successful remyelination in response to acute demyelination. Oligodendrocyte progenitor cells persist in the adult rodent CNS. In several models of transient demyelination oligodendrocytes progenitor proliferation occurs prior to remyelination. Several developmentally important trophins are expressed in normal adult rodent CNS, and may be more abundant in remyelinating rodent CNS. Specifically, these trophins include platelet derived growth factor A (PDGFA) and fibroblast growth factor 2 (FGF2) [25], and the neurotrophins nerve growth factor (NGF) and brain derived neurotrophic factor (BDNF) [26].

In principle, remyelination can be achieved by either promoting endogenous repair mechanisms or by providing an exogenous source of myelinating cells via transplantation. However, although promoting the endogenous repair of demyelinated lesions has shown some success [26], oligodendrocyte transplantation has yet to be proved successful [27].

1.3 BRAIN DERIVED NEUROTROPHIC FACTOR (BDNF)

BDNF was originally cloned in 1989 [28]. It is the second member of the neurotrophin family, which includes NGF and neurotrophin (NT)-3, -4/5, -6 and -7. The important role of BDNF is regulating the survival and differentiation of various neuronal populations. This role has been firmly established on sensory neurons, cerebellar neurons and spinal motor neurons. Neurons are the major source of BDNF in the nervous system [29]. Like many biologically active proteins, BDNF is synthesized and secreted as a 34kDa precursor protein, proBDNF, which is cleaved to produce active 13kDa BDNF [30].

1.3.1 NEUROTROPHIN RECEPTORS

Neurotrophins bind to three known tropomyosin-related kinase receptors (Trk), TrkA, TrkB and TrkC. TrkA binds to NGF. TrkB interacts with BDNF and NT-4. The biological responses of NT-3 are mediated by TrkC (although it binds with low affinity to TrkA and B). In addition, each of these neurotrophins binds with low affinity to the p75 neurotrophin receptor (p75^{NTR}), a member of the TNF receptor superfamily. BDNF signalling is most commonly associated with TrkB. Studies have shown that the mature form of BDNF signals via the TrkB receptor.

However, proBDNF interacts with the p75^{NTR} and mediates biological actions distinct from those of TrkB.

1.3.2 BDNF AND OLIGODENDROCYTES

Several studies have shown a role for BDNF in oligodendrocyte development *in vivo*. Specifically, BDNF induces oligodendrocyte progenitor cell proliferation [31], differentiation [32] and myelin formation [33]. BDNF increases the expression of the key myelin structural proteins including MBP [34], MAG, and PLP in mature oligodendrocytes [35]. Further, BDNF^{-/-} mice have reduced myelin, and decreased PLP and MBP mRNA [33]. These studies are consistent with the hypothesis that BDNF plays an active role in the structural integrity of myelin. Interestingly, studies have provided evidence that BDNF contributes to the remyelination of spinal cord lesions [36]. Delivery of exogenous BDNF to the CNS of mice induced to a state of EAE resulting in a significant increase in remyelination [37]. A study using EAE induced in a BDNF knockout showed that in the absence of BDNF, myelin structural damage was significantly increased during antigenically induced spinal cord myelin damage [38]. These results suggest that BDNF is critical to repair the compromised structural integrity of myelin resulting from MS. These studies also show that increased BDNF expression in the spinal cord facilitates myelin repair [26].

McTigue et al were one of the first groups to explore BDNF in spinal cord myelin damage and repair [26]. Their study showed significantly increased BDNF levels in the damaged spinal cord. In addition, they confirmed that the presence BDNF in the injured spinal cord promoted oligodendrocyte progenitor cell proliferation and re-myelination of damaged axons [26]. Another recent study showed that BDNF is critical for recovery from demyelination in the CNS [39]. Remyelination is preceded by an increase in oligodendrocyte precursor cells [25]. Several groups

have postulated a lack of oligodendrocyte progenitors as a cause of failed myelin repair [40]. Following myelin damage, reduced levels of BDNF impact the proliferating population of oligodendrocyte precursors, and the subsequent expression of myelin proteins following their differentiation. Thus, increasing the BDNF levels in the spinal cord after injury may act to increase the numbers of oligodendrocytes in and around the lesions that are then able to affect repair.

Published studies show that oligodendrocytes express p75^{NTR} [41]. Although there are no published studies addressing TrkB expression by spinal cord oligodendrocytes, there are studies showing that proBDNF promotes myelination via p75^{NTR}-mediated activity independent of TrkB [42]. Specifically, inhibition of the p75^{NTR} receptor activity prevented the expression of MAG [42]. MAG is essential for long-term axon–myelin stability, the structure of the nodes of Ranvier, and maintenance of the axon cytoskeleton [42]. Thus proBDNF appears to be critical for the structural integrity of the intact myelin sheath, through TrkB independent pathways. In addition to regulating oligodendrocyte lineage cells, BDNF also regulates other cell types (including astrocytes and neurons) that are critical for the formation of myelin [43].

While BDNF is a well-known survival factor during developmental myelination, the specific molecular mechanisms linking BDNF to myelin repair are not yet well defined. In an animal model of demyelination, treatment with glatiramer acetate (Copaxone), which is an immunomodulatory agent to treat relapsing-remitting MS, increased BDNF levels compared to controls [44]. This increase was sustained over the disease course and correlated with myelin repair [44]. In addition, mice receiving transformed bone marrow stromal cells producing BDNF exhibited delayed onset of disease, enhanced clinical recovery, reduced apoptosis, and reduced

demyelination following EAE [45]. Data from human studies provide further support for a beneficial role of BDNF in myelin repair associated with MS lesions. For example, higher serum levels of BDNF were detected during an MS attack in contrast to those seen during the stable phase of the disease [46]. These results suggest that during a MS attack, BDNF expression is upregulated in order to facilitate myelin repair, as evident by its subsequent recovery during the remission phase of the disease. There is no published longitudinal study describing changes in the expression levels of BDNF in correlation with MS relapses in humans. However, it has been shown that peripheral blood mononuclear cells of RRMS patients secrete lower levels of BDNF compared to those of healthy individuals [47]. This suggests that patients with RRMS have lower baseline BDNF levels that predispose them to myelin damage for which they cannot repair as efficiently as normal control subjects. Furthermore, other studies have confirmed that BDNF is expressed in and around human MS lesions [48] suggesting a key role in lesion repair possibly through induction of oligodendrocyte migration and/or precursor proliferation at the site of myelin injury. Recent human studies suggest that up-regulation of BDNF expression facilitates myelin repair [49]. At present, despite the beneficial roles of BDNF in myelin repair, the exact cellular source and target of BDNF responsible for this repair remains unknown. Our recently published study provides evidence that spinal cord BDNF levels may be derived from the sensory neurons of the DRG [50]. Further studies are required to fully characterise the specific cellular source of spinal cord derived BDNF during myelin repair of MS.

1.4 NEUROPATHIC PAIN

Neuropathic pain presents as a chronic pain syndrome. Pain is common in MS patients, with published prevalence estimates varying from 29–86% [51]. The clinical presentation of

neuropathic pain differs from nociceptive pain in those patients present with various sensory abnormalities such as numbness, burning, tingling and shooting pains that vary in severity, intensity and location. Often patients do not equate these abnormal sensations with pain or as a result of MS. At present, there is no known cure for neuropathic pain. Current treatment strategies at the best are only able to reduce pain to a more tolerable level. Neuropathic pain is treated differently from nociceptive pain. Treatment usually follows a careful algorithm, beginning with antidepressants (amitriptyline, venlafaxine or paroxetine), followed by antiepileptic drugs (gabapentin, carbamazepine or topiramate) and topical antineuralgics (capsaicin, ketamine, lidocaine). It can also include analgesics and narcotics. It should be noted that each agent must be given a sufficient trial period, usually at least four to eight weeks. Pharmacists should be able to explain to patients that the response to treatment may not be immediate, as may be the case when treating nociceptive pain with analgesics [52]. A detailed algorithm for the treatment of neuropathic pain has been published elsewhere [52].

1.4.1 PAIN PROCESSING LOOP

The pain process is composed of pain signaling and pain relieving pathways. It is a complex of equilibrium. The pain from the peripheral nervous system is a protective mechanism, which warns against tissue damage. Disease, drug, or injury can disrupt this mechanism and result in chronic pain. When nociceptors get stimulation, pain signals are transmitted to the DRG via sensory afferent fibers. Nociceptive impulses received by primary sensory neurons in the DRG are then transmitted to the spinal cord in the laminae II via dorsal roots. This impulse is relayed to the cortex for high degree process via ascending pathways such as the spinal thalamic tract. The pain-processing center in cortex releases neurotransmitters to inhibit the pain transmission,

which is originated from nociceptors via descending pain control pathways. Overall, the formation of pain processing loop is driven by nociceptive impulse input and pain transmission is suppressed by a descending antinociceptive input [52].

1.5 FRACTALKINE

Chemokines are small cytokines that are key mediators controlling the response of leukocytes to areas of inflammation. They also act as chemotactic cues for leukocytes via interactions with their G-protein coupled, cell membrane-spanning receptors. Fifty chemokines have been identified, which are divided into 4 subgroups, the XC, CC, CXC and CX3C chemokines [53]. Synthesis of chemokines occurs rapidly within infected or damaged tissues. They are thought to drive chronic inflammatory processes in order to attract appropriate cell populations to combat invading organisms and repair damaged tissues [53]. Recent studies have provided evidence that chemokines may serve to reduce neurological deficits including neuropathic pain in inflammatory disorders such as MS [54].

CX3CL1 (Fractalkine) is the only member of the fourth class of chemokines, with a CX3C motif in the mucine-like domain [55]. It is unique in that it is tethered to a cell membrane and is cleaved after an excitotoxic stimulus, to produce a soluble, diffusible protein [56]. CX3CL1 is usually expressed in the normal rodent brain by different neuronal cell sub-types [57]. In addition, it is also expressed in monocytes, NK cells and smooth muscle cells [58]. Recent evidence has shown that CX3CL1 and its receptor are known to be involved in the pathogenesis of several clinical diseases such as rheumatoid arthritis, chronic pancreatitis and neuropathic pain [59]. Further, CX3CL1 plays a critical role in neuroinflammation and neuroprotection by

regulating neuronal-microglial communication [60]. In the CNS, CX3CL1 is highly expressed by neurons while CX3CR1 is only expressed by microglia [57]. However, studies have shown that the expression of CX3CL1 changes during pain states [61].

1.5.1 FRACTALKINE AND PAIN

Several studies show that induction of neuropathic pain results in the synthesis and release of CX3CL1 in the sensory neurons of the dorsal root ganglion (DRG) [61]. Further, this increase is accompanied by upregulation of CX3CR1 in the spinal cord microglia, and correlates with the onset of neuropathic pain [61]. The most likely source of fractalkine in the spinal cord in neuropathic pain states is resident microglia which upregulate fractalkine in response to injury [61]. Activated T-cells, transmigrating across the blood brain barrier are an additional source for the increased CX3CR1-immunoreactivity in the spinal cord in neuropathic pain [62].

Further evidence of a role for CX3CL1 in neuropathic pain comes from a study using intrathecal injections of CX3CL1 [63]. That study showed that acute intrathecal injection of CX3CL1 resulted in the development of thermal hyperalgesia and mechanical allodynia in adult rats [64]. Administration of neutralizing antibodies against CX3CR1 attenuated the allodynia and hyperalgesia in a rat neuropathic pain model [64]. Interestingly, in a spared nerve injury model performed in CX3CR1 knockout mice Holmes et al. showed increased allodynia, suggesting an anti-allodynic role for CX3CL1/CX3CR1 signalling [63]. Therefore, antagonism of CX3CR1 appears to be a promising novel strategy to reduce neuropathic pain.

1.6 DORSAL ROOT GANGLIA (DRG)

The DRG are located midway between peripheral innervated tissue and the spinal cord, and are not part of the CNS. The DRG contain most of the body's primary sensory neurons, which transduce sensory signals from peripheral tissues to the CNS. The sensory neurons of the DRG have a 'pseudounipolar' morphology and it is the cell bodies that are located in the DRG. The sensory neurons are separated from one another by a layer of ensheathing satellite glial cells, which prevents synaptic interactions. However, during the course of neuroexcitability in neighbouring cells, DRG neurons do undergo (sub threshold) excitation [65].

DRG neurons are derived from common neural crest cells and differentiate into a heterogeneous population of sensory neurons, which differ in size, intermediate filament proteins, neuropeptide expression, neurotrophin receptors, target field innervation and function [65]. Most efforts to classify DRG neurons have been on size and other features such as specific neuropeptide content, cytoskeletal and calcium-binding proteins and surface hydrates [66].

According to size, there are three main morphological types of sensory neurons: large, intermediate and small [66]. These populations overlap, but still they show several physiological, biochemical and functional differences. Small neurons give rise to C fibers (non-myelinated, slow conducting), whereas the fibers of large neurons are of the A β types (myelinated, fast conducting). Many of the small cells contain substance P or calcitonin gene related peptide, and they are concerned with thermo- and mechanoreception, and many of them are nociceptive. The terminals of large neurons are low threshold mechanoreceptors [65].

Currently, there are four subdivisions of sensory afferent, which are: cutaneous, muscle, joint and visceral. There are three main types of cutaneous fibers: A β , A γ and C. The A β fibers

contain myelinated, large diameter sensory axons, which display a fast velocity. The A γ class contains intermediate sized sensory axons thinly myelinated. The unmyelinated C fibers represent the small sensory axons, which have a slow conduction velocity. Under normal conditions, only C and A γ can transmit nociceptive information. It has been suggested that A β fibers are responsive to touch, vibration, pressure and other non-noxious modes. Muscle and joint afferents are classed to group I (myelinated, rapid velocity), group II & III (thinly myelinated) and group IV (unmyelinated, slow velocity).

Although some order has emerged from such attempts, defining DRG neurons in this manner is inadequate, since intermediate size classes exist that express the various phenotypic properties usually assigned to one or the other size class. Neurons in DRG have no dendrites, and thus their structure is much simpler than that of most other neurons. They do not receive synapses, but are still endowed with receptors for numerous neurotransmitters.

1.7 EXPERIMENTAL AUTOIMMUNE ENCEPHALOMYELITIS (EAE)

Studies of MS are impeded by its complexity. Ethical and practical issues forbid experimental strategies such as the transfer of suspected pathogenic immune cells to healthy recipients. Further, disease pathology occurs in the CNS and is therefore inaccessible to experimental research. Thus, like most other human diseases, MS research depends on the availability of suitable experimental models to elucidate the pathogenic mechanisms and to develop effective and specific therapies. Many animal models are currently available and each represents certain isolated aspects of MS. A few models produce CNS lesions that cause both inflammation and demyelination. The classic and most common model of MS is actively induced EAE. It is usually induced in rodents. Myelin protein in complete Freund's adjuvant is used for the immunization. The dose and nature of immunization and the strains used determine the severity of the induced disease symptoms. This model has been used extensively to study MS and related symptoms associated with disease pathology.

1.8 PROJECT DESCRIPTION

In summary, we studied BDNF expression within the DRG in the early stages of inflammation associated with the development of EAE. Further, we studied BDNF transport from the DRG to the spinal cord in order to explore its promising function in myelin repair and neuroimmunomodulation. In addition, in order to study the exact role of BDNF in the events of myelin repair via TrkB/p75^{NTR} receptor in EAE spinal cord, we identified the BDNF responsive cells, which express TrkB in the spinal cord from an EAE animal model of MS.

Another objective of this research was to further understand the role of CX3CL1 and CX3CR1 in MS-induced neuropathic pain, as a result, we studied the expression of CX3CL1 and CX3CR1 at gene and protein levels within spinal cord in the early inflammatory stages associated with induction of MS prior to demyelination in an EAE disease model.

Finally, in order to find a method that would allow cryosectioning of the bone without loss of structural integrity of the underlying soft tissue we assess the efficacy of four different decalcifying reagents with respect to their effects on the cellular structure of the myelin of the grey and white matter of the spinal cord.

1.9 REFERENCES

1. Compston A. The story of Multiple Sclerosis. (1998) In: McAlpine's Multiple Sclerosis. 3rded. London: Churchill Livingstone
2. Noseworthy JH, Lucchinetti C, Rodriguez M, Weinshenker BG. (2000) Multiple sclerosis. *N Engl J Med* 343:938-52.
3. Simon J H, Jacobs L D, Campion M K, Rudick R A, Cookfair D L, Herndon R M, et al (1999). The Multiple Sclerosis Collaborative Research Group (MSCRG), A longitudinal study of brain atrophy in relapsing multiple sclerosis, *Neurology* 53: 139–148.
4. Galetta S L. (2001). The Controlled High Risk Avonex[®] Multiple Sclerosis Trial (CHAMPS STUDY), *J Neuroophthalmol.* 21: 292–295.
5. Beck, R. W., Chandler, D. L., Cole , S. R., Simon, J. H., Jacobs, L. D., Kinkel, R. P., et al. (2002). Interferon beta-1a for early multiple sclerosis: CHAMPS trial subgroup analyses, *Ann Neurol.* 51: 481–490.
6. The IFNB Multiple Sclerosis Study Group, (1993). Interferon beta-1b is effective in relapsing-remitting multiple sclerosis. I. Clinical results of a multicenter, randomized, double-blind, placebo-controlled trial, *Neurology.* 43: 655–661.
7. PRISMS (Prevention of Relapses and Disability by Interferon beta-1a Subcutaneously in Multiple Sclerosis) Study Group, (1998). Randomised double-blind placebo-controlled study of interferon beta-1a in relapsing/remitting multiple sclerosis, *Lancet.* 352; 1498–1504.

8. PRISMS Study Group and the University of British Columbia MS/MRI Analysis Group, PRISMS-4: (2001). Long-term efficacy of interferon-beta-1a in relapsing MS, *Neurology*. 56; 1628–1636.
9. Bornstein, M. B., Miller, A., Slagle, S., Weitzman, M., Crystal, H., Drexler E, et al. (1987). A pilot trial of Cop1 in exacerbating-relapsing multiple sclerosis, *N Engl J Med*. 317: pp. 408–414.
10. Johnson K P, Brooks B R, Cohen J A, Ford C C, Goldstein J, Lisak R P, et al, and The Copolymer 1 Multiple Sclerosis Study Group, (1995). Copolymer 1 reduces relapse rate and improves disability in relapsing-relapsing multiple sclerosis: results of a phase III multicenter, double-blind placebo-controlled trial, *Neurology*. 45; 1268–1276.
11. Millefiorini E, Gasperini C, Pozzilli C, D'Andrea F, Bastianello S, Trojano M, et al. (1997). Randomized placebo-controlled trial of mitoxantrone in relapsing-relapsing multiple sclerosis: 24-month clinical and MRI outcome, *J Neurol*. 244: 153–159.
12. Bunge, R. P. (1968). "Glial cells and the central myelin sheath." *Physiol Rev* 48(1): 197-251.
13. Rakic, S. and N. Zecevic (2003). "Early oligodendrocyte progenitor cells in the human fetal telencephalon." *Glia* 41(2): 117-27
14. Levison, S. W., C. Chuang, et al. (1993). "The migrational patterns and developmental fates of glial precursors in the rat subventricular zone are temporally regulated." *Development* 119(3): 611-22.
15. Campagnoni, A. T. (1988). "Molecular Biology of Myelin Proteins from the Central Nervous System." *Journal of Neurochemistry* 51(1): 1-14.

16. Harauz, G., V. Ladizhansky, et al. (2009). "Structural Polymorphism and Multifunctionality of Myelin Basic Protein." *Biochemistry*.
17. Tanaka, H., J. Ma, et al. (2009). "Mice with Altered Myelin Proteolipid Protein Gene Expression Display Cognitive Deficits Accompanied by Abnormal Neuron-Glia Interactions and Decreased Conduction Velocities." *J. Neurosci.* 29(26): 8363-8371.
18. Schnaar, R. L., B. E. Collins, et al. (1998). "Myelin-associated glycoprotein binding to gangliosides. Structural specificity and functional implications." *Ann N Y Acad Sci* 845: 92-105.
19. Kaplan, M. R., A. Meyer-Franke, et al. (1997). "Induction of sodium channel clustering by oligodendrocytes." *Nature* 386(6626): 724-8.
20. Rasminsky, M. and T. A. Sears (1972). "Internodal conduction in undissected demyelinated nerve fibres." *J Physiol* 227(2): 323-50.
21. Dyer, C. A. (2002). "The structure and function of myelin: from inert membrane to perfusion pump." *Neurochem Res* 27(11): 1279-92.
22. Frost, E., B. W. Kiernan, et al. (1996). "Regulation of oligodendrocyte precursor migration by extracellular matrix: evidence for substrate-specific inhibition of migration by tenascin-C." *Dev Neurosci* 18(4): 266-73.
23. Brosnan, C. F., Traugott, U., Raine, C. S. (1983). Analysis of humoral and cellular events and the role of lipid haptens during CNS demyelination. *Acta Neuropath.* 9: 59–70.
24. Raine C S. (1997). The Norton lecture: a review of the oligodendrocyte in the multiple sclerosis lesion. *J of Neuro.* 77: 135-52.

25. Frost, E. E., J. A. Nielsen, et al. (2003). "PDGF and FGF2 regulate oligodendrocyte progenitor responses to demyelination." *J Neurobiol* 54(3): 457-72.
26. McTigue, D. M., P. J. Horner, et al. (1998). "Neurotrophin-3 and Brain-Derived Neurotrophic Factor Induce Oligodendrocyte Proliferation and Myelination of Regenerating Axons in the Contused Adult Rat Spinal Cord." *J. Neurosci.* 18(14): 5354-5365.
27. Gout, O., A. Gansmuller, et al. (1988). "Remyelination by transplanted oligodendrocytes of a demyelinated lesion in the spinal cord of the adult shiverer mouse." *Neurosci Lett* 87(1-2): 195-9.
28. Leibrock J, Lottspeich F , Hohn A , Hofer M , Hengerer B, Masiakowski P, *et al.* (1989). Molecular cloning and expression of brain-derived neurotrophic factor. *Nature.* 341: 149–152.
29. Hofer M, Pagliusi S R, Hohn A, Leibrock A, Barde Y-A. (1990). Regional distribution of brain-derived neurotrophic factor mRNA in the adult mouse brain. *EMBO J.* 9: 2459–2464.
30. Kolbeck, R., S. Jungbluth, et al. (1994). "Characterisation of neurotrophin dimers and monomers." *Eur J Biochem* 225(3): 995-1003.
31. Van't Veer, A., Y. Du, et al. (2009). "Brain-derived neurotrophic factor effects on oligodendrocyte progenitors of the basal forebrain are mediated through trkB and the MAP kinase pathway." *J Neurosci Res* 87(1): 69-78.
32. Nakajima, H., K. Uchida, et al. (2010). "Targeted retrograde gene delivery of brain-derived neurotrophic factor suppresses apoptosis of neurons and oligodendroglia after spinal cord injury in rats." *Spine (Phila Pa 1976)* 35(5): 497-504.

33. Cellerino, A., P. Carroll, et al. (1997). "Reduced Size of Retinal Ganglion Cell Axons and Hypomyelination in Mice Lacking Brain-Derived Neurotrophic Factor." *Molecular and Cellular Neuroscience* 9(5-6): 397-408.
34. Djalali, S., M. Holtje, et al. (2005). "Effects of brain-derived neurotrophic factor (BDNF) on glial cells and serotonergic neurones during development." *Journal of Neurochemistry* 92(3): 616-627.
35. Du, Y., L. D. Lercher, et al. (2006). "Mitogen-activated protein kinase pathway mediates effects of brain-derived neurotrophic factor on differentiation of basal forebrain oligodendrocytes." *J Neurosci Res* 84(8): 1692-702.
36. De Santi, L., P. Annunziata, et al. (2009). "Brain-derived neurotrophic factor and TrkB receptor in experimental autoimmune encephalomyelitis and multiple sclerosis." *J Neurol Sci* 287(1-2): 17-26.
37. Makar, T. K., C. T. Bever, et al. (2009). "Brain-derived neurotrophic factor gene delivery in an animal model of multiple sclerosis using bone marrow stem cells as a vehicle." *J Neuroimmunol* 210(1-2): 40-51.
38. Lee, D. H., E. Geyer, et al. (2012). "Central nervous system rather than immune cell-derived BDNF mediates axonal protective effects early in autoimmune demyelination." *Acta Neuropathol* 123(2): 247-58.
39. VonDran, M. W., H. Singh, et al. (2011). "Levels of BDNF impact oligodendrocyte lineage cells following a cuprizone lesion." *J Neurosci* 31(40): 14182-90.

40. Blakemore, W. F., and Keirstead, H. S. (1999). "The origin of remyelinating cells in the central nervous system." *J Neuroimmunol* 98(1): 69-76.
41. Cohen, R. I., R. Marmor, et al. (1996). "Nerve growth factor and neurotrophin-3 differentially regulate the proliferation and survival of developing rat brain oligodendrocytes." *J Neurosci* 16(20): 6433-42.
42. Cosgaya, J. M., J. R. Chan, et al. (2002). "The neurotrophin receptor p75NTR as a positive modulator of myelination." *Science* 298(5596): 1245-8.
43. Emery, B. (2011). "Regulation of oligodendrocyte differentiation and myelination." *Science* 330(6005): 779-82.
44. Chen, M., R. M. Valenzuela, et al. (2003). "Glatiramer acetate-reactive T-cells produce brain-derived neurotrophic factor." *J Neurol Sci* 215(1-2): 37-44.
45. Makar, T. K., D. Trisler, et al. (2004). "Brain-derived neurotrophic factor (BDNF) gene delivery into the CNS using bone marrow cells as vehicles in mice." *Neurosci Lett* 356(3): 215-9.
46. Azoulay, D., Urshansky, N., et al. (2008). "Low and dysregulated BDNF secretion from immune cells of MS patients is related to reduced neuroprotection." *J Neuroimmunol* 195(1-2): 186-93.
47. Caggiula, M., A. P. Batocchi, et al. (2006). "Neurotrophic factors in relapsing remitting and secondary progressive multiple sclerosis patients during interferon beta therapy." *Clin Immunol* 118(1): 77-82.
48. Stadelmann, C., M. Kerschenstainer, et al. (2002). "BDNF and gp145trkB in multiple sclerosis brain lesions." *Brain* 125(1): 75-85.

49. Azoulay, D., Vachapova, V., et al. (2005). "Lower brain-derived neurotrophic factor in serum of relapsing remitting MS: reversal by glatiramer acetate." *J Neuroimmunol* 167(1-2): 215-8.
50. Zhu, W., E. Frost, et al. (2011). "The role of dorsal root ganglia activation and brain derived neurotrophic factor in multiple sclerosis." *J Cell Mol Med*.
51. O'Connor AB, Schwid SR, Herrmann DN, et al. (2008). Pain associated with multiple sclerosis: systematic review and proposed classification. *Pain* 1:96-111. Epub 2007 Oct 24.
52. Namaka M, Gramlich CR, Ruhlen D, et al. (2004). A treatment algorithm for neuropathic pain. *Clin Ther* 7:951-79.
53. Ransohoff, R. M. (2009). "Chemokines and chemokine receptors: standing at the crossroads of immunobiology and neurobiology." *Immunity* 31(5): 711-21.
54. Karpus, W. J. (2001). "Chemokines and central nervous system disorders." *J Neurovirol* 7(6): 493-500.
55. Bazan, J. F., Bacon, K. B., et al. (1997). "A new class of membrane-bound chemokine with a CX3C motif." *Nature* 385(6617): 640-4.
56. Chapman, G. A., K. Moores, et al. (2000). "Fractalkine cleavage from neuronal membranes represents an acute event in the inflammatory response to excitotoxic brain damage." *J Neurosci* 20(15): RC87.
57. Harrison, J. K., Y. Jiang, et al. (1998). "Role for neuronally derived fractalkine in mediating interactions between neurons and CX3CR1-expressing microglia." *Proceedings of the National Academy of Sciences of the United States of America* 95(18): 10896-10901.

58. Lindia, J. A., E. McGowan, et al. (2005). "Induction of CX3CL1 expression in astrocytes and CX3CR1 in microglia in the spinal cord of a rat model of neuropathic pain." *J Pain* 6(7): 434-8.
59. Haskell, C. A., W. W. Hancock, et al. (2001). "Targeted deletion of CX(3)CR1 reveals a role for fractalkine in cardiac allograft rejection." *J Clin Invest* 108(5): 679-88.
60. Lamb, B. (2012). "The roles of fractalkine signaling in neurodegenerative disease." *Mol Neurodegener* 7 Suppl 1: L21.
61. Verge, G. M., E. D. Milligan, et al. (2004). "Fractalkine (CX3CL1) and fractalkine receptor (CX3CR1) distribution in spinal cord and dorsal root ganglia under basal and neuropathic pain conditions." *Eur J Neurosci* 20(5): 1150-60.
62. Hu, P., A. L. Bembrick, et al. (2007). "Immune cell involvement in dorsal root ganglia and spinal cord after chronic constriction or transection of the rat sciatic nerve." *Brain Behav Immun* 21(5): 599-616.
63. Holmes, F. E., N. Arnott, et al. (2008). "Intra-neural administration of fractalkine attenuates neuropathic pain-related behaviour." *J Neurochem* 106(2): 640-9.
64. Johnston, I. N., E. D. Milligan, et al. (2004). "A role for proinflammatory cytokines and fractalkine in analgesia, tolerance, and subsequent pain facilitation induced by chronic intrathecal morphine." *J Neurosci* 24(33): 7353-65.
65. Devor M. (1999). Unexplained peculiarities of the dorsal root ganglion, *Pain Suppl.* 6:S27–S35.
66. Rambourg A, Clermont Y, Beaudet A. (1983). Ultrastructural features of six types of neurons in rat dorsal root ganglia. *J. Neurocytol.* 12: 47–66.

CHAPTER 2 – AN OVERVIEW OF RELAPSING REMITTING MULTIPLE SCLEROSIS AND CURRENT TREATMENT OPTIONS

Authors and affiliations: Wenjun Zhu, , Josee-Anne Le Dorze¹, Michael Prout, Emma Frost, ,
Mike Namaka, Faculty of Pharmacy, University of Manitoba, Winnipeg, MB, Canada

This paper was published in Pharmacy Practice, Nov 2010, CCCEP # 1065-2010-111-I-P.

2.1 STATEMENT OF CONTRIBUTION

For this paper, I completed the full literature search, I wrote the initial draft of the manuscript. I participated in intellectual discussions surrounding the editing of the manuscript. I wrote and edited the final manuscript and completed manuscript submission. In addition, I completed the proof reading and final document preparations for publication.

2.2 INTRODUCTION

Multiple sclerosis (MS) is a complex condition that affects individuals across the lifespan. Every day, research is being conducted to advance our understanding and knowledge of the etiology of this disease, as well as treatment and potential cures.

Despite the recognized gaps in knowledge, many aspects of MS have been elucidated. For example, certain pathophysiological aspects of the disease have been characterized, such as the process of demyelination. Furthermore, the epidemiology of MS has been well studied. MS is considered a disease of young adults [1]. It has been categorized as such because age at diagnosis is usually between 15 and 40 years. It affects women more frequently than men, in a ratio $>2:1$ [2]. Although women are more frequently affected, men are more likely to develop a higher degree of disability from MS [2]. The incidence of the disease averages 100 diagnosed patients per 100,000 individuals [3,4]. The global distribution of MS displays some intriguing geographical patterns. For example, Canada has been classified as a location with above average incidence of MS, with a prevalence of 132.5 individuals diagnosed per 100,000 [5, 6]. Countries bordering the equator appear to have low rates of MS, while countries further away are characterized by higher incidences of the disease at 30 or more cases per 100,000 individuals [6]. Although MS is not considered a genetic disease, having a first-degree family member with MS increases the risk for developing the disease by a factor of 20–40 compared to individuals in the general population [7]. As researchers continue to unveil key advancements in cellular mechanisms involved in the pathology of MS, the standard of care for individuals living with MS also continues to improve. Due to the diverse array of clinical symptoms induced by the disease, physicians have identified the need to merge with other health disciplines including

physiotherapists, occupational therapists, dieticians, nurses, social workers and pharmacists to provide holistic care to their patients.

2.2.1 ETIOLOGY AND PATHOPHYSIOLOGY

Although the exact etiology of MS remains elusive, evidence implicates multiple factors including the fact that MS is an autoimmune disease. Destruction of the myelin sheath around the axons of the central nervous system (CNS) follows a series of events including immunological activation, the infiltration of peripheral blood lymphocytes and macrophages into the CNS and the subsequent inflammatory response [8]. The net result is the immune-mediated destruction of myelin, oligodendrocytes (cells that produce myelin) and the axons that propagate electrical nerve impulses [9, 10].

The pathophysiological mechanism of MS is thought to begin when unknown, foreign antigens are introduced into the peripheral blood. These antigens are then captured and displayed by antigen presenting cells to inflammatory T-helper cells (Th1 cells), activating them. This leads to a series of events which culminate in the circulating Th1 cells being able to dock, adhere and aggregate at the surface of, and eventually cross, the endothelial lining of the blood brain barrier (BBB) [11-13]. Following migration into the CNS, Th1 cells are then reactivated to specific myelin antigen that share a similar amino acid sequence homology to that of the original causative antigen that initiated the immune response in the periphery. The reactivation of Th1 cells in the CNS results in a similar immune response to that which originally occurred in the periphery. This ultimately drives the phagocytic activity of additional inflammatory mediators such as B cells, macrophages, lymphocytes, and other antibodies that orchestrate a targeted

destruction of CNS myelin [11, 14, 15]. The CNS is composed of an intricate synaptic network of neurons and axons that constantly relay messages between the body and the brain in the form of electrical impulses. These electrical impulses are essential for normal bodily functioning. Analogous to an electrical circuit, the propagation of electrical impulses along these intricate synaptic axonal connections is facilitated by the insulation provided by the myelin sheath that surrounds nerve axons [16]. The pathogenic immune-mediated erosion of the myelin sheath results in the formation of lesions or plaques, which are detectable by magnetic resonance imaging. Ultimately, as the myelin coating is destroyed, the neuron's ability to conduct electrical impulses diminishes. The electrical impulses are unable to reach their target destination due to partial or complete dissipation of the electrical impulse through areas of eroded myelinated axons [17].

The interruptions in electrical signaling described above manifest clinically in the form of a broad array of symptoms. These symptoms include fatigue, muscle spasticity, neuropathic pain, bladder and bowel dysfunction, visual disturbances, depression, reduced cognition, sexual dysfunction, speech and swallowing problems, weakness, paresthesias, muscle rigidity, tremor and ataxia [12, 14].

2.2.2 CATEGORIZATION AND DIAGNOSIS OF MS

Traditionally, MS has been separated into the following categories based on distinct disease patterns. *Relapsing-remitting MS* (RRMS) is diagnosed in patients who have acute attacks, known as relapses, followed by periods of remission where disability is completely reversed. Most patients are diagnosed with this form of the disease. *Primary-progressive MS* (PPMS), on

the other hand, is a chronic disease state with no remissions where symptoms continuously accumulate. Lastly, *secondary progressive MS* (SPMS) occurs secondary to RRMS. At a certain point, patients initially diagnosed with RRMS may stop recovering completely following acute attacks or relapses and disability starts to accumulate gradually [18]. The diagnosis of patients with RRMS usually involves a review of the patient's medical history, a physical exam, a neurological exam, an MRI scan, electroencephalogram (EEG) and, occasionally, other procedures such as a lumbar puncture. MRI scans have become a critical tool in the diagnosis of MS. Patients with MS have characteristic white spots on their MRI scans, allowing for visualization of the areas affected by demyelination. Establishing a diagnosis of MS is often a long and drawn-out process of exclusion. Other pathophysiology must be excluded before the possibility of MS is entertained. In order for a patient to be diagnosed with RRMS, they must have experienced at least two clinical attacks or relapses, disseminated in time and space [19]. According to the New Diagnostic Criteria for MS: Guidelines for Research Protocols, a clinical attack or relapse is any major neurological dysfunction (such as a temporary loss of vision, tingling or numbness in a limb, or muscle spasticity) that lasts for more than 24 hours, often a few days or even several weeks [19]. Furthermore, the two attacks must be disseminated in time, meaning each attack must last at least 24 hours and the two attacks must be separated by a period of at least one month. They must also be disseminated in space, meaning each attack must involve a different part of the CNS [19]. For example, this may mean that one attack involves the optic nerve and presents as optic neuritis (ON) whereas the second attack could involve demyelination in the area of the spinal cord that signals the voiding reflex, and present itself as a bladder that fails to empty. The two attacks had different symptoms due to the fact that the areas of the CNS affected were different.

2.3 TREATMENT OPTIONS FOR RRMS

Despite the immense and ongoing progress we have witnessed in the field of MS research, there is currently no cure for MS. However, a variety of immunomodulatory therapies have been shown to decrease the frequency, intensity and duration of relapses, delay the onset of disability and reduce the number of active lesions as seen on MRI in RRMS patients. This section will focus on treatment for RRMS, since it is the most likely form that pharmacists will encounter in their patients. Additionally, the majority of treatments for MS are indicated only in RRMS. Ultimately, improvement in a patient's quality of life is the primary goal of therapy. Currently available immunomodulatory drugs which act to modify the course of MS include interferon beta-1b, interferon beta-1a, glatiramer acetate and natalizumab [20]. Although the exact disease modifying mechanisms of these drugs are not completely understood, it is known that they decrease the permeability of the BBB and suppress T-cell production, ultimately preventing the inflammatory cascade from escalation.

2.3.1 Interferon beta

Interferon beta is one treatment option frequently offered to patients with RRMS. Two forms of recombinant interferon beta, 1a and 1b, have been approved by Health Canada for the treatment of RRMS. Interferon beta-1a was approved in 1998 [21]. Interferons are endogenously produced by eukaryotic cells in response to certain biological triggers, including viruses [22]. It has been demonstrated that interferon beta-1a upregulates the production of interleukin-10 (IL-10), a potent immunosuppressor of many different inflammatory cytokines that have been implicated in the pathophysiology of MS, such as tumour necrosis factor alpha (TNF- α) [23]. It has been suggested that this may account for some of interferon beta-1a's therapeutic benefit. More

recently, its role in TNF receptor signaling has been suggested as another possible mechanism by which it provides therapeutic benefit [24]. Interferon beta-1a was tested in a multicenter trial involving 301 patients with RRMS and mild-to-moderate disability. Participants were randomized to receive intramuscular injections of 6 million units (30 μ g) of interferon beta-1a, or placebo for up to two years [25, 26]. The primary outcome was the length of time to the progression of disability, defined as a decrease in 1.0 points from baseline on the Expanded Disability Status Scale (EDSS), persisting for at least six months. Treatment with interferon beta-1a was found to significantly reduce the probability of disability progression [25, 27]. The second type of interferon available for the treatment of RRMS is interferon beta-1b. Although the full mechanism of action of interferon beta-1b remains unknown, it has been suggested that down regulating antigen presentation and increasing the expression of immunoglobulin-like transcript 3, an immunoinhibitory protein, may possibly contribute to its therapeutic benefit [22, 28]. Interferon beta-1b was tested in a multicenter trial involving 372 patients with RRMS and mild-to-moderate disability. Participants were randomized to receive 8 million units (250 μ g) of interferon beta-1b, 1.6 million units (50 μ g) of interferon beta-1b, or placebo, given by subcutaneous injection every other day for up to five years. Compared to treatment with placebo, treatment with the higher dose reduced the relapse by 31%, increased the proportion of patients who were relapse-free (27% vs. 17%), and reduced the number of patients who had moderate and severe relapses by a factor of two [29]. Both types of interferon beta are usually well tolerated. The most common side effects are influenza-like symptoms for 24–48 hours after each injection. These may subside after two to three months of treatment, but can persist. It is entirely appropriate for pharmacists to recommend pre-injection analgesia. Acetaminophen or ibuprofen can be taken one hour before the injection to minimize symptoms. Injection site reactions are

common but can be minimized by using proper injection technique, rotating injection sites, using corticosteroid creams and icing the area prior to injection [30]. Interferons may also result in liver toxicity, leukopenia or anemia [31]. As a result, baseline complete blood counts, platelet determinations and liver function tests should be administered prior to the start of therapy, at 1 month, every three months for one year and every six months thereafter [30]. Interferons may be related to the onset or worsening of depression. Interferon products should therefore be used with caution in patients with significant depression. Clinicians should monitor their patients carefully as there can be an increased risk of suicide [30]. Another clinically significant adverse event relates to the fact that interferon beta is immunogenic and can cause the body to form neutralizing antibodies, which can lead to decreased radiologic and clinical effectiveness [32].

2.3.2 Glatiramer acetate (GA)

Glatiramer acetate was approved by Health Canada for the treatment of RRMS in 1997. Glatiramer acetate is a mixture of synthetic polypeptides containing the four naturally-occurring amino acids L-glutamic acid, L-alanine, L-tyrosine and L-lysine. It is believed that its mechanism of action involves the induction and activation of suppressor T-cells in the periphery [33, 34]. Glatiramer acetate was tested in a trial involving 251 patients with RRMS and mild-to-moderate disability. Treatment consisted of daily subcutaneous injections of 20 mg of glatiramer acetate or placebo for two years [35]. Glatiramer acetate therapy produced a 20% reduction in relapse rates compared to placebo [35]. The most common side effects were mild injection site reactions, which occurred in 90% of patients given glatiramer acetate. After one or more injections, 15% of glatiramer recipients experienced brief episodes of flushing, chest tightness, shortness of breath, palpitations and anxiety, lasting no longer than twenty minutes [30]. Patients

can be reassured that this type of reaction is self-limiting and likely benign, unless they have a history of, or other evidence of, coronary artery disease [30]. Serum antibodies to glatiramer acetate were detected, although the presence of such antibodies demonstrated no appreciable effect on the clinical benefit of the drug [35]. Additionally, patients treated with glatiramer acetate did not experience an increased risk of depression, as those treated with interferons [30].

2.3.3 Natalizumab

Natalizumab is a monoclonal antibody originally approved for the treatment of RRMS by Health Canada in 2006. Its effectiveness in RRMS is a direct result of its role as a α 4-integrin antagonist. The protein α 4-integrin binds vascular cell adhesion molecule-1 on endothelial cells to permit migration of leukocytes into the CNS [36, 37]. As a result, this agent has the potential to prevent inflammation from occurring in the CNS by blocking the central migration of blood-borne activated Th1 cells.

Initial studies focusing on the efficacy of natalizumab had impressive results. One randomized, blinded and controlled study assigned MS patients to receive a 3 mg/kg, 6 mg/kg or placebo injection every 28 days for six months, with follow up for an additional six months. The primary outcome was the number of new gadolinium-enhancing lesions as seen on MRI. Secondary outcomes included the frequency of relapse, changes in score on the EDSS and the patients' perception of their own well-being. Results demonstrated that individuals in the placebo group had a mean of 9.6 new lesions, compared to 0.7 and 1.1 in the 3 mg/kg and 6 mg/kg groups, respectively. Clinically, 27 patients in the placebo group experienced a relapse, compared with 13 and 14 in the 3 mg/kg and 6 mg/kg groups, respectively ($p=0.02$ in both cases) [38]. Common

adverse effects of natalizumab include fatigue, non-IgE-mediated allergic reactions, headache, nausea, colds, as well as exacerbations in a minority of patients who suffer from Crohn's disease [39]. Additionally, patients receiving natalizumab are at risk of developing neutralizing antibodies, which can decrease the effectiveness of the drug. In addition to these common adverse effects, natalizumab, both as monotherapy and in combination with other immunomodulatory drugs, carries the risk of progressive multifocal leukoencephalopathy (PML). PML is an opportunistic infection with high mortality rates, resulting from infection with the JC virus; a variant of the human polyomavirus [40, 41]. Concerns about the development of PML resulted in this agent's withdrawal from the market. Natalizumab was reintroduced into the market in 2007, but only as monotherapy for the treatment of RRMS in patients who have had an inadequate response to, or who are unable to tolerate, other therapies [42-45]. In 2010, Health Canada issued another warning relating to PML following the use of natalizumab. A total of 46 cases of PML have been reported worldwide. The incidence of PML increases with longer duration of treatment. Rates of PML jumped from one per 1,000 to 1.6 per 1,000 after 24 months of therapy. As a result, Health Canada strongly advises health care professionals to re-evaluate treatment after 24 months of natalizumab therapy [46].

2.3.4 Other agents

Other immunosuppressive agents such as methotrexate, cyclophosphamide and mitoxantrone have been found to decrease the activity of the immune system. These agents have been recommended for use in specific sub-populations of MS patients—specifically those in whom first line therapies fail, or those who are unable to tolerate first-line therapies [47]. In addition to the above-standard therapies, there are some promising new drugs for the treatment of MS

currently undergoing trials. Cladribine is a synthetic anti-neoplastic agent with immunosuppressive properties commonly used in the treatment of leukemia. It is an analog of the purine nucleoside, adenosine, which plays an important part in DNA synthesis [48]. Fingolimod, on the other hand, is a structural analogue of sphingosine that undergoes phosphorylation in vivo and causes the internalization of a receptor usually present on lymphocytes [49]. As a result of this internalization, the lymphocyte is left unable to respond to signals which would cause its exit from secondary lymphoid tissues, thus reducing the amount of circulating lymphocytes. Both agents are given orally and are currently undergoing Phase III trials (Cladribine is being evaluated in ORACLE and results of this trial are expected in October 2012, whereas fingolimod is being evaluated in FREEDOMS II, with results expected in March 2011) [49].

2.3.1 SYMPTOM MANAGEMENT IN MS

MS is inherently a neurological disease in which myelinated axons are eventually destroyed. Although our ultimate goal is to find a way to stop and repair this damage, this has not yet been achieved. As a result, pharmacists are often involved in managing MS-induced symptoms such as neuropathic pain, optic neuritis, bladder dysfunction, spasticity and fatigue.

Neuropathic pain presents as a chronic pain syndrome. Pain is common in MS patients, with published prevalence estimates varying from 29–86% [50]. The clinical presentation of neuropathic pain differs from nociceptive pain in that patients present with various sensory abnormalities such as numbness, burning, tingling and shooting pains that vary in severity,

intensity and location. Often patients don't equate these abnormal sensations with pain or as a result of MS. Therefore, it is critical that pharmacists, during consultation with their patients, take care to ask patients whether they are experiencing any unusual sensations above and beyond the traditional definition of pain. Neuropathic pain is treated differently than nociceptive pain. Treatment usually follows a careful algorithm, beginning with antidepressants (amitriptyline, venlafaxine or paroxetine), followed by antiepileptic drugs (gabapentin, carbamazepine or topiramate) and topical antineuralgics (capsaicin, ketamine, lidocaine). It can also include analgesics and narcotics. It should be noted that each agent must be given a sufficient trial period, usually at least four to eight weeks. Pharmacists should be able to explain to patients that the response to treatment may not be immediate, as may be the case when treating nociceptive pain with analgesics [51]. A detailed algorithm for the treatment of neuropathic pain has been published elsewhere [51].

Optic neuritis (ON) is the first presenting symptom in approximately 20% of MS cases. It can be described as painful vision loss without accompanying systemic or neurological symptoms. Visual function recovery occurs spontaneously within two to three weeks in approximately 80% of those afflicted by ON. Of those afflicted, 93% recover to a visual acuity of at least 20/40 within twelve months [52]. Short-term, high-dose corticosteroid treatment may be considered. This generally consists of intravenous methylprednisolone (250 mg QID for three days) followed by oral prednisone (1 mg/kg for 11 days), followed by a tapering period [52-54]. Although this type of treatment does not provide any long-term benefit, it can shorten the duration of visual impairment providing short-term benefits to the patient [52].

Urinary problems secondary to bladder dysfunction are very common in the MS patient. Frequently, the myelin on nerve axons innervating the bladder has eroded, leading to the dissipation of electrical impulses to this tissue and causing symptoms that may include urgency, hesitancy, frequency and incontinence. The clinician should first eliminate the possibility of an infection, treating with antibiotics if necessary. Oral agents such as terazosin and prazosin, which relax the smooth muscle in the bladder, can be used to treat symptoms of hesitancy. If the problem is due to a constant full bladder, catheterization may be the most beneficial approach. On the other hand, if the patient's bladder is frequently contracting, anticholinergic agents such as oxybutynin can be tried [55]. Pharmacists can make nonpharmacological recommendations to help patients with these symptoms, such as fluid management, pelvic floor exercises and bladder emptying exercises.

Spasticity is another common symptom in MS patients. It can manifest as limitations in the range of movement and/or pain, which can affect an individual's ability to complete daily tasks of living [56]. All pharmacological treatments for spasticity should be preceded and accompanied by physical therapy and occupational therapy. Oral baclofen has been used successfully to treat spasticity [57]. Other oral agents used in the treatment of spasticity include tizanidine and cannabinoids [58, 59]. Occasionally, intrathecal baclofen or botulinum toxin injections are also used to treat spasticity [60, 61].

Fatigue is another frequent MS induced symptom, affecting 80–97% of MS patients [62]. Occupational and physical therapists can help MS patients manage their energy more efficiently. In addition, pharmacological management with amantadine and modafinil are reasonable options

to manage MS-induced fatigue [63, 64]. Methylphenidate has been shown to be effective in treating HIV induced fatigue and may also be an option for MS patients [65]. Pharmacists can be involved in the treatment of fatigue by helping patients to manage the side effects of these drugs, such as increased alertness during the night.

2.3.2 NONPHARMACOLOGICAL TREATMENTS

As for any patient with neurologic deficits, a multifaceted approach is important to limiting the progression of the disease and overcoming disability. Simple things, such as avoiding heat, can prevent the worsening of MS symptoms. Heat has been shown to slow electrical impulses along nerve axons [66]. Since electrical impulses are already slowed due to demyelination, it is easy to see how avoiding heat may be beneficial for the MS patient.

2.4 PHARMACIST'S ROLE

The practice of pharmacy has evolved beyond simply providing pharmaceutical care. The drugs are no longer the primary focus of patient care; instead, they merely act as vehicles to deliver the desired healthcare goals. Pharmacists have expert knowledge on drugs and can provide insight as how to best achieve these goals. As a result of the demonstrated benefits of pharmacist involvement, clinical pharmacy practitioners have gained acceptance and integration in the overall health care team [67, 68]. The integration of a pharmacist within an inter-professional team to provide care for MS patients has potential benefits. Frequently, these patients are on numerous medications and require increased access and support from the healthcare system. Often, many different medications will be used to treat a patient's varied symptoms, and

pharmacists are well informed to ensure that a patient's drugs are being used appropriately. Frequently, a drug used to treat one symptom may actually have the side effect of worsening another symptom. Pharmacists can help patients weigh the benefits and risks of each drug as it is being added to their drug regimen. The pharmacist thus can play an important role in MS clinics across the country. Similarly, community pharmacists are important in the care of MS patients as they are often more accessible than doctors and neurologists and are likely to be the first healthcare professional a patient approaches regarding new drug-related questions or problems.

2.5 SUMMARY

MS is a chronic inflammatory demyelinating disease that affects the CNS. The most common course of the disease is the relapsing-remitting subtype, which is characterized by unpredictable relapses followed by periods of relative remission with no signs of new disease activity. The pharmacist plays an important role in the holistic approach to patient care.

2.6 REFERENCES

1. Wingerchuk DM, Lucchinetti CF, Noseworthy JH. Multiple sclerosis: current pathophysiological concepts. *Lab Invest* 2001; 3: 263-81.
2. Sadovnick AD, Ebers GC. Epidemiology of multiple sclerosis: a critical overview. *Can J Neurol Sci* 1993; 1: 17-29.
3. Shum J. Drug management of Multiple Sclerosis. *The CE Advisor* 1994; 1-8.
4. Teasell R W. Managing advanced multiple sclerosis. *Can Fam Physician* 1993; 1127-30, 1133-4, 1137-41.
5. Multiple Sclerosis International Federation. Atlas of MS (accessed May 23, 2010, 2010)
6. Kurtzke J F. Multiple sclerosis in time and space—geographic clues to cause. *J Neurovirol* 2000;Suppl 2:S134-S140.78
7. Kalman B, Albert RH, Leist TP. Genetics of multiple sclerosis: determinants of autoimmunity and neurodegeneration. *Autoimmunity* 2002;4:225-34.
8. Raine CS, Scheinberg LC. On the immunopathology of plaque development and repair in multiple sclerosis. *J Neuroimmunol* 1988;2-3:189-201.
9. Burt RK, Traynor AE, Cohen B, et al. T cell-depleted autologous hematopoietic stem cell transplantation for multiple sclerosis: report on the first three patients. *Bone Marrow Transplant* 1998;6:537-41.
10. Werner P, Pitt D, Raine CS. Glutamate excitotoxicity—a mechanism for axonal damage and oligodendrocyte death in Multiple Sclerosis? *J Neural Transm Suppl.* 2000;60:375-85.
11. Noseworthy JH, Lucchinetti C, Rodriguez M, et al. Multiple sclerosis. *N Engl J Med* 2000;13:938-52.

12. Namaka M, Pollitt-Smith M, Gupta A, et al. The clinical importance of neutralizing antibodies in relapsing-remitting multiple sclerosis. *Curr Med Res Opin* 2006;2:223-39.
13. Cui JY. Multiple sclerosis: an immunologic perspective. *Phys Med Rehabil Clin N Am* 2005;2:351-8.
14. Sobel RA. The pathology of multiple sclerosis. *Neurol Clin* 1995;1:1-21.
15. Rodriguez M. Multiple sclerosis: basic concepts and hypothesis. *Mayo Clin Proc* 1989;5:570-6.
16. Ozenci V, Kouwenhoven M, Link H. Cytokines in multiple sclerosis: methodological aspects and pathogenic implications. *Mult Scler* 2002;5:396-404.
17. Bainbridge J, Corboy J, Gidal B. Multiple Sclerosis. In: JT Dipiro. *Pharmacotherapy-A Pathophysiologic Approach*. Toronto: McGraw-Hill 2002:1019-1030.
18. Lublin FD, Reingold SC. Defining the clinical course of multiple sclerosis: results of an international survey. National Multiple Sclerosis Society (USA) Advisory Committee on Clinical Trials of New Agents in Multiple Sclerosis. *Neurology* 1996;4:907-11.
19. Poser CM, Paty DW, Scheinberg L, et al. New diagnostic criteria for multiple sclerosis: guidelines for research protocols. *Ann Neurol* 1983;3:227-31.
20. Bainbridge J, Corboy J and Gidal B. Multiple Sclerosis. In: JT Dipiro. *Pharmacotherapy - A Pathophysiologic Approach*. Toronto: McGraw-Hill 2002: 1019-30.
21. Drug Product Database Online Query: AVONEX and REBIF. <http://webprod.hc-sc.gc.ca/dpd-bdpp/info.do?lang=eng&code=61126> (accessed May 23, 2010, 2010)
22. Jiang H, Milo R, Swoveland P, et al. Interferon beta-1b reduces interferon gamma-induced antigen-presenting capacity of human glial and B cells. *J Neuroimmunol* 1995;1:17-25.

23. Rudick RA, Ransohoff RM, Peppler R, et al. Interferon beta induces interleukin-10 expression: relevance to multiple sclerosis. *Ann Neurol* 1996;4:618-27.
24. Reuss R, Pohle S, Retzlaff K, et al. Interferon beta-1a induces tumor necrosis factor receptor 1 but decreases tumor necrosis factor receptor 2 leukocyte mRNA levels in relapsing-remitting multiple sclerosis. *Neuroimmunomodulation* 2009; 3:171-6 Epub 2009 Feb 24.
25. Jacobs LD, Cookfair DL, Rudick RA, et al. Intramuscular interferon beta-1a for disease progression in relapsing multiple sclerosis. The Multiple Sclerosis Collaborative Research Group (MSCRG). *Ann Neurol* 1996;3:285-94.
26. Jacobs LD, Cookfair DL, Rudick RA, et al. A phase III trial of intramuscular recombinant interferon beta as treatment for exacerbating-remitting multiple sclerosis: design and conduct of study and baseline characteristics of patients. Multiple Sclerosis Collaborative Research Group (MSCRG). *Mult Scler* 1995;2:118-35.
27. Rudick RA, Goodkin DE, Jacobs LD, et al. Impact of interferon beta-1a on neurologic disability in relapsing multiple sclerosis. The Multiple Sclerosis Collaborative Research Group (MSCRG). *Neurology* 1997;2:358-6
28. Jensen MA, Yanowitch RN, Reder AT , et al. Immunoglobulin-like transcript 3, an inhibitor of T cell activation, is reduced on blood monocytes during multiple sclerosis relapses and is induced by interferon beta-1b. *Mult Scler* 2009;1:30-8.
29. Interferon beta-1b is effective in relapsing-remitting multiple sclerosis. I. Clinical results of a multicenter, randomized, double-blind, placebo-controlled trial. The IFNB Multiple Sclerosis Study Group. *Neurology* 1993;4:655-61.
30. Bainbridge J, Corboy J. Multiple Sclerosis. In: JT Dipiro. *Pharmacotherapy - A Pathophysiologic Approach*. Toronto: McGraw-Hill 2008:913-926.

31. Interferon beta-1b in the treatment of multiple sclerosis: final outcome of the randomized controlled trial. The IFNB Multiple Sclerosis Study Group and The University of British Columbia MS/MRI Analysis Group. *Neurology* 1995;7:1277-85.
32. Goodin DS, Frohman EM, Hurwitz B, et al. Neutralizing antibodies to interferon beta: assessment of their clinical and radiographic impact: an evidence report: report of the Therapeutics and Technology Assessment Subcommittee of the American Academy of Neurology. *Neurology* 2007;13:977-84.
33. Johnson KP, Brooks BR, Cohen JA, et al. Copolymer 1 reduces relapse rate and improves disability in relapsing-remitting multiple sclerosis: results of a phase III multicenter, double-blind placebo-controlled trial. The Copolymer 1 Multiple Sclerosis Study Group. *Neurology* 1995;7:1268-76.
34. Weber MS, Hohlfeld R, Zamvil SS. Mechanism of action of glatiramer acetate in treatment of multiple sclerosis. *Neurotherapeutics* 2007;4:647-53.
35. Johnson KP, Brooks BR, Cohen JA, et al. Copolymer 1 reduces relapse rate and improves disability in relapsing-remitting multiple sclerosis: results of a phase III multicenter, double-blind placebo-controlled trial. The Copolymer 1 Multiple Sclerosis Study Group. *Neurology* 1995;7:1268-76.
36. Frenette PS, Wagner DD. Adhesion molecules--Part 1. *N Engl J Med* 1996;23:1526-9.
37. Frenette PS, Wagner DD. Adhesion molecules--Part II: Blood vessels and blood cells. *N Engl J Med* 1996;1:43-5.
38. Miller DH, Khan OA, Sheremata WA, et al. A controlled trial of natalizumab for relapsing multiple sclerosis. *N Engl J Med* 2003;1:15-23.

39. Sands BE, Kozarek R, Spainhour J, et al. Safety and tolerability of concurrent natalizumab treatment for patients with Crohn's disease not in remission while receiving infliximab. *Inflamm Bowel Dis* 2007;1:2-11.
40. Kleinschmidt-DeMasters BK and Tyler KL. Progressive multifocal leukoencephalopathy complicating treatment with natalizumab and interferon beta-1a for multiple sclerosis. *N Engl J Med* 2005;4:369-74.
41. Langer-Gould A, Atlas SW, Green AJ, et al. Progressive multifocal leukoencephalopathy in a patient treated with natalizumab. *N Engl J Med* 2005;4:375-81.
42. Yednock TA , Cannon C, Fritz LC, et al. Prevention of experimental autoimmune encephalomyelitis by antibodies against alpha 4 beta 1 integrin. *Nature* 1992;364:63-6.
43. Baron JL, Madri JA, Ruddle NH, et al. Surface expression of alpha 4 integrin by CD4 T cells is required for their entry into brain parenchyma. *J Exp Med* 1993;1:57-68.
44. Kent SJ, Karlik SJ, Cannon C, et al. A monoclonal antibody to alpha 4 integrin suppresses and reverses active experimental allergic encephalomyelitis. *J Neuroimmunol* 1995;1:1-10.
45. Hartung HP, Reiners K, Archelos JJ, et al. Circulating adhesion molecules and tumor necrosis factor receptor in multiple sclerosis: correlation with magnetic resonance imaging. *Ann Neurol* 1995;2:186-93.
46. TYSABRI (natalizumab) - New Safety Information Regarding Progressive Multifocal Leukoencephalopathy (PML) - For Health Professionals. http://hc-sc.gc.ca/dhp-mps/medeff/advisories-avis/prof/_2010/tysabri_3_hpccps-eng.php (accessed June 29, 2010)
47. Neuhaus O, Kieseier BC, Hartung HP. Immunosuppressive agents in multiple sclerosis. *Neurotherapeutics* 2007;4:654-60.

48. Sipe JC. Cladribine for multiple sclerosis: review and current status. *Expert Rev Neurother* 2005;6:721-7.
49. Conway D, Cohen J A. Emerging oral therapies in multiple sclerosis. *Curr Neurol Neurosci Rep* 2010;5:381-8.
50. O'Connor AB, Schwid SR, Herrmann DN, et al. Pain associated with multiple sclerosis: systematic review and proposed classification. *Pain* 2008;1:96-111. Epub 2007 Oct 24.
51. Namaka M, Gramlich CR, Ruhlen D, et al. A treatment algorithm for neuropathic pain. *Clin Ther* 2004;7:951-79.
52. Shams PN, Plant GT. Optic neuritis: a review. *Int MS J* 2009;3:82-9.
53. Beck RW. The Optic Neuritis Treatment Trial. *Arch Ophthalmol* 1988;8:1051-3.
54. Osborne BJ, Volpe NJ. Optic neuritis and risk of MS: differential diagnosis and management. *Cleve Clin J Med* 2009;3:181-90.
55. Schapiro RT . The symptomatic management of multiple sclerosis. *Ann Indian Acad Neurol* 2009;4:291-5.
56. Kesselring J, Beer S. Symptomatic therapy and neurorehabilitation in multiple sclerosis. *Lancet Neurol* 2005;10:643-52.
57. Paisley S, Beard S, Hunn A, et al. Clinical effectiveness of oral treatments for spasticity in multiple sclerosis: a systematic review. *Mult Scler* 2002;4:319-29.
58. Turcotte D, Le Dorze JA, Esfahani F, et al. Examining the roles of cannabinoids in pain and other therapeutic indications: a review. *Expert Opin Pharmacother* 2010;1:17-31.
59. Vakhapova V, Auriel E and Karni A. Nightly sublingual tizanidine HCl in multiple sclerosis: clinical efficacy and safety. *Clin Neuropharmacol* 2010;3:151-4.

60. Dario A, Tomei G. Management of spasticity in multiple sclerosis by intrathecal baclofen. *Acta Neurochir Suppl* 2007; Pt 1:189-92.
61. Snow BJ, Tsui JK, Bhatt MH, et al. Treatment of spasticity with botulinum toxin: a double-blind study. *Ann Neurol* 1990;4:512-5
62. Bagert B, Camplair, Bourdette D. Cognitive dysfunction in multiple sclerosis: natural history, pathophysiology and management. *CNS Drugs* 2002; 7: 445-55.
63. Krupp LB, Coyle PK, Doscher C, et al. Fatigue therapy in multiple sclerosis: results of a double-blind, randomized, parallel trial of amantadine, pemoline, and placebo. *Neurology* 1995; 11: 1956-61.
64. Rammohan KW, Rosenberg JH, Lynn DJ, et al. Efficacy and safety of modafinil (Provigil) for the treatment of fatigue in multiple sclerosis: a two centre phase 2 study. *J Neurol Neurosurg Psychiatry* 2002; 2: 179-83.
65. Breitbart W, Rosenfeld B, Kaim M et al. A randomized, double-blind, placebo-controlled trial of psychostimulants for the treatment of fatigue in ambulatory patients with human immunodeficiency virus disease. *Arch Intern Med* 2001; 3: 411-20.
66. Davis SL, Wilson TE, White AT, et al. Thermoregulation in Multiple Sclerosis. *J Appl Physiol* 2010;29.
67. McAuley JW, Mott DA, Schommer JC, et al. Assessing the needs of pharmacists and physicians in caring for patients with epilepsy. *J Am Pharm Assoc (Wash)* 1999;4: 499-504.
68. Henry S. Drug treatment for new Parkinson's patients should await specialist diagnosis. *The Pharmaceutical Journal* 2001; 266: 454.

CHAPTER 3 – THE ROLE OF DORSAL ROOT GANGLIA ACTIVATION AND BRAIN DERIVED NEUROTROPHIC FACTOR IN MULTIPLE SCLEROSIS

Authors and affiliations - Wenjun Zhu¹, Emma Frost¹, Farhana Begum², Parvez

Vora¹, Kelvin Au¹, Yüewen Gong¹, Brian MacNeil³, Prakash Pillai^{1,2}, Mike Namaka^{1,2}

1. Faculty of Pharmacy, 2. Department of Human Anatomy and Cell Science, 3. School of Medical Rehabilitation, University of Manitoba, Winnipeg, MB, Canada

This is an Accepted Article that has been peer-reviewed and approved for publication in the *Journal of Cellular and Molecular Medicine*. It has been published electronically, but has yet to be published in hard copy. Please cite this article as an “Accepted Article”; doi: 10.1111/j.1582 4934. 2011. 01481.x

3.1 STATEMENT OF CONTRIBUTION

For this study, I was responsible for the induction of the EAE rats (including neurological disability testing, sacrifice, harvesting and preparation of tissue for analysis), and completion of immunohistochemistry, ELISA, real-time RT-PCR, and analyzing the data. I participated in the experimental design, and intellectual discussions surrounding the data interpretation. I drafted the manuscript, prepared the figures for publication and proof read the final manuscript prior to publication.

3.2 ABSTRACT

Multiple sclerosis (MS) is characterized by focal destruction of the white matter of the brain and spinal cord. The exact mechanisms underlying the pathophysiology of the disease are unknown.

Many studies have shown that MS is predominantly an autoimmune disease with an inflammatory phase followed by a demyelinating phase. Recent studies alongside current treatment strategies, including glatiramer acetate, have revealed a potential role for brain derived neurotrophic factor (BDNF) in MS. However, the exact role of BDNF is not fully understood. We used the experimental autoimmune encephalomyelitis (EAE) model of MS in adolescent female Lewis rats to identify the role of BDNF in disease progression. DRG and spinal cords were harvested for protein and gene expression analysis every 3 days post-disease induction (dpi) up to 15 days. We show significant increases in BDNF protein and gene expression in the DRG of EAE animals at 12 dpi, which correlates with peak neurological disability. BDNF protein expression in the spinal cord was significantly increased at 12 dpi, and maintained at 15 dpi. However, there was no significant change in mRNA levels. We show evidence for the anterograde transport of BDNF protein from the DRG to the dorsal horn of the spinal cord via the dorsal roots. Increased levels of BDNF within the DRG and spinal cord in EAE may facilitate myelin repair and neuroprotection in the CNS. The anterograde transport of DRG derived BDNF to the spinal cord may have potential implications in facilitating central myelin repair and neuroprotection.

Keywords: Multiple Sclerosis, MS, EAE, BDNF, DRG, anterograde transport

3.3 INTRODUCTION

Multiple sclerosis (MS) is a chronic, neuroinflammatory disease characterized by immune-cell mediated white matter damage in the central nervous system (CNS) [1]. Myelin reactive Th1-cells transmigrate across the blood brain barrier into the CNS. These Th1-cells promote neuroinflammation by the sustained production of cytokines such as interleukins (IL), tumor necrosis factor- α (TNF α), and interferon- γ (IFN γ) [2, 3]. The consequent myelin damage results in a variety of disease-induced symptoms including: fatigue, cognitive dysfunction and sensory abnormalities [1, 4].

Current early MS treatments are directed at inflammation and neuroprotection [1, 5]. However, the exact inflammatory mechanisms that underlie the disease are largely unknown. Studies show that changes in neurotrophins and/or their receptors play a critical role in neuroimmunomodulation [6, 7]. One candidate neurotrophin in MS associated inflammation is brain-derived neurotrophic factor (BDNF) [6-9]. BDNF is a potent mitogen for neurons during CNS development [10-12], and an important regulator of neuronal maturation and protection [8, 13]. Studies have shown an association of BDNF production by immune cells and disease activity, in addition higher BDNF serum levels were observed during relapse in contrast to those seen during the stable phase of the disease [6, 8, and 14]. In addition, BDNF is expressed in and around MS lesions [15]. Further evidence for the importance of BDNF in MS comes from the use of glatiramer acetate (GA). GA is an approved treatment for relapsing remitting MS (RRMS) [5]. It acts by increasing the production and release of BDNF by Th-cells [9, 16-19]. However, the exact role for BDNF in MS is still unknown.

We have previously shown that the dorsal root ganglion (DRG) is a pivotal reservoir of the inflammatory cytokine TNF α in the early inflammatory stage of experimental autoimmune encephalomyelitis (EAE) [20]. We hypothesized that BDNF expression is increased within the DRG in the early stages of inflammation associated with the development of EAE, and that this BDNF is anterograde transported from the DRG to the dorsal horn of the spinal cord.

This study is the first published study showing evidence that BDNF levels are increased in the dorsal root ganglia (DRG) and spinal cord of rats induced to a state of EAE in accordance with our model of disease induction [20]. Further, we show that BDNF protein is anterogradely transported from the DRG to the dorsal root entry zone, via kinesin mediated active transport. Our study provides novel information relating to the mechanisms underlying the efficacy of current immunomodulatory therapies used to ameliorate MS symptoms. In addition, we show a previously unrecognized mechanism of BDNF transport into the spinal cord after immune induction.

3.4 MATERIALS AND METHODS

3.4.1 EAE MODEL

Experimental autoimmune encephalomyelitis (EAE) was induced using MBP, in adolescent female Lewis rats (Charles River, Montreal, QC) as previously described [20]. Adolescent female Lewis rats were randomly assigned to 3 experimental groups: naïve control (NC), active control (AC) and active EAE (EAE). For each group there were 5 time points for sacrifice at 3, 6, 9, 12 and 15 days post induction (dpi). All animal experiments were conducted according to

protocols approved by the University of Manitoba Animal Protocol Management and Review Committee, in full compliance with the Canadian Council on Animal Care.

3.4.2 TISSUE HARVESTING AND SECTIONING

For immunohistochemical (IHC) analysis of protein expression, animals were perfusion fixed with 4% paraformaldehyde as previously described [20]. Spinal columns were dissected free of overlying muscle and connective tissue, and decalcified according to previously described protocols [21]. For gene expression analysis, the DRG and spinal cord were harvested as previously described [20]. Tissue was stored in RNAlater stabilization reagent (Qiagen, cat. no. 76106, Washington DC, USA) until processed. Total RNA, DNA, and proteins were isolated as previously described [22].

3.4.3 WESTERN BLOT

Protein concentration for each sample was assessed using the Bradford protein assay [23]. For each sample, 30 µg total protein was analyzed by western blot as previously described [20]. Anti-BDNF antibody (1:500, R&D system Minneapolis, MN, USA) was used to detect BDNF protein. Following incubation with anti-rabbit secondary antibody (1:10,000, Jackson ImmunoResearch, West Grove, PA, USA), immunoreactivity was detected by chemiluminescence (Alpha Innotech, Santa Clara, CA, USA).

3.4.4 IMMUNOHISTOCHEMISTRY

Qualitative immunofluorescent analysis of cryostat sections was conducted to detect the protein expression of BDNF according to previously described methods [20, 22]. Double-labeled immunofluorescence using monoclonal antibodies against the neuronal markers NF-160 (1:40, Invitrogen, Burlington, ON, Canada) or NeuN (1:1000; Chemicon, Billerica, MA, USA) were conducted in conjunction with the polyclonal antibody for BDNF (polyclonal chicken anti-BDNF antibody (1:100, R&D system Minneapolis, MN, USA)). This antibody detects the mature form of BDNF, at 14 kDa, that acts via the TrkB receptor to exert its biological effect in the tissue being assessed [24]. BDNF and NeuN were identified using chicken anti-BDNF antibody, and mouse monoclonal NeuN antibody [22]. Secondary antibodies were biotinylated - chicken IgY (1:100, R&D Systems Inc., Minneapolis, MN, U.S.A) and goat anti-mouse FITC (1:50, Jackson, West Grove, PA, USA), Streptavidin-Alexa Fluor 568 (TRITC/Texas red, 1:500, Molecular Probes/Invitrogen, Burlington, ON, Canada). The slides were imaged using an Olympus BX51 configured with FV5000 Confocal laser scanning capability; images were captured in Fluoview Version 4.3. Cell diameter measurements and pseudocoloring were performed using Image Pro Express software (Media Cybernetics, Bethesda, MD, USA). Image sizing, black background balancing and final collation for publication were performed using Adobe Creative Suite 2 v9.0.2 (Adobe Systems Inc., San Jose, CA, USA). No image manipulations were performed other than those described.

3.4.5 REVERSE TRANSCRIPTION POLYMERASE CHAIN REACTION (RT-PCR) AND REAL TIME PCR

Real time RT-PCR was conducted on tissue samples as previously described [20, 22]. The PCR reaction was performed using a Light-Cycler-DNA master SYBR green 1 kit following manufacturers protocols (Roche, Indianapolis, IN, USA). BDNF primers were: forward: 5'-TTC TTG TGC AGT GCC AGC CTC GTC-3; reverse; 5'-GCC GTT GAA CTT GCC GTG GGT AGA- 3' and annealing temperature at 54 °C. qRT-PCR results were analyzed using 1-way analysis of variance (ANOVA) followed by Tukey's post hoc comparisons. Statistical significance was confirmed using two-tailed Students *t*-test. The model detected differences between main effects day and group values; and the interaction effect day x group values, which were considered significant at $p < 0.05$. Normality and homogeneity of error variance of dependent variable was tested by using Kolmogorov-Smirnov and Levene's test.

3.4.7 ENZYME LINKED IMMUNOSORBENT ASSAY

Total protein was extracted from the samples as described above, and total protein concentration assessed using the Bradford assay [23]. The protein concentrations of the samples were adjusted to 30µg in the sample volume of 100µl. Sandwich-style ELISA was performed using the BDNF Emax ImmunoAssay System (Promega, Madison, WI) according to the manufacturer's instructions [25]. BDNF content was interpolated from standard curve runs for each plate (linear range of 7.8–500). For a given DRG and spinal cord segment, samples from the groups of AC and EAE and the naïve control rats were determined in a single run. Each sample was assayed in three separate ELISA assays, with three replicates per sample per ELISA.

3.4.8 STATISTICAL ANALYSIS

Statistics was performed using GraphPad Prism version 4.03 for Windows (GraphPad Software, San Diego California USA, www.graphpad.com). Statistical analysis was performed using ANOVA with Tukey's Multiple Comparison post hoc test. Student's *t*-test was used to assess significance of differences between the groups.

3.5 RESULTS

3.5.1 NEUROLOGICAL DISABILITY SCORES

All animals in the EAE groups were assessed for neurological disability according to a previously described global neurological disability assessment tool [20]. Prior to day 6 post-EAE induction (6 dpi), none of the animals displayed clinical neurological deficits thereby scoring zero. However, by 9 dpi all animals started to display clinical signs of neurological disability (mean 0.57 ± 0.45). Neurological disability progressively worsened upon daily assessment until 12 dpi (peak disability; mean 6.42 ± 5.35), then subsided by 15 dpi (mean 1.5 ± 1.41) as the animals entered the remission phase of disease induction, well characterized for this animal model [26] (**Figure 1**).

3.5.2 IMMUNOHISTOCHEMICAL ANALYSIS OF BDNF PROTEIN EXPRESSION IN DRG

Comparative IHC analysis of EAE versus AC animals euthanized at 6, 9, 12 and 15 dpi, revealed markedly increased BDNF immunoreactivity in the EAE animals' at 6 dpi through 15 dpi relative to that seen in the AC group at the same experimental time points and/or the NC group

(**Figure 2a**). Judging by easily detectable sensory neuron morphological criteria, and NeuN double labeling, the increased signal intensity for cytoplasmic BDNF appears to be localized to the sensory neuron population of the DRG. In addition, the satellite cells within the DRG were immunoreactive for BDNF. The overall increase in BDNF from the collaborative effects of satellite cells and neuronal cells appears to reach peak expression around 12 dpi (**Figure 2a**). These results suggest that the transient neuronal expression of BDNF in the DRG peaks at day 12 and subsides by day 15 post induction. A double blind analysis of the EAE group relative to the two control groups showed that the percentage of DRG neurons identified as BDNF positive significantly increased from 9 dpi ($19.0 \pm 5.0\%$) to a relative peak 12 dpi ($42 \pm 3.0\%$; $p=0.0169$), and decreased again at 15 dpi ($27.0 \pm 3.0\%$) (**Figure 2b**). However, the same increase in neuronal expression of BDNF was not seen in either of the control groups. In NC DRG only $11.2 \pm 2.1\%$ of neurons were identified as BDNF positive. In AC controls the percentage of BDNF positive cells did not significantly change between days 9, 12 and 15 post induction (15.5 ± 3.4 , 15.0 ± 3.0 , 11.0 ± 2.5 respectively). EAE DRG had significantly more BDNF positive neurons compared to AC DRG at both 12 and 15 dpi ($p=0.0031$ and 0.0149 respectively). A sub-analysis of the BDNF positive neurons identified significant changes in cell sizes across the three groups (**Figure 2c**). The mean cell size of BDNF positive neurons in AC9 DRG is significantly larger than in NC DRG ($31.93 \pm 5.50 \mu\text{m}$ compared to $26.55 \pm 3.82 \mu\text{m}$; $p<0.0001$). There is no significant difference in mean cell sizes between any of the AC DRG at 9, 12 or 15 dpi (31.93 ± 5.50 , 31.46 ± 6.65 , and $28.83 \pm 6.47 \mu\text{m}$ respectively). The cell sizes are significantly larger in EAE DRG compared to AC DRG at all-time points assayed (34.97 ± 7.79 , 40.05 ± 8.96 , and $35.09 \pm 7.01 \mu\text{m}$ at 9, 12 and 15 dpi respectively). Thus, by 9 dpi, the mean BDNF positive cell size is significantly increased in EAE animals compared to AC animals ($p=0.0091$). At 12 dpi,

the mean cell sizes are highly significantly different between EAE and AC animals ($p=0.0001$). At 15 dpi, the BDNF positive cell sizes are also highly significantly different ($p=0.0001$). In order to assess potential changes in cell type expressing BDNF, we compared the location of BDNF positive cells in NC DRG to those in the DRG of EAE 12. We found in EAE 12 DRG that BDNF was expressed by small to medium DRG neurons in similar stereological locations to the BDNF positive cells in the NC DRG. In addition, we also saw BDNF expression in medium to large size neurons located in different regions from those seen in the NC DRG (**Figure 2d**). Our results show that there are more BDNF expressing medium size neurons in the EAE DRG than in the NC group. Thus, these data reveal a change in the cell type expressing BDNF, from predominantly small neurons ($<30\ \mu\text{m}$), to predominantly medium diameter sensory neurons ($30\text{-}50\ \mu\text{m}$). This corresponds to C and A γ fibers respectively.

3.5.3 ENZYME LINKED IMMUNOSORBENT ASSAY ANALYSIS OF BDNF PROTEIN EXPRESSION IN THE DRG

The values for the BDNF expression in the lumbar DRG are presented as the absolute quantity of BDNF per μg of total protein. Levels in NC DRG were $0.599 \pm 0.044\ \text{pg}/\mu\text{g}$ total protein. AC DRG levels of BDNF were significantly higher ($p=0.0004$) at 0.915 ± 0.012 , 0.951 ± 0.089 and $1.014 \pm 0.023\ \text{pg}/\mu\text{g}$ total protein for 9, 12 and 15 dpi respectively. BDNF levels in day 9 EAE DRG were not significantly different from AC 9 dpi at $1.007 \pm 0.053\ \text{pg}/\mu\text{g}$ total protein, nor were BDNF levels in day 15 EAE DRG different from AC 15 dpi ($1.073 \pm 0.022\ \text{pg}/\mu\text{g}$ total protein). However, at 12 dpi in the EAE DRG, BDNF levels were significantly increased compared to AC day 12 DRG, at $1.371 \pm 0.039\ \text{pg}/\mu\text{g}$ total protein compared to $0.951 \pm 0.089\ \text{pg}/\mu\text{g}$ total protein ($p=0.0049$) see **Figure 3a**.

3.5.6 BDNF GENE EXPRESSION ANALYSIS IN THE DRG

Real time reverse transcription polymerase chain reaction (qRT-PCR) analysis was conducted on DRG from all lumbar, thoracic and cervical regions of the spinal column from the three experimental groups, at the pre-determined experimental time points. The BDNF mRNA expression was assessed in parallel with that of the housekeeping gene Glyceraldehyde-3-phosphate dehydrogenase (GAPDH). The mRNA expression for BDNF within the DRG obtained from the three experimental groups revealed peak expression in the EAE group at 12 dpi compared to all other experimental groups (**Figure 3b**). Specifically, mRNA in EAE 12 dpi is significantly higher than other groups (NC and AC) ($p=0.0493$).

3.5.7 BDNF PROTEIN AND GENE EXPRESSION IN THE SPINAL CORD

IHC analysis for BDNF protein expression in the spinal cord reveals marked increases in immunoreactivity in the dorsal horn of the active EAE spinal cord at 12 dpi, compared to AC and NC animals (**Figure 4a**). The increased levels of BDNF immunoreactivity in AC animals relative to the NC is expected as there is a significant immune response resulting from the Freund's adjuvant, MT and PT injections. ELISA analysis of BDNF expression was conducted on spinal cord of animals at 9, 12 and 15 dpi. NC spinal cord contained 0.63 ± 0.06 pg/ μ g total protein. AC rats at 9, 12 and 15 dpi showed a significantly increased level of BDNF compared to NC at 0.92 ± 0.012 ; 0.97 ± 0.056 ; 1.01 ± 0.023 pg/ μ g total protein respectively ($p>0.01$) (**Figure 4b**). EAE animals showed a significant increase ($p=0.0195$) in BDNF expression in the caudal spinal cord at 12 dpi at 1.41 ± 0.016 pg/ μ g total protein compared to days 9 and 12 at $.01 \pm 0.05$ and 1.07 ± 0.02 pg/ μ g total protein respectively (**Figure 4b**). The qRT-PCR analysis of gene

expression changes revealed no significant differences in BDNF mRNA in the spinal cord of any of the groups across all time points studied (**Figure 4c**).

3.5.8 BDNF PROTEIN EXPRESSION IN THE DORSAL ROOTS

Based on our model of MS induction [20], we hypothesized that BDNF expression is induced in the DRG and translocated to the dorsal horn along the dorsal roots. To test our hypothesis we assessed the presence of BDNF in the dorsal root in the EAE animals. We show markedly increased BDNF immunoreactivity in the dorsal roots of active EAE animals compared to NC (**Figure 5a**). Several previous studies have shown that BDNF is anterogradely transported in vesicles, from the neuronal cell body along the axon to the synapse [27, 28]. Vesicles are moved around in the cell along the cytoskeleton, controlled by motor proteins, the kinesin and dynein protein families [29]. Kinesin has been shown to regulate the anterograde transport of BDNF from the neuronal cell body to the synapse [30, 31]. We demonstrate anterograde transport of BDNF along the dorsal roots, using co-localization of BDNF with the motor protein kinesin [30]. Kinesin-BDNF double immunohistochemistry showed co-localization of the two proteins throughout the dorsal root, and dorsal root entry zone, which indicates that BDNF is anterogradely transported to dorsal horn from DRG (**Figure 5B**).

3.6 DISCUSSION

The current study was designed to test our hypothesis that BDNF expression is up-regulated in the DRG and spinal cord in the EAE model of MS. We used MBP to induce EAE in Lewis rat as our research was focused on the early antigenic induction of inflammation rather than the chronic

demyelination aspects of the disease [32]. In this study we show a direct correlation between antigenic immune activation and increased expression of BDNF, at both the gene and protein level within DRG, which peaks at 12 dpi in correlation with peak neurological disability [20]. Further, we show peak BDNF levels in spinal cord at day 12, with maintenance of increased levels at day 15, in contrast to DRG levels, which return to normal by day 15. Our results indicate that medium sized sensory neurons of the DRG represent the principle source of BDNF production, and that this BDNF is anterogradely transported from DRG along the roots to the dorsal horn.

The death of oligodendrocytes and subsequent demyelination of the brain and spinal cord, which characterize MS, occur as a direct result of T-cell activation [3]. We have previously shown activation of DRG neurons in the inflammatory stage of EAE, with increased expression of the proinflammatory cytokine TNF α [20]. This lead to the hypothesis that DRG neurons are a primary source of inflammatory mediators in the very early stages of neuroinflammatory disorders such as MS [20]. Although the exact molecular events underlying the pathophysiology of MS remain unclear, immunomodulatory therapies have proven effective for some MS patients [5]. One such therapy is glatiramer acetate (GA) [33]. While the mechanism of action of GA is unknown, studies have shown that GA-active T-cells produce a significantly increased level of BDNF, which is directly neuroprotective and/or neuroregenerative [19, 34]. Although GA-specific Th1, Th2 and Th0 cells are all involved in BDNF production, larger *in vitro* studies have suggested that Th2 cells play a predominant role in GA modulation of RRMS [19, 35]. Further evidence of a role for BDNF in MS comes from a study showing that BDNF treatment has a beneficial effect on disease progression in EAE [36, 37]. Thus BDNF may play a significant role in the induction and progression of neuronal and oligodendrocyte damage. Our study provides

evidence that BDNF expression is upregulated in the early inflammatory stage of neuroinflammation. In addition, we show that BDNF levels are maintained in the spinal cord after amelioration of neurological symptoms, suggesting a role for BDNF in the prevention of immediate cell damage resulting from the initial inflammation. Further longitudinal studies are required to clarify the role of BDNF in neuroprotection in the later, demyelinating stages of disease progression.

In order to characterize the specific cellular source of the BDNF protein, we used cell soma size to identify the sensory neuron subtypes present in the DRG. Our results show that medium diameter (30-50 μm : A γ) sensory neurons appear to be the predominant source of BDNF in the EAE DRG. Further, it appears that the specific location of the BDNF positive cells indicates that the cellular source of BDNF in the EAE DRG is changing from the small C fibers, to the medium A γ fibers. Based on Aoki's paper in 2004, the neurons on the outer edge of the DRG are the small NGF dependent (substance P and CGRP expressing) nociceptive neurons, which are critical for inflammatory hyperalgesia [38]. This cellular source differs from the source of TNF α in the EAE DRG, which is predominantly produced by small diameter (<30 μm : C) neurons [20]. Interestingly, BDNF enhances the excitability of small diameter neurons, and potentiates their action potential firing, via p75^{NTR} signaling [39]. A study using CFA injection into the rat paw to initiate a pain response showed TrkB, the high affinity BDNF receptor, expression in medium to large sensory neurons of the lumbar DRG, and expression of the low affinity BDNF receptor, p75^{NTR} in the small diameter neurons [39]. Further, microglia activated by peripheral nerve injury secretes high levels of BDNF, which subsequently results in the development of neuropathic pain [40]. Further studies are required to identify the BDNF responsive cells in the DRG of the EAE model.

Neurotrophins and cytokines interact to co-regulate their expression in inflammatory states [41, 42]. For example, TNF α induces the expression of BDNF expression in astrocytes and neurons [41, 42]. Based on our established model [20], we hypothesize that BDNF works in concert with cytokines such as TNF α and other neurotrophins, such as NGF, to regulate cellular effects on myelin [41,43]. The current study, in conjunction with our previously published studies [20, 22], provides support for the importance of cytokine - neurotrophin interactions in the induction of neuroinflammatory disorders.

Anterograde and retrograde transport of neurotrophins are known to occur between the DRG and spinal cord [44]. We show evidence for the active transport of BDNF from the DRG to the dorsal root entry zone, via kinesin mediated anterograde transport. Kinesin is a dimeric molecule that attaches to protein filled vesicles, and walks towards the plus end of a microtubule, transporting the proteins to the synapse. This form of transport is known as anterograde transport. Vesicular transport is the fastest mechanism of transporting proteins at 50-400 mm/day compared to the slower transport of proteins, at less than 8 mm/day [29]. This provides a plausible explanation for the increase in BDNF protein seen in the dorsal horn, even though levels of BDNF mRNA are not increased. This corroborates previous studies showing anterograde transport of BDNF along microtubules via transport vesicles [45]. Our results are also consistent with other studies that have shown transport of TNF α and BDNF in rodent models of nerve injury [22, 44].

Since BDNF is known to affect myelin function [46], it is possible that DRG derived BDNF contributes to the recovery of the inflammatory damage to myelin that has been shown in previous studies [6]. This potential mechanism of disease induction expands the potential for targeted strategies aimed at attenuating white matter disorders such as MS. One caveat to this therapeutic strategy is the potential for the development of pain, as previous studies have shown

that elevated BDNF in the dorsal horn correlates with the development of pain [47]. In addition, we have shown the induction of pain in this model of neuroinflammation, associated with the peak neurological disability (MacNeil, Begum et al., unpublished observations)

3.7 SUMMARY

Our study offers new insights into the role of the DRG derived BDNF in the inflammatory response preceding myelin damage in the early stages of MS. We demonstrate significantly increased BDNF gene and protein levels in the DRG correlating with peak neurological disability. In addition, we show increased BDNF protein levels in the dorsal horn without an increase in mRNA levels, which suggests that BDNF is transported into, rather than synthesized in, the dorsal horn. We show that medium diameter DRG sensory neurons are an important source of BDNF, which is anterogradely transported to the spinal cord during the early stage of autoimmune induced neuroinflammation. Further, our findings provide support for the immune activation of the DRG as a critical step in the development of myelin disorders of the CNS. This is the first study to identify changes in BDNF expression and transport in the early inflammatory stages of neuroimmune induction.

Acknowledgements - We would like to thank Elizabeth Tran, Samantha Kendall, Jeremy Paterson, Joumana Mustapha and Kim Madec for technical assistance. We would also like to thank our funding & supporting agencies: Biogen Idec Canada Inc (MN & EEF), Manitoba Medical Services Foundation (EEF & MN), Manitoba Institute of Child Health (MN & EEF), Manitoba Health Research Council (EEF), Pfizer UK Global (MN & EEF), and Purdue Pharma

(MN & EEF). WZ was the recipient of a Canada Millennium Scholarship Foundation award. PV and FB were recipients of MHRC Studentships. WZ, FB, BM, PP and PV performed the research. WZ, BM and EEF analyzed the data. EEF wrote the paper. MN and EEF designed the research study.

Conflict of Interest Statement

The authors confirm that there are no conflicts of interest.

3.8 REFERENCES

1. Namaka MP, Ethans K, Jensen B, *et al.* Multiple Sclerosis. Therapeutic Choices/e-Therapeutic. Ottawa: Canadian Pharmacists Association Publishers, Inc, 2011. pp. 309-19
2. Bar-Or A. The immunology of multiple sclerosis. *Semin Neurol.* 2008; 28: 29-45.
3. Codarri L, Fontana A, Becher B. Cytokine networks in multiple sclerosis: lost intranotation. *Curr Opin Neurol.* 2010; 23: 205-11.
4. Zhu W, Le Dorze JA, Prout M, *et al.* An Overview of Relapsing Remitting Multiple Sclerosis (RRMS) and Current Treatment Options. *Pharmacy Practice* 2010; 9.
5. Namaka M, Leong C, Prout M, *et al.* Emerging Therapies for the Management of Multiple Sclerosis. *Clinical Medicine Insights: Therapeutics.* 2010; 2: 1-13.
6. De Santi L, Annunziata P, Sessa E, Bramanti P. Brain-derived neurotrophic factor and TrkB receptor in experimental autoimmune encephalomyelitis and multiple sclerosis. *J Neurol Sci.* 2009; 287: 17-26.
7. Linker R, Gold R, Luhder F. Function of neurotrophic factors beyond the nervous system: inflammation and autoimmune demyelination. *Crit Rev Immunol.* 2009; 29: 43-68.
8. Azoulay D, Urshansky N, Karni A. Low and dysregulated BDNF secretion from immune cells of MS patients is related to reduced neuroprotection. *J Neuroimmunol.* 2008; 195: 186-93.
9. Azoulay D, Vachapova V, Shihman B, *et al.* Lower brain-derived neurotrophic factor in serum of relapsing remitting MS: reversal by glatiramer acetate. *J Neuroimmunol.* 2005; 167:215-18.
10. Leibrock J, Lottspeich F, Hohn A, *et al.* Molecular cloning and expression of brain-derived neurotrophic factor. *Nature.* 1989; 341: 149-52.

11. Djalali S, Holtje M, Grosse G, *et al.* Effects of brain-derived neurotrophic factor (BDNF) on glial cells and serotonergic neurones during development. *Journal of Neurochemistry*. 2005; 92: 616-27.
12. Lykissas MG, Batistatou AK, Charalabopoulos KA, Beris AE. The role of neurotrophins in axonal growth, guidance, and regeneration. *Curr Neurovasc Res*. 2007; 4: 143-51.
13. Cunha C, Brambilla R, Thomas KL. A simple role for BDNF in learning and memory? *Front Mol Neurosci*. 2010; 3: 1. 18
14. Nishimura K, Nakamura K, Anitha A, *et al.* Genetic analyses of the brain-derived neurotrophic factor (BDNF) gene in autism. *Biochemical and Biophysical Research Communications*. 2007; 356: 200-6.
15. Stadelmann C, Kerschenstainer M, Misgeld T, *et al.* BDNF and gp145trkB in multiple sclerosis brain lesions. *Brain*. 2002; 125: 75-85.
16. Brandes DW. The role of glatiramer acetate in the early treatment of multiple sclerosis. *Neuropsychiatr Dis Treat*. 2010; 6: 329-36.
17. Kala M, Miravalle A, Vollmer T. Recent insights into the mechanism of action of glatiramer acetate. *J Neuroimmunol*. 2011; 235: 9-17.
18. Arnon R, Aharoni R. Neuroprotection and neurogeneration in MS and its animal model EAE effected by glatiramer acetate. *J Neural Transm*. 2009; 116: 1443-49.
19. Ziemssen T, Kumpfel T, Klinkert WE, *et al.* Glatiramer acetate-specific T-helper 1- and 2-type cell lines produce BDNF: implications for multiple sclerosis therapy. Brain-derived neurotrophic factor. *Brain*. 2002; 125: 2381-91.

20. Melanson M, Miao P, Eisenstat D, *et al.* Experimental autoimmune encephalomyelitis induced upregulation of tumor necrosis factor-alpha in the dorsal root ganglia. *Mult Scler.* 2009; 15: 1135-45.
21. Begum F, Zhu W, Namaka MP, Frost EE. A novel decalcification method for adult rodent bone for histological analysis of peripheral-central nervous system connections. *Journal of Neuroscience Methods.* 2010; 187: 59-66.
22. Miao P, Madec K, Gong Y, *et al.* Axotomy-induced up-regulation of tumor necrosis factor alpha in the dorsal root ganglia. *Neurol Res.* 2008; 30: 623-31.
23. Bradford MM. A rapid and sensitive method for the quantitation of microgram quantities of protein utilizing the principle of protein-dye binding. *Anal Biochem.* 1976; 72: 248-54.
24. Chadwick W, Magnus T, Martin B, *et al.* Targeting TNF-alpha receptors for neurotherapeutics. *Trends Neurosci.* 2008; 31: 504-11.
25. Grimm JW, Lu L, Hayashi T, *et al.* Time-dependent increases in brain-derived neurotrophic factor protein levels within the mesolimbic dopamine system after withdrawal from cocaine: implications for incubation of cocaine craving. *J Neurosci.* 2003; 23: 742-47.
26. Mix E, Meyer-Rienecker H, Zettl U. Animal models of multiple sclerosis for the development and validation of novel therapies – potential and limitations. *Journal of Neurology.* 2008; 255: 7-14.
27. Von Bartheld CS, Wang X, Butowt R. Anterograde axonal transport, transcytosis, and recycling of neurotrophic factors: the concept of trophic currencies in neural networks. *Mol Neurobiol.* 2001; 24: 1-28.

28. Gauthier LR, Charrin BC, Borrell-Pages M, *et al.* Huntingtin controls neurotrophic support and survival of neurons by enhancing BDNF vesicular transport along microtubules. *Cell*. 2004; 118: 127-38.
29. Caviston JP, Holzbaur EL. Microtubule motors at the intersection of trafficking and transport. *Trends Cell Biol*. 2006; 16: 530-37.
30. Miki H, Okada Y, Hirokawa N. Analysis of the kinesin superfamily: insights into structure and function. *Trends Cell Biol*. 2005; 15: 467-76.
31. Park JJ, Cawley NX, Loh YP. A bi-directional carboxypeptidase E-driven transport mechanism controls BDNF vesicle homeostasis in hippocampal neurons. *Mol Cell Neurosci*. 2008; 39: 63-73.
32. Mannie M, Swanborg RH, Stepaniak JA. Experimental Autoimmune Encephalomyelitis in the rat. *Current Protocols in Immunology*. 2009; 15: 15.2.
33. Skihar V, Silva C, Chojnacki A, *et al.* Promoting oligodendrogenesis and myelin repair using the multiple sclerosis medication glatiramer acetate. *Proc Natl Acad Sci U S A*. 2009; 106: 17992-97.
34. Lalive PH, Neuhaus O, Benkhoucha M, *et al.* Glatiramer acetate in the treatment of multiple sclerosis: emerging concepts regarding its mechanism of action. *CNS Drugs*. 2011; 25: 401-14.
35. La Mantia L, Munari LM, Lovati R. Glatiramer acetate for multiple sclerosis. *Cochrane Database Syst Rev*. 2010; 5: CD004678.
36. Makar TK, Bever CT, Singh IS, *et al.* Brain-derived neurotrophic factor gene delivery in an animal model of multiple sclerosis using bone marrow stem cells as a vehicle. *J Neuroimmunol*. 2009; 210: 40-51.

37. Makar TK, Trisler D, Eglitis MA, *et al.* Brain-derived neurotrophic factor (BDNF) gene delivery into the CNS using bone marrow cells as vehicles in mice. *Neurosci Lett.* 2004; 356: 215-19.
38. Woolf CJ, Allchorne A, Safieh-Garabedian B, Poole S. Cytokines, nerve growth factor and inflammatory hyperalgesia: the contribution of tumour necrosis factor alpha. *Br J Pharmacol.* 1997; 121: 417-24.
39. Zhang YH, Chi XX, Nicol GD. Brain-derived neurotrophic factor enhances the excitability of rat sensory neurons through activation of the p75 neurotrophin receptor and the sphingo myelin pathway. *J Physiol.* 2008; 586: 3113-27
40. Coull JAM, Beggs S, Boudreau D, *et al.* BDNF from microglia causes the shift in neuronal anion gradient underlying neuropathic pain. *Nature.* 2005; 438: 1017-21.
41. Aloe L, Properzi F, Probert L, *et al.* Learning abilities, NGF and BDNF brain levels in two lines of TNF-alpha transgenic mice, one characterized by neurological disorders, the other phenotypically normal. *Brain Res.* 1999; 840: 125-37.
42. Saha R, Liu X, Pahan K. Up-regulation of BDNF in Astrocytes by TNF- α : A Case for the Neuroprotective Role of Cytokine. *Journal of Neuroimmune Pharmacology.* 2006; 1: 212-22.
43. Takei Y, Laskey R. Tumor Necrosis Factor alpha Regulates Responses to Nerve Growth Factor, Promoting Neural Cell Survival but Suppressing Differentiation of Neuroblastoma Cells. *Mol Biol Cell.* 2008; 19: 855-64.
44. Zweifel LS, Kuruvilla R, Ginty DD. Functions and mechanisms of retrograde neurotrophin signalling. *Nat Rev Neurosci.* 2005; 6: 615-25.
45. Altar CA, DiStefano PS. Neurotrophin trafficking by anterograde transport. *Trends Neurosci.* 1998; 21: 433-37.

46. McTigue DM, Horner PJ, Stokes BT, Gage FH. Neurotrophin-3 and Brain-Derived Neurotrophic Factor Induce Oligodendrocyte Proliferation and Myelination of Regenerating Axons in the Contused Adult Rat Spinal Cord. *J Neurosci*. 1998; 18: 5354-65.
47. Merighi A, Salio C, Ghirri A, BDNF as a pain modulator. *Progress in Neurobiology*. 2008; 85: 297-317.

3.9 FIGURES

Figure 1: Neurological Disability Score for EAE animals induced to a state of MS.

Disability scores range from a mean clinical disability score of 0 (no disability) to 15 (maximum disability). The bell shaped distribution outlining peak neurological disability in response to EAE induction occurred at day 12 post-EAE induction. Neurological disability is scored according to the following criteria: Tail: 0 = normal; 1 = partially paralyzed, weakness; 2 = completely paralyzed, Bladder: 0 = normal; 1 = incontinence: limp: Right hind limb: 0 = normal; 1 = weakness; 2 = dragging with partial paralysis; 3 = complete paralysis: Left hind limb: 0 = normal; 1 = weakness; 2 = dragging with partial paralysis; 3 = complete paralysis: Right forelimb: 0 = normal; 1 = weakness; 2 = dragging, not able to support weight; 3 = complete paralysis: Left forelimb: 0 = normal; 1 = weakness; 2 = dragging, not able to support weight; 3 = complete paralysis:

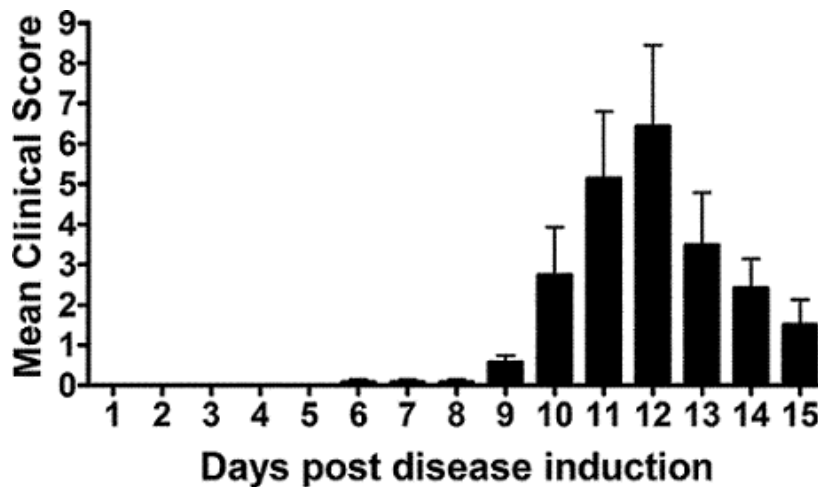


Figure 2 (a) BDNF immunoreactivity in rat DRG. Images shown depict BDNF label (red) colocalised with NeuN (green) in active EAE, active control and naïve animals. 10 µm sections of DRG were stained with BDNF (R&D Systems Minneapolis, MN). Marked elevations in BDNF labeling were noted in the active EAE animal group at day 12 relative to all other treatment groups. Images were taken at a total magnification of 10x and were exposed for 810 msec, Bar = 50 µm. Dpi = days post induction of EAE. **(b) Percentage of BDNF positive (+) sensory DRG neurons compared to total neurons found within some groups at the various experimental time points.** Significantly increased proportions of BDNF +ve sensory neurons were identified in the active EAE group, which peaks at 12 dpi (**=p<0.005; *=p<0.05, ANOVA followed by Students *t*-test). **(c) Analysis of size of the BDNF positive neurons in DRG.** Analysis of the size of BDNF +ve neurons obtained from the active EAE group reveals a change in the cell size distribution from small to predominantly medium diameter (<30µm) sensory neurons which corresponds to C and A γ fibers respectively (*= p<0.05, ***=p<0.001, ANOVA with Tukey's post test, Student's *t*-test was used to assess differences between the means). NC=Naïve control; AC=Active control; 9, 12 and 15 stand for rat sacrificed date. **(d) Comparison of BDNF positive neurons in different area of DRG** Analysis of the size and location of BDNF +ve neurons obtained from the active EAE group reveals there are more BDNF +ve neurons with larger size in different area from NC group.

Figure 2a

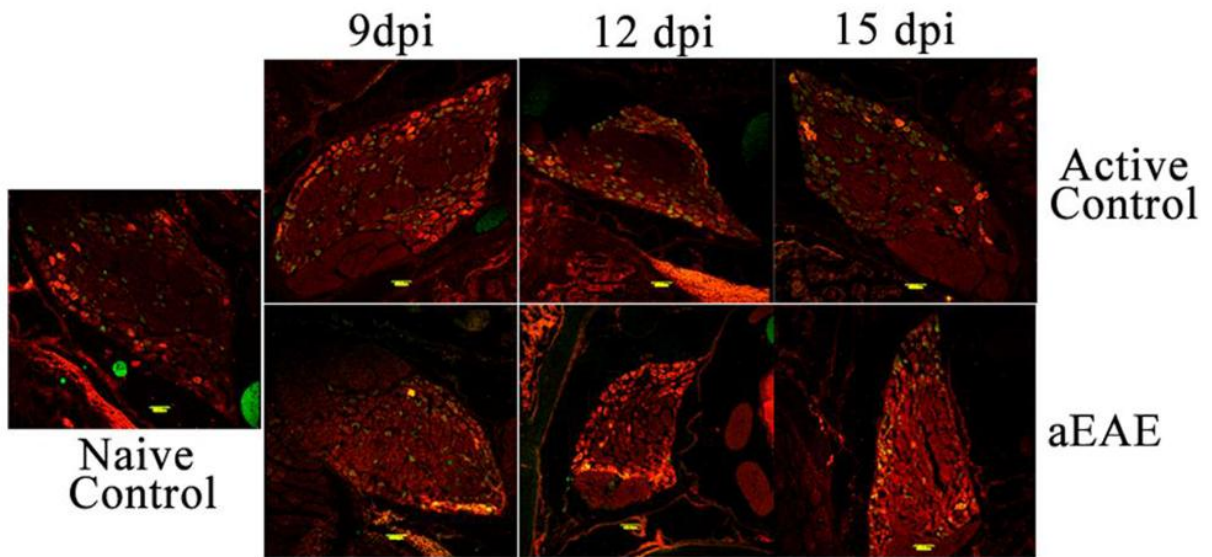


Figure 2b

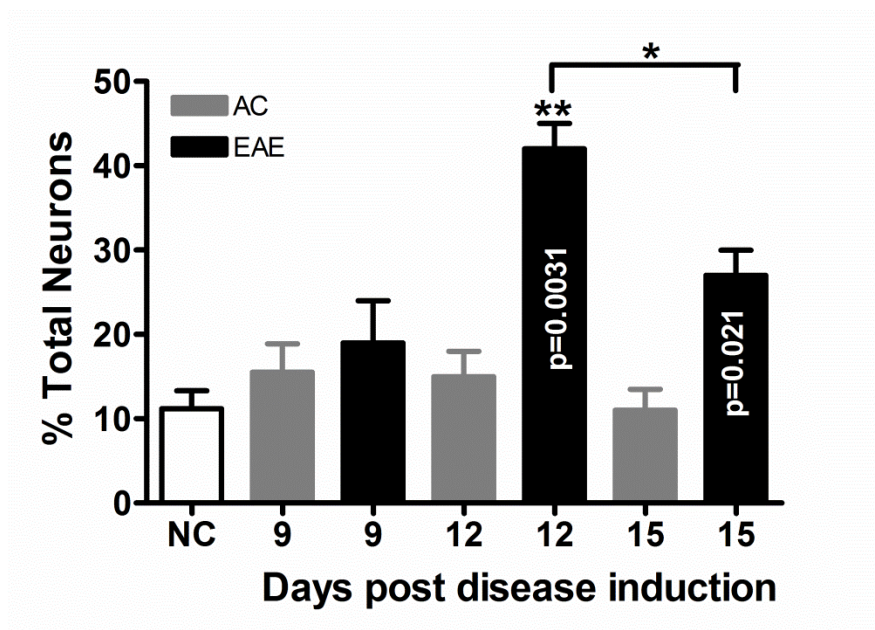


Figure 2c

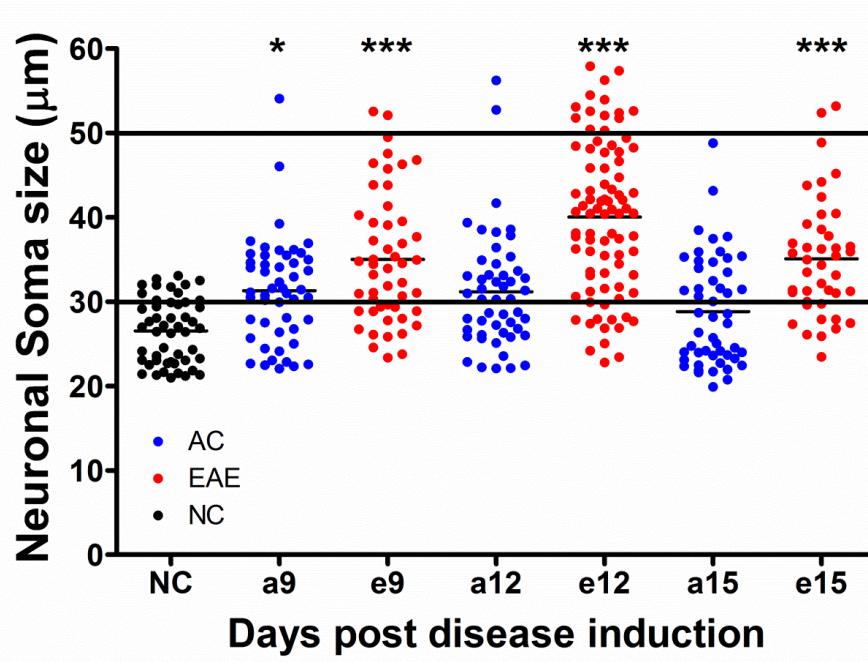


Figure 2d

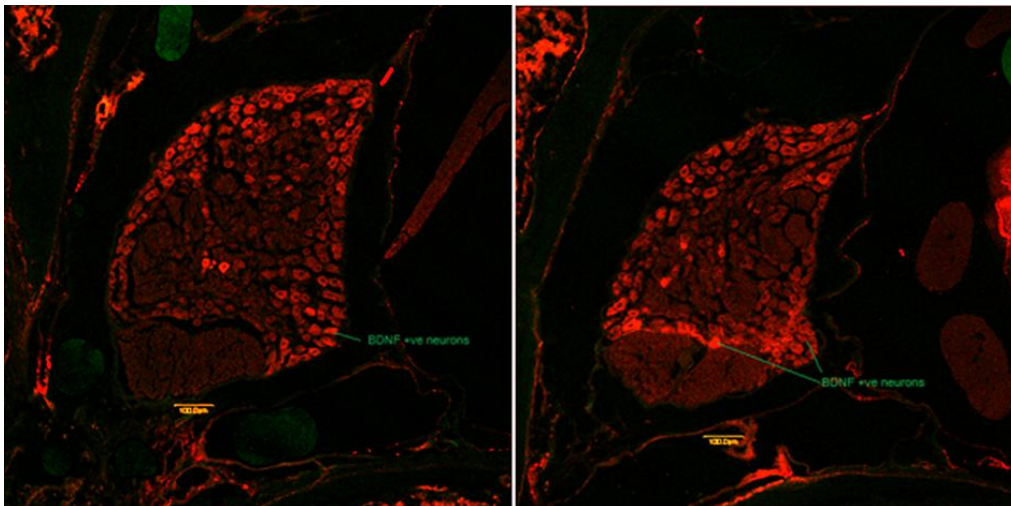


Figure 3 (a) ELISA quantification of BDNF expression in the DRG. BDNF expression in the lumbar DRG was quantified using ELISA. Rats induced to a state of EAE show significantly increased BDNF expression compared to NC animals (**= $p < 0.005$; ***= $p < 0.001$, ANOVA followed by Student's *t*-test). Results are shown as pg/ml BDNF/ μ g total protein. (b) Real-time RT-PCR results of BDNF expression within DRG. The BDNF mRNA expression of DRG for animals of the active EAE group (red bars), euthanized at day 12 is significantly higher than other groups (naive control (blue bar) and active control (green bars)) (*= $p = 0.049$) with a one way ANOVA and Tukey's post test based on two factors (day and group) using software SPSS 16.0.

Figure 3a

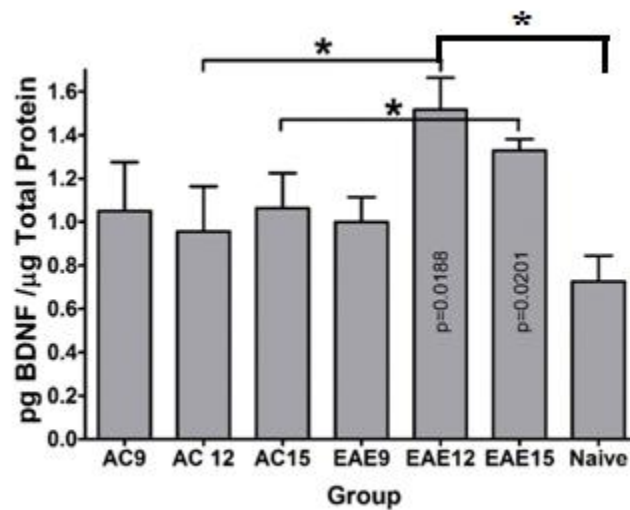


Figure 3b

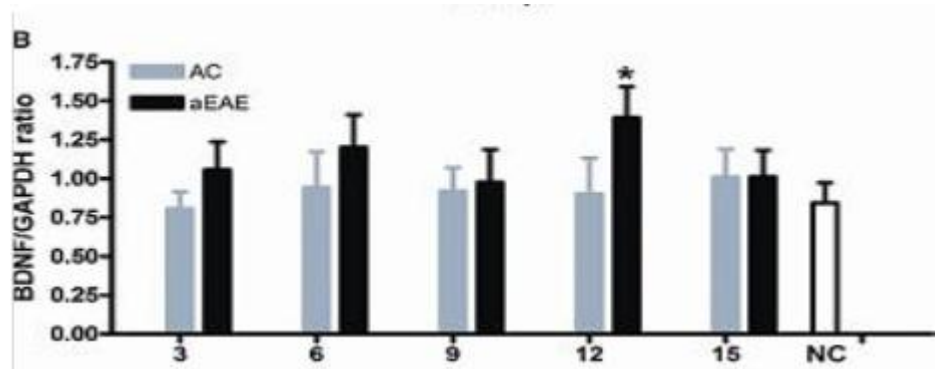


Figure 4 (a) BDNF immunoreactivity in spinal cord. Comparative IHC analysis of 10 μ m sections of spinal cord showed markedly increased BDNF immunoreactivity at active EAE 12 dpi relative to active control. Active control spinal cord also shows increased BDNF immunoreactivity at 12 dpi, however, by 15 dpi, immunoreactivity is markedly reduced compared to active EAE spinal cord. Reticulocyte staining shows clearly in the dura of the active EAE spinal cord (arrow head). All images were taken at a total magnification of 100X and were exposed for 764 msec with BDNF positive cells brightly labeled with red. Bar=100 μ m. (b) ELISA quantification of BDNF expression in the spinal cord. BDNF expression in the lumbar DRG was quantified using ELISA. Rats induced to a state of EAE show significantly increased BDNF expression compared to NC animals ($*=p<0.05$). Results are shown as pg/ml BDNF/ μ g total protein. (c) Real-time RT-PCR results of BDNF expression within spinal cord. The BDNF mRNA expression of spinal cord for animals of the active EAE group (grey bars), at 12 dpi, is higher than other groups with an increasing trend (naive control (white bar) and active control (black bars)) ($*=p>0.05$) with a one way ANOVA and Tukey's post test based on two factors (day and group) using software SPSS 16.0.

Figure 4a

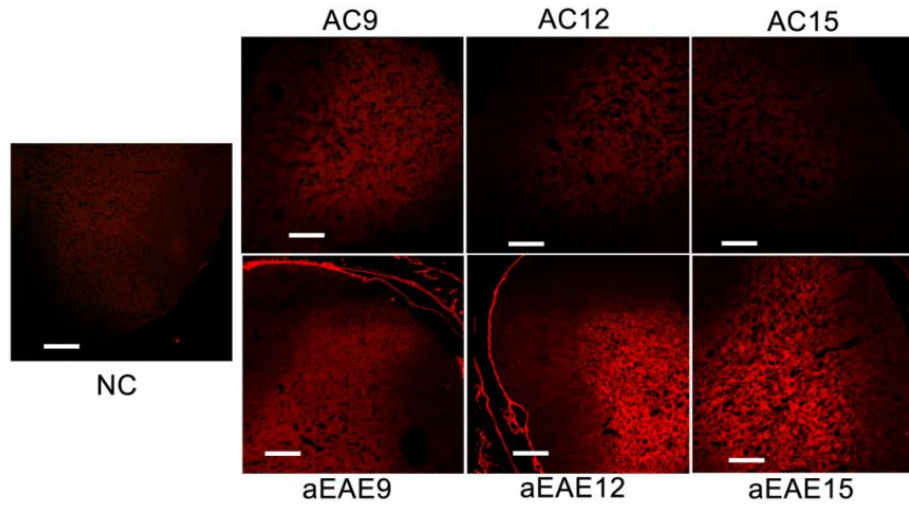


Figure 4b

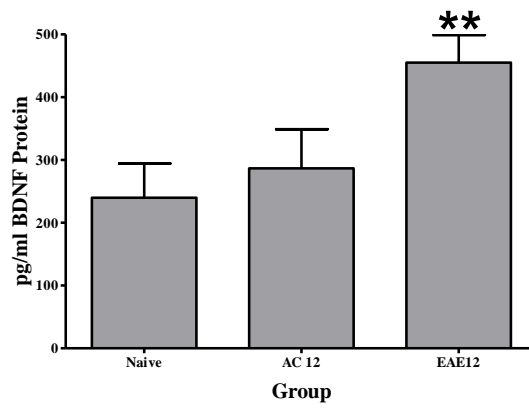


Figure 4c

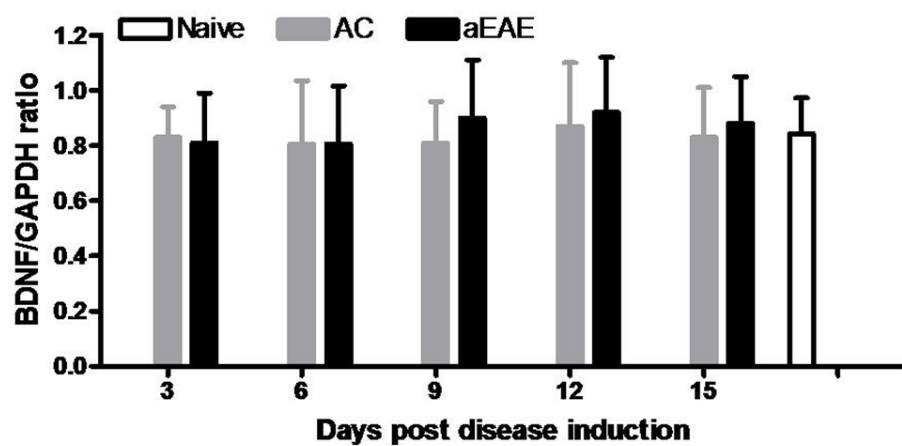


Figure 5 (a) BDNF Immunoreactivity in the dorsal roots. Representative sections of dorsal root entry zones from the lumbar spinal cord of Lewis rats induced to a state of EAE. A marked increase in BDNF immunoreactivity (red) is seen in the dorsal roots of active EAE compared to active control animals and NC animals. *Panel A* – Naïve animals have no BDNF immunoreactivity in the dorsal roots (DR). *Panel B* – Active control animals have noticeable BDNF immunoreactivity in the satellite cells of the dorsal root, and in the grey matter of the dorsal horn, *Panel C* – Active EAE animals appear to have increased levels of BDNF immunoreactivity in the satellite cells of the dorsal root, as identified as small brightly stained cell surrounding the axons of the root. In addition, there is a marked increase in punctuate staining in the length of the roots. Further, the grey matter of the dorsal horn has a markedly increased immunoreactivity compared to the active control animals. DR = Dorsal root, SC = spinal cord. Bar = 10 μ m. (b) Anterograde transport of BDNF along the dorsal root is mediated by kinesin. Double immunolabeling of frozen sections of EAE spinal cord shows BDNF (red) co-localized to the motor protein kinesin (red) (arrow). Kinesin is distributed throughout the dorsal root (DR) and spinal cord (SC). BDNF immunoreactivity is markedly higher in the dorsal root entry zone than the root. Co-labeling shows as yellow. Bar = 10 μ m

Figure 5a

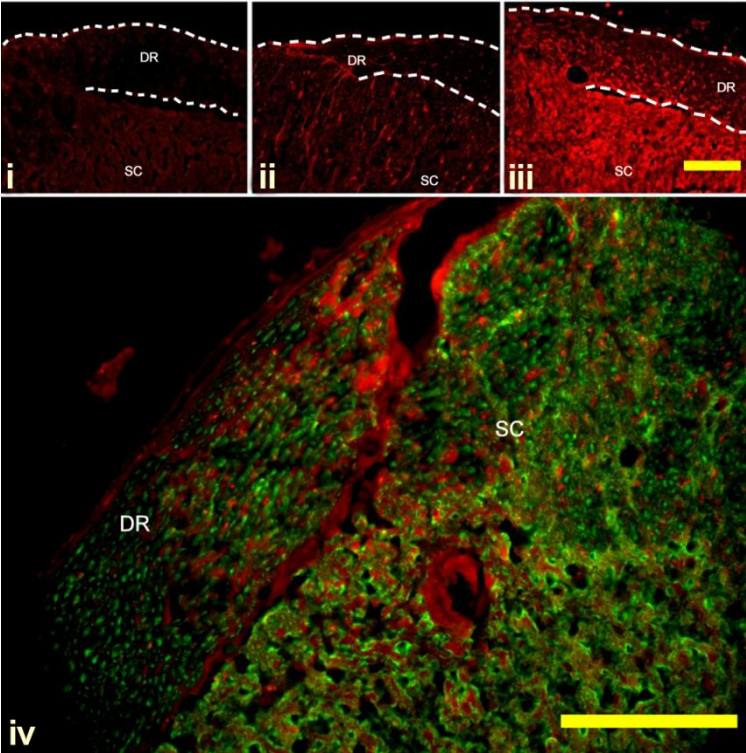
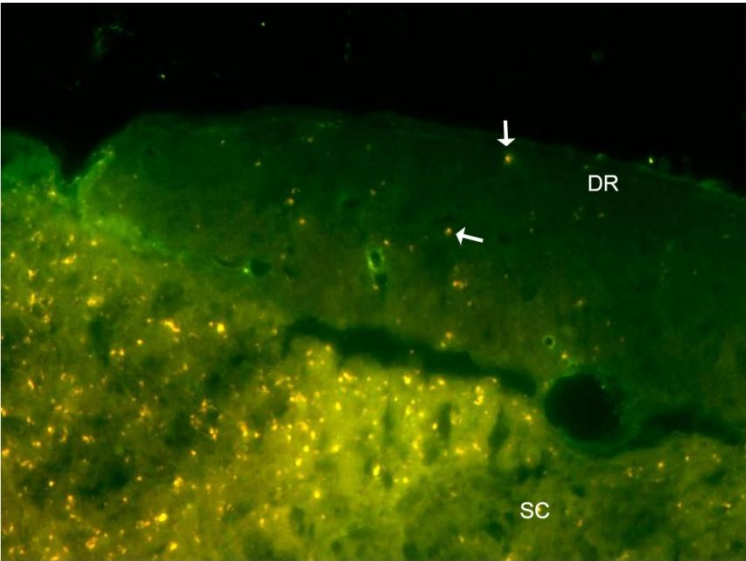


Figure 5b



CHAPTER 4 – THE IDENTIFICATION OF BDNF RESPONSIVE CELLS IN SPINAL CORD FROM AN EAE ANIMAL MODEL OF MS

Authors and affiliations:

Wenjun Zhu¹, Crystal Acosta¹, Brian Macneil², Emma Frost^{1*}, Mike Namaka¹

1. Faculty of Pharmacy, University of Manitoba, Winnipeg, Manitoba, Canada 2. Medical Rehabilitation, University of Manitoba, Winnipeg, Manitoba, Canada

This manuscript was submitted to International Journal of Molecular Sciences in May 2012 .

4.1 STATEMENT OF CONTRIBUTION

For this study, I was responsible for the experimental design, induction of the EAE rats (including neurological disability testing, sacrifice, harvesting and preparation of tissue for analysis), and completion of immunohistochemistry, Western blot, real-time RT-PCR, writing the manuscript and preparing for submission. In addition, I supervised the other graduate student (Crystal Acosta) as she assisted with the RT-PCR analysis.

4.2 ABSTRACT

Multiple sclerosis (MS) is a chronic inflammatory autoimmune disease in the central nervous system (CNS), which is characterised by demyelination. The exact pathophysiology of MS is still unknown but it is associated with infiltration of T-cells, activation of glia cells that result in axonal and subsequent neuronal damage. The proposed role for brain derived neurotrophic factor (BDNF) and its receptor tropomyosin-related kinase receptor (TrkB) in the myelin repair and

neuroprotection places this neurotrophin in a potentially strategic position in regard to the pathological events of MS. In this study, we used the experimental autoimmune encephalomyelitis (EAE) rat model of MS determine the role of BDNF in the early stage of MS. Protein and gene expression analysis were through Western blot and real time RT-PCR respectively. Significant increases in protein expression of TrkB was shown in the spinal cord in the EAE rats at 12 day post induction relative to controls, which correlates with peak neurological disability. The up-regulated expression of TrkB and identifications of specific BDNF responsive cells within spinal cord may represent a critical link to promising therapeutic treatment for inflammatory and demyelinating diseases such as MS.

Keywords: MS; EAE; TrkB; BDNF; myelin repair

4.3 INTRODUCTION

Multiple sclerosis (MS) is a chronic inflammatory disease of the central nervous system (CNS) [1]. Active T-cells infiltrating the CNS cause myelin disruption and axonal damage [2]. Demyelination and neuronal loss represent the main pathological features of MS [3, 4]. Current therapeutic intervention in MS involves treatment of inflammation and the prevention of demyelination due to oligodendrocyte death and axonal loss [5]. The current treatments of MS

including immunomodulation and immunosuppression do control inflammation, but the desire to reduce the disability progression has spurred research on alternative therapeutic strategies such as remyelination and neuroprotection [5]. One promising candidate is brain-derived neurotrophic factor (BDNF), which is a potent neurotrophin that promotes axonal growth and neuronal survival [6]. Several studies have shown a role for BDNF in oligodendrocyte development *in vivo*. Specifically, BDNF induces oligodendrocyte progenitor proliferation [7], differentiation [8] and myelin formation [9, 10]. Further, in RRMS patients, treatment with glatiramer acetate increased BDNF levels. However, despite the beneficial roles of BDNF in myelin repair, its exact mechanism is still unknown [5]. BDNF increases the expression of the key myelin structural proteins including myelin basic protein (MBP) [11], myelin associated glycoprotein (MAG), and proteolipid protein (PLP) in mature oligodendrocytes [12]. Interestingly, studies have provided evidence that BDNF contributes to the remyelination of spinal cord lesions [13, 14]. Delivery of exogenous BDNF to the CNS of mice induced to a state of EAE resulted in a significant increase in remyelination [14]. These studies are consistent with the hypothesis that BDNF plays an active role in the myelin repair in MS. Our previous study showed that BDNF levels are increased in EAE dorsal root ganglion (DRG) coincidental with peak neurological disability [6]. Further, we showed that increased spinal cord BDNF levels are partly due to the anterograde transport of BDNF protein from the DRG along the dorsal roots [6].

Like other neurotrophins, BDNF is synthesized and secreted as a 34kDa precursor protein, proBDNF, which is cleaved to produce mature 13kDa BDNF [15-17]. BDNF signalling is regulated via two different receptor classes, the tropomyosin-related kinase receptor (TrkB) [18, 19] and the p75^{NTR} receptor, a member of the TNF receptor superfamily [19, 20]. The mature form of BDNF signals only via the TrkB receptor [18]. However, proBDNF interacts with the

p75^{NTR} [21] and mediates biological actions distinct from those of TrkB [19, 22, 23]. Published studies show that oligodendrocytes express p75^{NTR} [24, 25]. Although there are no published studies addressing TrkB expression by spinal cord oligodendrocytes, there are studies showing that proBDNF promotes myelination via p75^{NTR}-mediated activity independent of TrkB [26, 27]. Specifically, inhibition of the p75^{NTR} receptor activity prevented the expression of MAG [26]. MAG is essential for long-term axon–myelin stability, the structure of the nodes of Ranvier, and maintenance of the axon cytoskeleton [26]. In addition to regulating oligodendrocyte lineage cells, BDNF also regulates other cell types (including astrocytes and neurons) that are critical for the formation of myelin [28].

At present, despite the beneficial roles of BDNF in myelin repair, the exact cellular source and target of BDNF responsible for this repair remains unknown. Our recently published study shows that increased BDNF expression at gene and protein levels in rat EAE spinal cord and provides evidence that spinal cord BDNF levels may be derived from the sensory neurons of the DRG [6]. Thus, we hypothesized that BDNF facilitates the downstream cellular cascade of events of myelin repair via TrkB/p75NTR receptor in EAE spinal cord. We show the gene and protein expression of TrkB significantly increased in a rat EAE model induced by MBP. In addition the increased TrkB levels seen are in accordance with progression of neurological disability in this EAE model of MS. Moreover, we show a detailed immunohistochemical (IHC) description of the cellular distribution of TrkB receptor in the EAE spinal cord. Our study provides novel information about BDNF/TrkB related molecular signaling mechanisms underlying myelin repair in MS.

4.4 EXPERIMENTAL SECTION

4.4.1 EAE MODEL

EAE was induced using MBP, in adolescent female Lewis rats (Charles River, Montreal, QC) as previously described [20, 29], Adolescent female Lewis rats were randomly assigned to 3 experimental groups: naïve control (NC), active control (AC) and active EAE (EAE). For each group there were 5 time points for sacrifice at 3, 6, 9, 12 and 15 days post induction (dpi). All animal experiments were conducted according to protocols approved by the University of Manitoba Animal Protocol Management and Review Committee, in full compliance with the Canadian Council on Animal Care.

4.4.2 REAL TIME REVERSE TRANSCRIPTION POLYMERASE CHAIN REACTION

Total RNA was isolated from DRG and spinal cord tissues using TRIzol reagent (Invitrogen, Carlsbad, CA, USA) according to manufacturer's protocol. The mRNA was transcribed to cDNA and quantitative real time RT-PCR was conducted for measuring target gene as previously described methods [6]. The PCR reaction was performed using a Light-Cycler-DNA master SYBR green 1 kit following manufacturer's protocols (Bio-Rad, Hercules, CA, USA). TrkB primers were: forward: 5'-acgtcaccaatcacacggagtacc-3'; reverse; 5'-ctggcagagtcacgctcgttgc-3' and annealing temperature at 62 °C. The cDNAs were amplified for a total 37 cycles. PCR product was calculated to a length of 430bp, as was confirmed on agarose gel electrophoresis stained with ethidium bromide.

4.4.3 WESTERN BLOT

Protein concentration for each sample was assessed using the Bradford protein assay (Bradford 1976). For each sample, 30 µg total protein was analyzed by western blot as previously described [6]. Anti-TrkB antibody (1:500, R&D system Minneapolis, MN, USA) was used to detect BDNF protein. Following incubation with anti-rabbit secondary antibody (1:10,000, Jackson ImmunoResearch, West Grove, PA, USA), the enhanced chemiluminescence signal was detected by chemiluminescence (Alpha Innotech, Santa Clara, CA, USA). Signals were normalized to GAPDH.

4.4.4 IMMUNOHISTOCHEMISTRY (IHC)

For IHC analysis of protein expression, animals were perfused and fixed with 4% paraformaldehyde as previously described [6]. Spinal columns were dissected free of overlying muscle and connective tissue, and decalcified according to previously described protocols [6]. Qualitative immunofluorescent analysis of cryostat sections was conducted to detect the protein expression of TrkB according to previously described methods [6]. Double-labeled immunofluorescence using monoclonal antibodies of NeuN (1:1000; Chemicon, Billerica, MA, USA), MBP (1:50, Santa Cruz), GFAP (1:100, Santa Cruz), CD68 (ED1) (1:100, Santa Cruz), PDGFR- α (1:50, Santa Cruz), CD4 (1:100, Santa Cruz), and neuron specific β -III Tubulin (1:50, R&D) were conducted in conjunction with the polyclonal antibody TrkB, respectively (1:100, R&D system Minneapolis, MN, USA). This antibody detects the mature form of TrkB at 145 kDa. The slides were imaged using an Olympus BX51 configured with FV5000 Confocal laser scanning capability; images were captured in Fluoview Version 4.3. The immunostaining images were performed using Image Pro Express software (Media Cybernetics, Bethesda, MD, USA).

Image sizing, black background balancing and final collation for publication were performed using Adobe Creative Suite 2 v9.0.2 (Adobe Systems Inc., San Jose, CA, USA). No image manipulations were performed other than those described.

4.4.5 STATISTICAL ANALYSIS

Statistics was performed using GraphPad Prism version 4.03 for Windows (GraphPad Software, San Diego California USA, www.graphpad.com). Results are expressed as mean \pm SEM. The data were analyzed by one-way ANOVA with Tukey's Multiple Comparison post hoc test. Student's *t*-test was used to assess significance of differences between the groups. Normality and homogeneity of error variance of dependent variable was tested by using Kolmogorov-Smirnov and Levene's test. A value of $p < 0.05$ was considered significant.

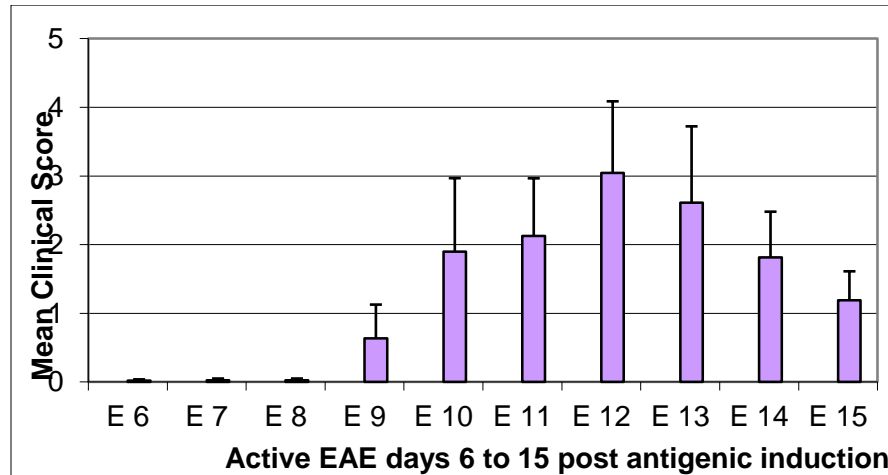
4.5 RESULTS AND DISCUSSION

4.5.1 ESTABLISHMENT OF AN MBP-INDUCED EAE MODEL

All animals in the EAE groups were assessed for neurological disability according to a previously described global neurological disability assessment tool [6]. None of the animals displayed clinical neurological deficits prior to day 6 post-EAE induction (6-dpi) as evident by their scoring of zero. However, all animals started to display clinical signs of neurological disability (0.57 ± 0.45) by 9- dpi representing the early inflammatory stage of disease induction with peak neurological disability score (6.42 ± 5.35) achieved by 12-dpi which subsequently subsided by 15-dpi (1.5 ± 1.41) as the animals entered the remission phase of disease induction,

which is well characterized for this animal model. In contrast, the naïve control and active control group animals did not displayed clinical neurological symptoms.

Figure 1. EAE animals Neurological Disability Clinical Score.



This figure illustrates clinical scores in the EAE animals, at different times in the disease progression. Global Neurological Disability Score for EAE animals induced to a state of Multiple Sclerosis. Disability scores range from a mean clinical disability score of 0 (no disability) to 15 (maximal disability). It shows that EAE animals developed the clinical symptom from day 6 and has the highest clinical score at day 12.

4.5.2 EXPRESSION OF TRKB MRNA IN THE EAE SPINAL CORD

Real time-PCR was used to test TrkB 145 mRNA expression from all naïve, active control and active EAE groups. We found very low expression of TrkB 145 mRNA in all groups. The data was normalized with GAPDH expression from all groups. The results show that there was no statistically significant change of TrkB mRNA expression between any two groups (data not shown).

4.5.3 UP-REGULATION OF TRKB PROTEIN IN THE EAE SPINAL CORD

Western blot was used to test TrkB protein expression from naïve, active control and active EAE groups. In general, the data shows that significantly increased TrkB protein expression in EAE9 and EAE 12 groups compared to naïve and AC9 and AC12 groups. Naïve control animals show TrkB protein expression at 0.235 ± 0.02 . Active control animals (grey bars) shown increased protein expression of TrkB relative to naïve control at day 9 and day 12. (AC9 = 0.576 ± 0.12 ; AC12 = 0.807 ± 0.15). In comparison, active EAE animals show a significant increase in TrkB expression in the spinal cord over naïve and active control at day 9 and 12 (EAE9 = 2.124 ± 0.24 $P < 0.05$ and EAE12 = 2.24 ± 0.26 , $P < 0.05$) [Figure 2&3].

Figure 2. TrkB protein expressions in the spinal cord by Western Blot

This figure illustrates that full length TrkB (145 kDa) protein is detected in naïve, active control and active EAE groups at the different time points. GAPDH protein is also detected at 40 kDa.

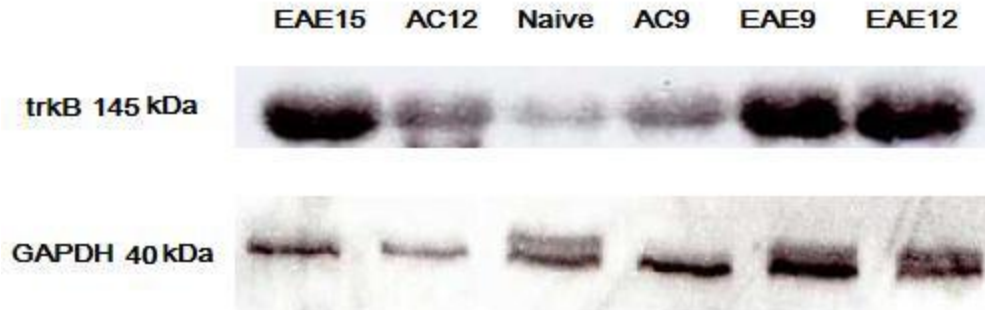
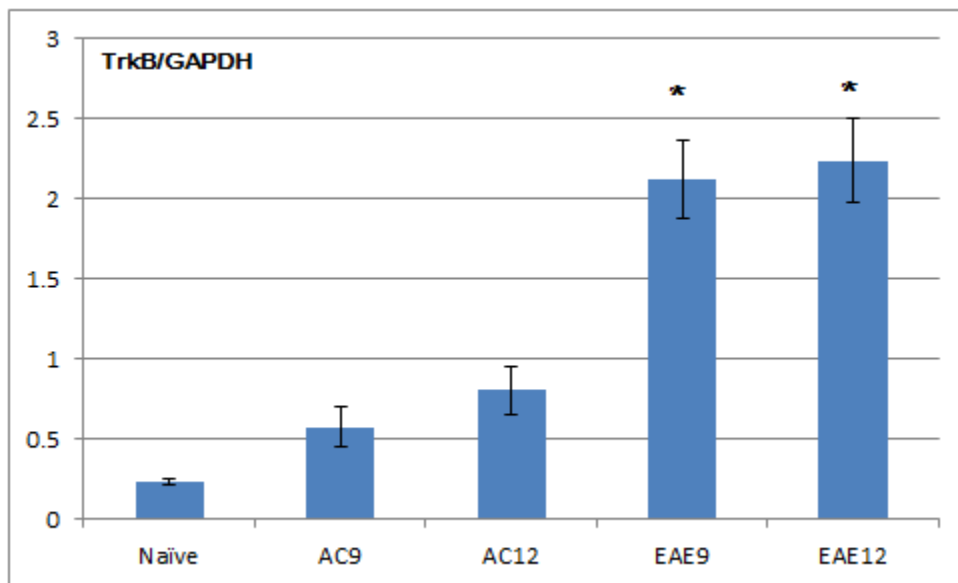


Figure 3. TrkB protein expressions in the spinal cord by Western Blot

This figure shows TrkB protein expression in the spinal cord, at different times in the disease progression. Naïve control animals show TrkB protein expression at 0.235 ± 0.02 . Active control animals (grey bars) showed an increased protein expression of TrkB to naïve control at day 9 and day 12. (AC9 = 0.576 ± 0.12 ; AC12 = 0.807 ± 0.15). In comparison, active EAE animals show a significant increase of TrkB expression in the spinal cord over naïve and active control at day 9 and 12 (EAE9 = 2.124 ± 0.24 P<0.05 and EAE12 = 2.24 ± 0.26 , P<0.05).



4.5.4 IHC ANALYSIS OF BDNF RESPONSIVE CELLS IN THE SPINAL CORD

In order to investigate the role of BDNF in the EAE spinal cord, double fluorescent staining was conducted to determine BDNF responsive cells (TrkB expressing cells). As shown in Figure 8 & 9, TrkB protein was co-localized with NeuN and β -III-tubulin. This means in the EAE spinal cord, neuronal cell bodies and axons are expressing TrkB protein. Furthermore, TrkB immunoreactivity enhanced in active EAE groups compared to naïve and active control groups. We also found in EAE spinal cord TrkB protein is co-localized with CD4⁺ T-cells [Figure 10] and Th17 cells [Figure 11]. This result shows immune cells also express TrkB receptor in EAE spinal cord. In addition, the markers including CD68, GFAP, MBP and PDGFR- α were used to determine the expression of TrkB on glial cells. Our results show that TrkB is not expressed on microglia, astrocytes, mature oligodendrocytes or oligodendrocyte precursors in the EAE spinal cord [Figure 4, 5, 6, and 7].

Figure 4. TrkB and MBP double labeling in EAE spinal cord

This figure illustrates that IHC results (MBP labeling red and TrkB labeling green) show TrkB is not co-localized with mature oligodendrocytes. Images were taken at a total magnification of 1000X from active EAE 12 group.

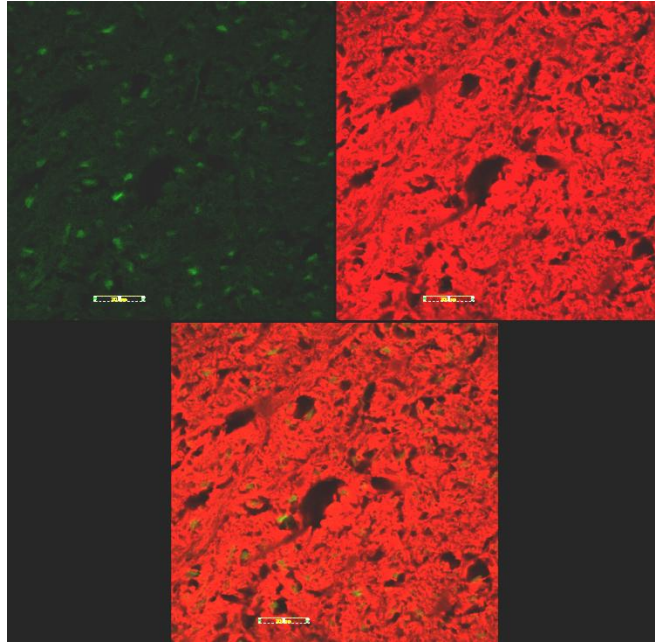


Figure 5. TrkB and PDGFR- α double labeling in EAE spinal cord

This figure illustrates that IHC results (PDGFR- α labeling red and TrkB labeling green) show TrkB is not co-localized with oligodendrocyte precursors. Images were taken at a total magnification of 1000X from active EAE 12 group.

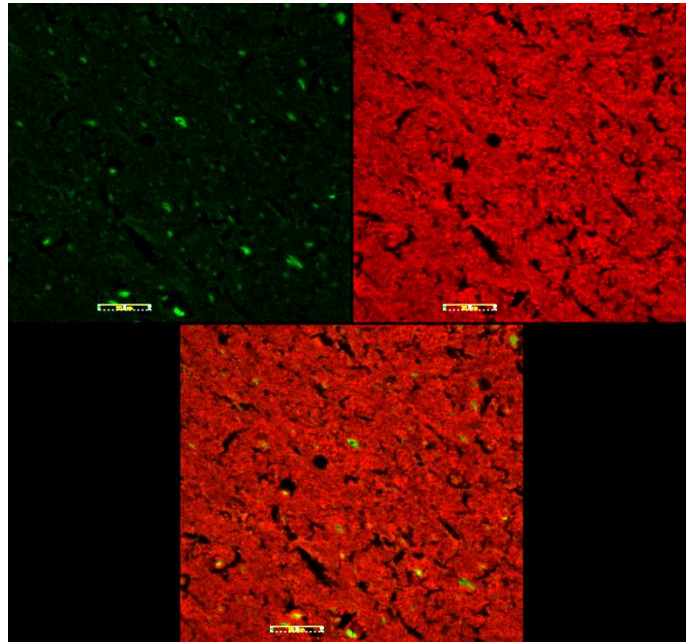


Figure 6. TrkB and GFAP double labeling in EAE spinal cord

This figure illustrates that IHC results (GFAP labeling red and TrkB labeling green) show TrkB is not co-localized with astrocytes. Images were taken at a total magnification of 1000X from active EAE 12 group.

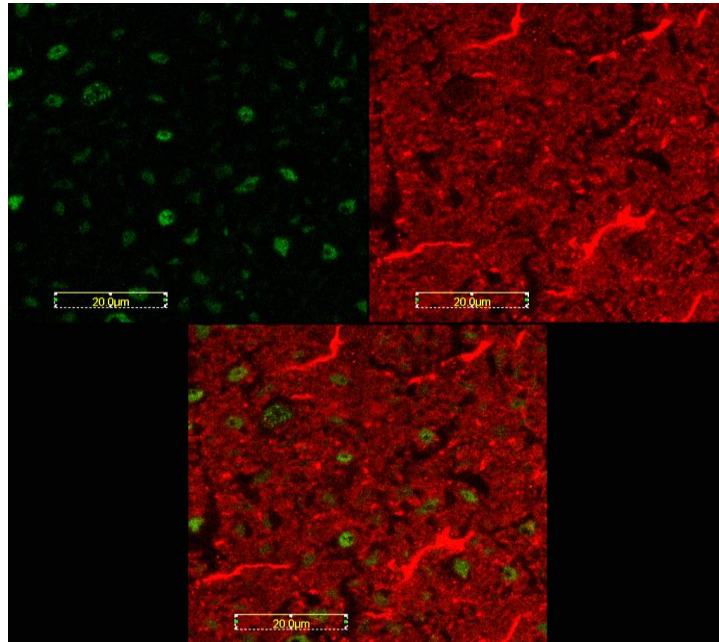


Figure 7. TrkB and CD68 double labeling in EAE spinal cord

This figure illustrates that IHC results (CD68 labeling red and TrkB labeling green) show TrkB is not co-localized with microglia cells. Images were taken at a total magnification of 1000X from active EAE 12 group.

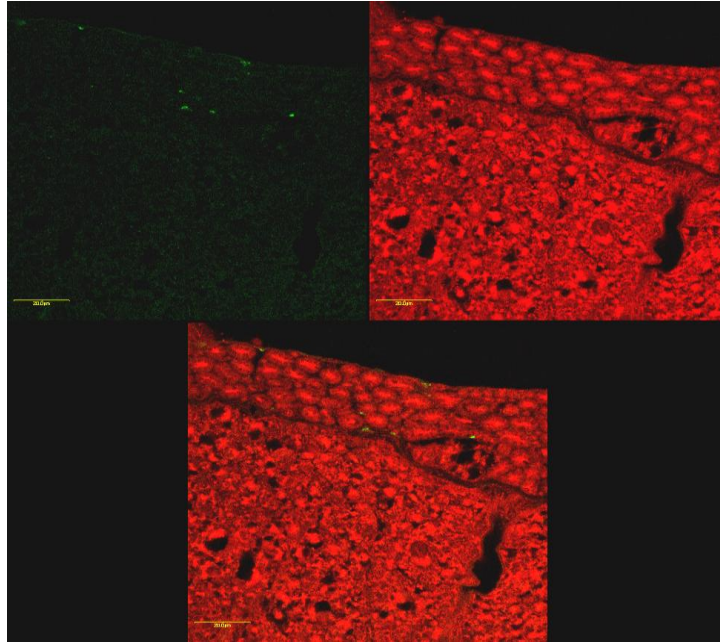


Figure 8. TrkB and NeuN double labeling in EAE spinal cord

This figure illustrates that IHC results (TrkB labeling red and NeuN labeling green) show TrkB is co-localized with neurons (yellow points). Images were taken at a total magnification of 400X from active EAE 12 group.

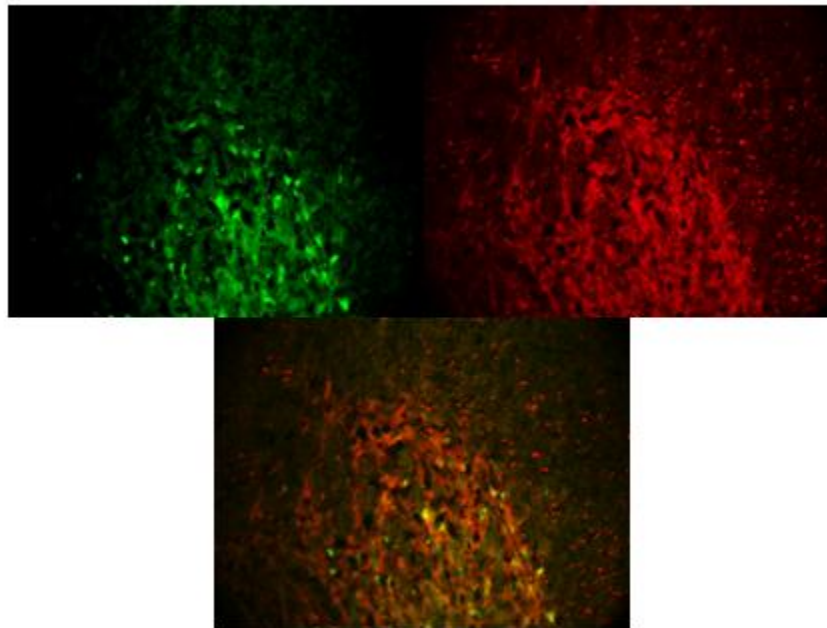


Figure 9. TrkB and β -III Tubulin double labeling in EAE spinal cord

This figure illustrates that IHC results (TrkB labeling red and β -III Tubulin labeling green) show TrkB is co-localized with neuronal axons (yellow points). Images were taken at a total magnification of 1000X from active EAE 12 group.

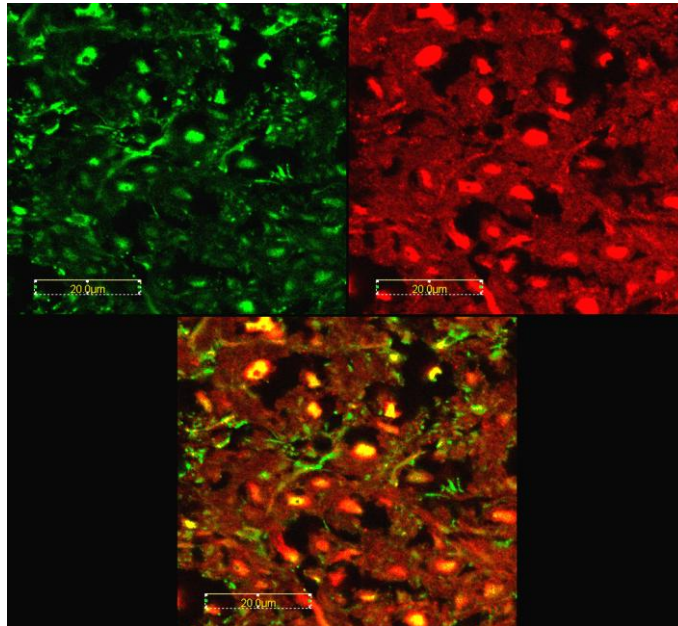


Figure 10. TrkB and CD4 double labeling in EAE spinal cord

This figure illustrates that IHC results (TrkB labeling red and CD4 labeling green) show TrkB is co-localized with CD4⁺ T-cells (yellow points). Images were taken at a total magnification of 400X from active EAE 12 group.

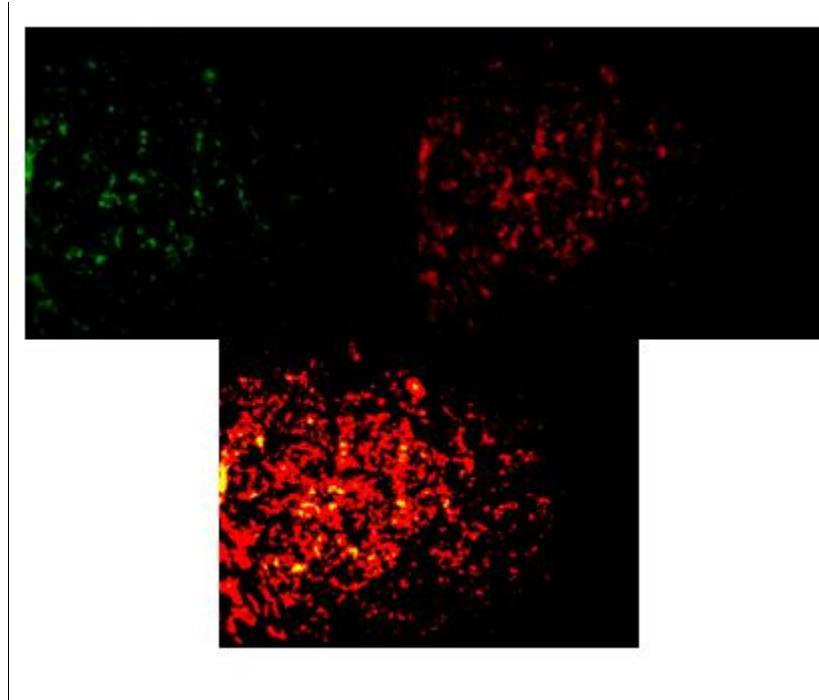
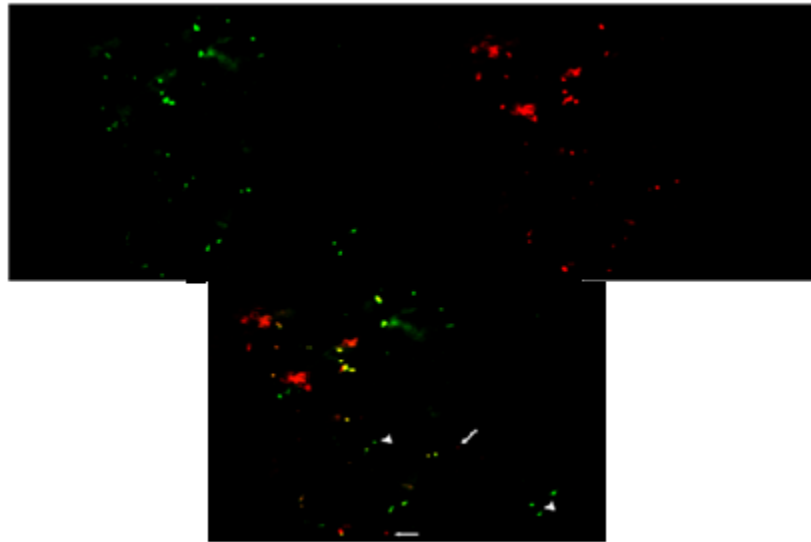


Figure 11. TrkB and Th17 double labeling in EAE spinal cord

This figure illustrates that IHC results (TrkB labeling red and Th17 labeling green) show TrkB is co-localized with Th17 cells (yellow points). Images were taken at a total magnification of 400X from active EAE 12 group.



4.6 DISCUSSION

Several recent studies identified BDNF as a critical component in the molecular pathology of MS [6]. Yet there is little understanding of the role of BDNF in MS. BDNF has been shown to promote neuronal survival and to support oligodendrocyte proliferation and axon remyelination [29, 30]. Our previous study showed significantly increased expression of BDNF at the mRNA and protein levels in the EAE spinal cord [6]. Thus, in this study, in order to determine the exact role of BDNF, we focused on the expression changes of TrkB, which is the high-affinity receptor for BDNF in the spinal cord. Our data clearly shows that the protein levels of TrkB are significantly increased in EAE spinal cord induced by MBP compared to naïve and active control rats.

TrkB is the high-affinity receptor of mature BDNF [31]. The TrkB receptor contains an extracellular domain with three leucine-rich motifs and two immunoglobulin-like C2 type domains (Ig-C2), an intracytoplasmic domain with kinase activity and a transmembrane domain [32]. When BDNF binds to TrkB, several intracellular signaling pathways are triggered including Ras/Raf-MAPK, PI3K-Akt and PLC γ -PKC cascades. These pathways promote neuronal survival and differentiation [32]. Thus, our results indicate that BDNF may promote neuronal survival in the spinal cord in the early inflammatory stage of EAE.

However, qRT-PCR data show that there is no significant change in TrkB mRNA expression between active EAE and naïve/active control groups. These results suggest that increased spinal cord TrkB protein expression may be a translation effect in the early stage of EAE. There are two possibilities to explain why there is protein up regulation without mRNA change. One is that increased protein may be stored in local neurons and released from cells in this time. Another reason is that TrkB protein might be transported from DRG to dorsal horn of spinal cord and

released from axonal terminals. Our immunostaining data shows that TrkB protein is expressed on the axonal terminals in EAE spinal cord.

Our study shows that TrkB immunoreactivity is localized on neurons and axons in the rat spinal cord. So, it is conceivable that BDNF exerts its effects on neurons through its neuroprotective function. On the other hand, BDNF may work on neurons to provide a guidance cue for myelin events in the spinal cord. By IHC analysis, we also found TrkB immunoreactivity is localized on CD4⁺ T and Th17 cells. Our results suggest that BDNF may exert its effects on immune cells thereby regulating their immunomodulatory effects. Inflammatory responses can provide regenerative and protective effects during CNS damage [33]. The TrkB⁺ T-cells could play an important role in MS immunopathogenesis by modulating autoreactive T-cells survival and behavior.

Furthermore, through IHC analysis, we found that TrkB protein is not expressed on mature oligodendrocytes or oligodendrocyte precursors. These results further suggest that in the early inflammatory stage, BDNF is not working on oligodendrocytes or oligodendrocyte precursors through TrkB receptor. BDNF may not exert function in myelin repair because there is no demyelination in the early inflammatory stage of EAE spinal cord. Furthermore, our IHC data show that TrkB is not expressed on spinal cord astrocytes or microglia. This result indicates that BDNF may not be involved in microglia activation in the early inflammatory stage of EAE.

Our study provides key information relating to the cellular source of TrkB expression in an EAE rat model of MS. Furthermore, by determining the direct role of BDNF on BDNF responsive TrkB expressing spinal cord cells; we provide novel information that may have the diverse applicability to other diseases the CNS such as epilepsy, Schizophrenia and cerebral palsy [5].

Further studies are required to study the expression of P75^{NTR} receptor in EAE spinal cord to determine the effect of TrkB independent BDNF activity. Activation of P75^{NTR} has been associated with multiple cell specific functions including cell survival, proliferation and apoptosis [32] and myelination [26]. Furthermore, P75^{NTR} can modulate the affinity of BDNF/TrkB interactions [34]. The determination of P75^{NTR} expression in the EAE spinal cord will provide more information underlying BDNF role in MS. Although our study show BDNF may not exert its function of myelin repair via TrkB receptor in the early inflammatory stage of MS, it may promote myelination via P75^{NTR} with TrkB- independent pathway.

4.7 CONCLUSIONS

In this research, we have found that significantly increased protein expression of BDNF receptor (TrkB 145) in EAE spinal cord without mRNA increase. In addition, we identified BDNF responsive cells (neurons, CD4+ T-cells and Th17 cells) in the EAE spinal cord. However, the glial cells including oligodendrocytes, microglial cells and astrocytes do not expressing BDNF receptor TrkB B 145. Our findings provided novel information about BDNF direct roles via TrkB signaling (neuroprotection and immunomodulation) in the early inflammatory stage of neuroimmune activation. However, BDNF may exert its effects via P75^{NTR} with TrkB independent pathway for myelin repair.

Acknowledgments

We would like to thank our funding & supporting agencies: Biogen Idec Canada Inc (MN & EEF), Manitoba Medical Services Foundation (EEF & MN), Manitoba Institute of Child Health

(MN & EEF), Manitoba Health Research Council (EEF), Pfizer UK Global (MN & EEF), Pfizer Canada (MN & EEF), and Purdue Pharma (MN & EEF). WZ was the recipient of a Canada Millennium Scholarship Foundation award.

4.8 REFERENCES AND NOTES

1. Compston, A.; Coles, A. Multiple sclerosis. *Lancet* 2008, 372, 1502–17.
2. Sospedra, M.; Martin, R. Immunology of multiple sclerosis. *Annu Rev Immunol* 2005, 23, 683–747.
3. Trapp, B.D.; Peterson, J.; Ransohoff, R.M.; Rudick, R.; Mörk, S.; Bö L. Axonal transection in the lesions of multiple sclerosis. *N Engl J Med* 1998, 338, 278–85.
4. Kutzelnigg A, Lucchinetti C.F, Stadelmann C, Brück W, Rauschka H, Bergmann M, et al. Cortical demyelination and diffuse white matter injury in multiple sclerosis. *Brain* 2005, 128, 2705–12.
5. Namaka, M.P.; Ethans, K.; Jensen, B., *et al.* Multiple Sclerosis. Therapeutic Choices/e-Therapeutic. *Ottawa: Canadian Pharmacists Association Publishers, Inc*, 2011, 309-319.
6. Zhu, W.; Frost, E.; Begum, F.; Vora, P.; Au, K.; Gong, Y.; MacNeil, B.; Pillai, P.; and Namaka, M., The role of dorsal root ganglia activation and brain derived neurotrophic factor in multiple sclerosis. *J Cell Mol Med*, 2011 Nov 2. doi: 10.1111/j.1582-4934.2011.01481.x. [Epub ahead of print]
7. Van't Veer, A.; Du, Y.; Fischer, T.Z.; Boetig, D.R.; Wood, M.R.; Dreyfus, C.F. Brain-derived neurotrophic factor effects on oligodendrocyte progenitors of the basal forebrain are mediated through TrkB and the MAP kinase pathway. *J Neurosci Res*, 2009, 87, 69-78.
8. Nakajima, H.; Uchida, K.; Yayama, T.; Kobayashi, S.; Guerrero, A.R.; Furukawa, S.; Baba, H. Targeted retrograde gene delivery of brain-derived neurotrophic factor suppresses apoptosis of

neurons and oligodendroglia after spinal cord injury in rats. *Spine (Phila Pa 1976)* 2010, 35, 497-504.

9. Vondran, M.W.; Clinton-Luke, P.; Honeywell, J.Z.; Dreyfus, C.F. BDNF^{+/-} mice exhibit deficits in oligodendrocyte lineage cells of the basal forebrain. *Glia* 2010, 58, 848-856.

10. Cellerino, A.; Carroll, H.; Thoenen, P.; Barde, Y.-A. Reduced Size of Retinal Ganglion Cell Axons and Hypomyelination in Mice Lacking Brain-Derived Neurotrophic Factor. *Molecular and Cellular Neuroscience* 1997, 9, 397-408.

11. Djalali, S.; Holtje, M.; Grosse, G.; Rothe, T.; Stroh, T.; Grosse, J.; Deng, D.R.; Hellweg, R.; Grantyn, R.; Hortnagl, H.; Ahnert-Hilger, G. Effects of brain-derived neurotrophic factor (BDNF) on glial cells and serotonergic neurons during development. *Journal of Neurochemistry* 2005, 92, 616-627.

12. Du, Y., L.D. Lercher, R. Zhou, and C.F. Dreyfus, Mitogen-activated protein kinase pathway mediates effects of brain-derived neurotrophic factor on differentiation of basal forebrain oligodendrocytes. *J Neurosci Res* 2006, 84,1692-1702.

[13] De Santi, L., Annunziata, P., Sessa, E., Bramanti, P. Brain-derived neurotrophic factor and TrkB receptor in experimental autoimmune encephalomyelitis and multiple sclerosis. *J Neurol Sci*, 2009, 287, 17-26.

14. Makar, T.K., Bever, C.T., Singh, I.S., Royal, W., Sahu, S.N., Sura, T.P. Brain-derived neurotrophic factor gene delivery in an animal model of multiple sclerosis using bone marrow stem cells as a vehicle. *J Neuroimmunol*, 2009, 210, 40-51.

15. Seidah, N.G., Benjannet, S., Pareek, S., Chretien, M., Murphy, R.A. Cellular processing of the neurotrophin precursors of NT3 and BDNF by the mammalian proprotein convertases. *FEBS Lett*, 1996, 379, 247-250.
16. Pang, P.T., Teng, H.K., Zaitsev, E., Woo, N.T., Sakata, K., Zhen, S., Teng, K.K., Yung, W.H., Hempstead, B.L., Lu, B. Cleavage of proBDNF by tPA/plasmin is essential for long-term hippocampal plasticity. *Science*, 2004, 306, 487-491.
17. Kolbeck, R., Jungbluth, S., Barde, Y.A. Characterisation of neurotrophin dimers and monomers. *Eur J Biochem*, 1994, 225, 995-1003.
18. Patapoutian, A., Reichardt, L.F. Trk receptors: mediators of neurotrophin action. *Curr Opin Neurobiol*, 2001, 11, 272-280.
19. Bibel, M., Hoppe, E., Barde, Y.A. Biochemical and functional interactions between the neurotrophin receptors trk and p75NTR. *EMBO J*, 1999, 18, 616-622.
20. Lee, F.S., Kim, A.H., Khursigara, G., Chao, M.V. The uniqueness of being a neurotrophin receptor. *Curr Opin Neurobiol*, 2001, 11, 281-286.
21. Binder, D.K., Scharfman, H.E. Brain-derived neurotrophic factor. *Growth Factors*, 2004, 22, 123-131.
22. Schecterson, L.C., Bothwell, M. Neurotrophin receptors: Old friends with new partners. *Dev Neurobiol*, 2010, 70, 332-338.
23. Shamovsky, I.L., Ross, G.M., Riopelle, R.J., Weaver, D.F. The interaction of neurotrophins with the p75NTR common neurotrophin receptor: a comprehensive molecular modeling study. *Protein Sci*, 1999, 8, 2223-2233.

24. Althaus, H.H., Kloppner, S., Klopfleisch, S., Schmitz, M. Oligodendroglial cells and neurotrophins: a polyphonic cantata in major and minor. *J Mol Neurosci*, 2008, 35, 65-79.
25. Cohen, R.I., Marmur, R., Norton, W.T., Mehler, M.F., Kessler, J.A. Nerve growth factor and neurotrophin-3 differentially regulate the proliferation and survival of developing rat brain oligodendrocytes. *J Neurosci*, 1996, 16, 6433-6442.
26. Cosgaya, J.M., Chan, J.R., Shooter, E.M. The neurotrophin receptor p75NTR as a positive modulator of myelination. *Science*, 2002, 298, 1245-1248.
27. Teng, H.K., Teng, K.K., Lee, R., Wright, S., Tevar, S., Almeida, R.D., Kermani, P., Torkin, R., Chen, Z.Y., Lee, F.S., Kraemer, R.T., Nykjaer, A., Hempstead, B.L. ProBDNF induces neuronal apoptosis via activation of a receptor complex of p75NTR and sortilin. *J Neurosci*, 2005, 25, 5455-5463.
28. Emery, B., Regulation of oligodendrocyte differentiation and myelination. *Science*, 2011, 330, 779-782.
29. Gravel, C., Götz, R., Lorrain, A., Sendtner, M. Adenoviral gene transfer of ciliaryneurotrophicfactor and brain-derived neurotrophic factor leads to long-term survival of axotomized motor neurons. *Nat Med* 1997, 3, 765–70.
30. McTigue, D.M., Horner, P.J., Stokes, B.T., Gage, F.H. Neurotrophin-3 and brain-derived neurotrophic factor induce oligodendrocyte proliferation and myelination of regenerating axons in the contused adult rat spinal cord. *J Neurosci* 1998, 18, 5354–65.

31. Klein, R., Nanduri, V., Jing, S. A., Lamballe, F., Tapley, P., Bryant, S., et al. The TrkB tyrosine protein kinase is a receptor for brain-derived neurotrophic factor and neurotrophin-3. *Cell* 1991, 66, 395–403.
32. Arévalo, J.C., Wu, S.H. Neurotrophin signaling: many exciting surprises! *Cell Mol Life Sci* 2006, 63, 1523–1537.
33. Moalem, G., Leibowitz-Amit, R., Yoles, E., Mor, F., Cohen, I.R., Schwartz, M. Autoimmune T-cells protect neurons from secondary degeneration after central nervous system axotomy. *Nat Med* 1999, 5, 49–55.
34. Copray, S., Küst, B., Emmer, B., Young, Lin. M., Liem, R., Amor, S., et al. Deficient p75 low affinity neurotrophin receptor expression exacerbates experimental allergic encephalomyelitis in C57/BL6 mice. *J Neuroimmunol* 2004; 148, 41–53.

CHAPTER 5 – FRACTALKINE (CX3CL1) AND FRACTALKINE RECEPTOR (CX3CR1) EXPRESSION IN THE SPINAL CORD ASSOCIATED WITH EXPERIMENTAL AUTOIMMUNE ENCEPHALOMYELITIS (EAE) INDUCED NEUROPATHIC PAIN

Authors and affiliations- Wenjun Zhu¹, Crystal Acosta¹, Brian MacNeil² Emma Frost¹, Mike Namaka¹

1 Faculty of Pharmacy, 2 Medical Rehabilitation, University of Manitoba, Winnipeg, Manitoba, Canada

This manuscript was submitted to the journal of Neuron Glia Biology in 2012 May.

5.1 STATEMENT OF CONTRIBUTION

For this study, I was responsible for the experimental design, induction of the EAE rats (including neurological disability testing, sacrifice, harvesting and preparation of tissue for analysis), and completion of immunohistochemistry, ELISA, real-time RT-PCR, writing the manuscript and preparing for submission. In addition, I supervised the other graduate student (Crystal Acosta) as she assisted with the statistical analysis.

5.2 ABSTRACT

Multiple sclerosis (MS) is a chronic inflammatory autoimmune disease, characterised by demyelination in the central nervous system (CNS). The exact pathophysiology of MS is still unknown but it is associated with infiltration of T-cells, and activation of microglia that results in myelin damage leading to neurological deficits including neuropathic pain. The proposed role for the chemokine CX3CL1 and its receptor CX3CR1, in the control of microglia activation and leukocyte infiltration places this chemokine in a potentially strategic position in regard to the pathological events of MS-induced neuropathic pain. In this study, the experimental autoimmune encephalomyelitis (EAE) rat model of MS was used to determine the role of CX3CL1 during the antigenic induction of neuropathic pain. Protein and gene expression was analyzed using ELISA and real time RT-PCR respectively. Significant increases in protein and mRNA expression of CX3CL1 and CX3CR1 were shown in dorsal root ganglia and spinal cord in the EAE rats at 12 days post induction, relative to controls. This increase correlates with peak neurological disability as well as sensory disturbances indicative of neuropathic pain. The up-regulated expression of CX3CL1 within spinal cord may represent a critical link to advanced understanding of pathology associated with neuropathic pain due to autoimmune diseases such as MS.

Keywords: Multiple sclerosis, experimental autoimmune encephalomyelitis, CX3CL1, CX3CR1, neuropathic pain

5.3 INTRODUCTION

Multiple sclerosis (MS) is a chronic inflammatory autoimmune disease of the central nervous system (CNS), which is characterised by inflammation, and subsequent demyelination of brain and spinal cord [1]. The exact pathophysiology of MS is still unknown but it is associated with infiltration of T-cells, activation of microglia and astrocytes resulting in myelin damage, which in turn leads to axonal and neuronal destruction. The disease often develops with various neurological manifestations including ataxia, cognitive dysfunction, and sensory abnormalities such as neuropathic pain [2].

Chemokines are small cytokines that are key mediators controlling the response of leukocytes to areas of inflammation. They also act as chemotactic cues for leukocytes via interactions with their G-protein coupled, cell membrane-spanning receptors. Fifty chemokines have been identified, which are divided into 4 subgroups, the XC, CC, CXC and CX3C chemokines [3]. Synthesis of chemokines occurs rapidly within infected or damaged tissues. They are thought to drive chronic inflammatory processes in order to attract appropriate cell populations to combat invading organisms and repair damaged tissues [3]. Recent studies have provided evidence that chemokines may serve to reduce neurological deficits such as neuropathic pain in inflammatory disorders such as MS [4].

CX3CL1 (Fractalkine) is the only member of the fourth class of chemokines, with a CX3C motif in the mucine-like domain [5]. It is unique in that it is tethered to a cell membrane and is cleaved after an excitotoxic stimulus, to produce a soluble, diffusible protein [6]. CX3CL1 is usually expressed in the normal rodent brain by different neuronal cell sub-types [7]. In addition, it is also expressed in monocytes, NK cells and smooth muscle cells. Recent evidence has shown that CX3CL1 and its receptor are known to be involved in the pathogenesis of several clinical

diseases such as rheumatoid arthritis, chronic pancreatitis and neuropathic pain [8]. Further, CX3CL1 plays a critical role in neuroinflammation and neuroprotection by regulating neuronal-microglial communication [9]. In the CNS, CX3CL1 is highly expressed by neurons while CX3CR1 is only expressed by microglia [10]. However, studies have shown that the expression of CX3CL1 changes during pain states [11].

Several studies show that induction of neuropathic pain results in the synthesis and release of CX3CL1 in the sensory neurons of the dorsal root ganglion (DRG) [11]. Further, this increase is accompanied by upregulation of CX3CR1 in the spinal cord microglia, and correlates with the onset of neuropathic pain [11]. The most likely source of fractalkine in the spinal cord in neuropathic pain states are resident microglia which upregulate fractalkine in response to injury [11]. Activated T-cells, transmigrating across the blood brain barrier are an additional source for the increased CX3CR1-immunoreactivity in the spinal cord in neuropathic pain [12].

Further evidence of a role for CX3CL1 in neuropathic pain comes from a study using intrathecal injections of CX3CL1 [13]. That study showed that acute intrathecal injection of CX3CL1 resulted in the development of thermal hyperalgesia and mechanical allodynia in adult rats [14]. Administration of neutralizing antibodies against CX3CR1 attenuated the allodynia and hyperalgesia in a rat neuropathic pain model [14]. Interestingly, in a spared nerve injury model performed in CX3CR1 knockout mice Holmes et al. showed increased allodynia, suggesting an anti-allodynic role for CX3CL1/ CX3CR1 signalling [13]. Therefore, antagonism of CX3CR1 appears to be a promising novel strategy to reduce neuropathic pain.

5.4 OBJECTIVE

We hypothesized that CX3CL1 and CX3CR1 expression are increased within spinal cord in correlation with the onset of neuropathic pain in an EAE model of MS.

To further understand the role of CX3CL1 and CX3CR1 in MS-induced neuropathic pain, we assessed the gene and protein expression of CX3CL1 and CX3CR1 in a rat EAE model induced by myelin basic protein (MBP) [15]. Our study shows significant increases in both CX3CL1 and its receptor CX3CR1, in addition the increased CX3CL1 and CX3CR1 levels correlate with progression of behavioral changes consistent with neuropathic pain in this EAE model. Moreover, we show a detailed immunohistochemical (IHC) analysis of the cellular distribution of CX3CL1 and CX3CR1 in the EAE spinal cord. Our study provides novel information about chemokine expression changes underlying MS-induced neuropathic pain.

5.5 METHODS

5.5.1 EXPERIMENTAL AUTOIMMUNE ENCEPHALOMYELITIS (EAE) MODEL

Experimental EAE was induced using MBP in adolescent female Lewis rats (Charles River, Montreal, QC) as previously described [15]. The rats were randomly assigned to 3 experimental groups: naïve control (NC), active control (AC) and active EAE. There were 5 time points for sacrifice at 3, 6, 9, 12 and 15 days post induction in AC and active EAE groups. All animal experiments were conducted according to protocols approved by the University of Manitoba Animal Protocol Management and Review Committee, in full compliance with the Canadian Council on Animal Care. Neurological disability is scored according to the following criteria: Tail: 0 = normal; 1 = partially paralyzed, weakness; 2 = completely paralyzed, limp; Bladder: 0 =

normal; 1 = incontinence: Right hind limb: 0 = normal; 1 = weakness; 2 = dragging with partial paralysis; 3 = complete paralysis: Left hind limb: 0 = normal; 1 = weakness; 2 = dragging with partial paralysis; 3 = complete paralysis: Right forelimb: 0 = normal; 1 = weakness; 2 = dragging, not able to support weight; 3 = complete paralysis: Left forelimb: 0 = normal; 1 = weakness; 2 = dragging, not able to support weight; 3 = complete paralysis.

5.5.2 TISSUE HARVESTING AND SECTIONING

For IHC analysis of protein expression, animals were perfusion fixed with 4% paraformaldehyde as previously described [15]. Spinal columns were dissected and decalcified according to previously described protocols [15]. For gene expression analysis, the DRG and spinal cord were harvested as previously described [15]. Tissue was stored in RNA later stabilization reagent (Qiagen, cat. no. 76106, Washington DC, USA) until processed. Total RNA, DNA, and proteins were isolated as previously described [15].

5.5.3 THERMAL SENSORY TESTING

Withdrawal latencies to a radiant heat stimulus [16] were assessed for each mouse using a Model 336G Plantar/Tail Stimulator Analgesia Meter (IITC Life Sciences, Woodland Hills, CA) according to previously described methods [17]. Rats were habituated to the testing apparatus for 30 min 2 days prior to any testing and for 10 min prior to testing on each test day. Baseline withdrawal latencies were measured for each animal on three separate days prior to immunization. Each experimental group was tested every day after immunization.

5.5.4 IMMUNOHISTOCHEMISTRY

Immunofluorescent analysis of cryostat sections was conducted to detect cellular location of the protein expression according to previously described methods [15]. Double-labeled immunofluorescence using polyclonal antibodies against the neuronal markers NeuN (1:100; Chemicon, Billerica, MA, USA), GFAP (1:100, Santa Cruz, CA, USA), CD68 (ED1) (1:100, Santa Cruz, CA, USA) were conducted in conjunction with the polyclonal antibody for CX3CL1 (1:100, eBioscience, San Diego, CA, USA) and CX3CR1 (1:100, eBioscience, San Diego, CA, USA). Secondary antibodies were goat anti-mouse FITC (1:100, Jackson, West Grove, PA, USA) and goat anti-rabbit TRITC (1:100, Jackson, West Grove, PA, USA). The slides were imaged using the Nikon DS-US camera and images were captured and colorized in Image pro plus 6.2. Image sizing, black background balancing and final collation for publication were performed using Adobe Creative Suite 2 v9.0.2 (Adobe Systems Inc., San Jose, CA, USA). No image manipulations were performed other than those described.

5.5.5 REAL TIME REVERSE TRANSCRIPTION POLYMERASE CHAIN REACTION

Real time RT-PCR was conducted on tissue samples as previously described methods [15]. The PCR reaction was performed using a Light-Cycler-DNA master SYBR green 1 kit following manufacturers protocols (Bio-Rad, Hercules, CA, USA). CX3CL1 primers were: forward: 5'-gaattcctggcgggtcagcacctcggcata-3'; reverse; 5'-aagcttttacagggcagcggctctggtggt-3' and annealing temperature at 60°C. CX3CR1 primers were: forward: 5'-agctgctcaggacctcacat-3'; reverse; 5'-gttggtggaggccctcatggctgat-3' and annealing temperature at 60°C. The cDNAs were amplified by 35 cycles of PCR. Expression levels were normalized to glyceraldehyde-3-phosphate dehydrogenase (GAPDH). GAPDH is an enzyme associated with cell metabolism and is used as

a standard housekeeping gene for expression pattern comparisons [18]. GAPDH primers were purchased from SuperArray. The quantification technique used the standard curve method.

5.5.6 ENZYME LINKED IMMUNOSORBENT ASSAY (ELISA)

Total protein was extracted from the samples as described above and total protein concentration assessed using the Bradford assay [19]. The protein concentrations of the samples were adjusted to 10 µg total protein for fractalkine and 1 µg total protein for CX3CR1 in the sample volume of 100 µl. Sandwich-style ELISA was performed using the RayBio rat CX3CL1 ELISA kit (RayBio, Norcross, GA, USA) and rat chemokine CX3CR1 ELISA kit (Mybiosource, San Diego, CA, USA) according to the manufacturer's instructions. CX3CL1 and CX3CR1 content were measured from standard curve runs for each plate (linear range of 0–2000 ng for CX3CL1; 0-10 ng for CX3CR1). Samples from the groups of AC and EAE and the naïve control rats were determined in each run. Each sample was assayed with 6 replicates per ELISA.

5.5.7 STATISTICAL ANALYSIS

Statistics was performed using GraphPad Prism version 4.03 for Windows (GraphPad Software, San Diego California USA, www.graphpad.com). Statistical analysis was performed using ANOVA with Tukey's Multiple Comparison post hoc test. Student's *t*-test was used to confirm significance of differences between the groups.

5.6 RESULTS

5.6.1 NEUROLOGICAL DISABILITY SCORES

All animals in the EAE groups were scored for neurological disability according to a previously described global neurological disability assessment tool [15]. Prior to day 6 post-EAE induction (6dpi), none of the animals displayed clinical neurological deficits thereby scoring zero. At 6dpi neurological deficits manifest in some animals as tail weakness. By 9dpi all animals started to display clinical signs of neurological disability (mean 0.57 ± 0.45). Neurological disability progressively worsened upon daily assessment until 12dpi (peak disability; mean 6.42 ± 5.35), then subsided by 15dpi (mean 1.5 ± 1.41) as the animals entered the remission phase of disease induction, well characterized for this animal model (Mix, Meyer-Rienecker et al. 2008) (Figure 1A). A box and whisker plot of the mean neurological disability score (NDS) plotted by day of disease onset, shows the variation of clinical symptoms seen in this model (Figure 1B). On the first day of disease onset the mean NDS is 1.98 ± 3.2 with a range of 0 to 10.33, on the second day the mean NDS is 4.01 ± 4.90 with a range of 0 to 14.33. The mean NDS for days 3 and 4 days after disease onset are 4.16 ± 4.59 and 4.022 ± 3.09 respectively, with ranges of 0.83 to 11.50 and 1.67 to 8.00 respectively. Significant variation in the presentation of NDS in this model represents the characteristics of the human MS disease (Namaka, Turcotte et al. 2008; Namaka, Ethans et al. 2011).

5.6.2 THERMAL SENSORY TESTING

Normalized thermal withdrawal latencies in EAE15 rats for tail relative to time of disease onset are shown in Figure 2A. Thermal withdrawal latency is measured each day throughout the

experiment. Due to the inherent variability in the neurological disability scoring, day 0 is set to be the first day of clinical symptoms/signs for each individual animal. Values are normalized to average baseline responses before induction and displayed as means \pm standard deviations. Withdrawal latencies for the tail were significantly elevated at day 1 (post disease onset) compared to all 4 days before induction (* = $p < 0.05$; ANOVA followed by Tukey's posthoc test). Two way analysis of variance (ANOVA) shows that there is an extremely significant difference in the thermal withdrawal latency of the animals with time ($p < 0.0001$).

Thermal sensory testing results in the limbs from EAE animals, at different times in the disease progression, shows significant reduced thermal withdrawal latency scores for the hind feet (Figure 2B) and the front right foot (Figure 2C). This indicates that the animals are showing signs of hyperalgesia, in accordance with previously published studies (Aicher, Silverman et al. 2004). For the hind feet, withdrawal latencies were significantly elevated at day 4 compared to all days before except Day 3 (Repeated measures ANOVA, $p > 0.05$, Tukey's posthoc test). ANOVA by SITE for DAY effect is significant for front left and rear left. For the front right foot, withdrawal latency is significantly increased at 4 days post disease onset (Figure 2C). Data are shown aligned to day of onset of clinical disease; Day 0 is the first day of clinical symptoms/signs for each individual animal.

5.6.3 CX3CL1 GENE EXPRESSION ANALYSIS IN THE DRG

Real time reverse transcription polymerase chain reaction (qRT-PCR) analysis was conducted on DRG isolated from the three experimental groups, at the pre-determined experimental time points (Figure 3A). The CX3CL1 mRNA expression was assessed in parallel with that of the

housekeeping gene Glyceraldehyde-3-phosphate dehydrogenase (GAPDH). Naïve control animals (white bars) show CX3CL1 mRNA expression at 0.0419 ± 0.005782 . Active control animals (grey bars) shown a similar mRNA expression of CX3CL1 to naïve control at all-time points (AC3 = 0.04557 ± 0.002845 ; AC6 = 0.0434 ± 0.004139 ; AC9 = 0.04493 ± 0.004672 ; AC12 = 0.04157 ± 0.006467 ; AC15 = 0.0540 ± 0.003517). In comparison, active EAE animals (black bars) show a significant increase of CX3CL1 expression in DRG over naïve control at day 9, 12 and 15 (EAE9 = 0.09827 ± 0.006542 , $p < 0.005$; EAE12 = 0.1323 ± 0.01539 , $p < 0.005$ and EAE15 = 0.1208 ± 0.01021 , $P < 0.005$). However, there is no significant change of CX3CL1 expression between active EAE and Naïve control at days 3 and 6 (EAE3 = 0.05203 ± 0.0006028 and EAE6 = 0.05747 ± 0.0044664). And also, Active EAE animals show significant increase in mRNA expression over active control group at days 9, 12 and 15 ($p < 0.005$, $p < 0.005$ and $p < 0.005$). (* = $p < 0.05$; ** = $p < 0.01$; *** = $p < 0.005$; ns = Not Significant; ANOVA followed by Tukey's posthoc test) (Figure 3A).

5.6.4 CX3CL1 PROTEIN EXPRESSION ANALYSIS IN THE DRG BY ELISA

Total CX3CL1 protein expression is significantly altered in the lumbar dorsal root ganglia of EAE rats in correlation with the peak neurological disability (Figure 3B). Results are given as ng CX3CL1 per 10 μ g total protein for each sample. Naïve control animals (white bars) show CX3CL1 protein expression at 44.42 ± 13.58 ng/10 μ g total protein. Active control animals (grey bars) showed a similar protein expression of CX3CL1 to naïve control at all-time points (AC3 = 43.85 ± 5.543 ng/10 μ g total protein; AC6 = 51.22 ± 17.60 ng/10 μ g total protein; AC9 = 41.86 ± 5.43 ng/10 μ g total protein; AC12 = 41.25 ± 6.31 ng/10 μ g total protein; AC15 = 30.87 ± 7.77 ng/10 μ g total protein). In comparison, active EAE animals (black bars) show a significant

increase of CX3CL1 expression in DRG over active control at day 12 and 15 (EAE12 = 61.74 ± 10.98 ng/10 μ g total protein, $p < 0.05$ and EAE15 = 53.48 ± 8.873 ng/10 μ g total protein, $p < 0.05$). However, there is no significant change of CX3CL1 expression between active EAE and active control at days 3, 6 and 9 (EAE3 = 48.18 ± 13.79 ng/10 μ g total protein; EAE6 = 43.44 ± 4.33 ng/10 μ g total protein and EAE9 = 56.82 ± 8.87 ng/10 μ g total protein). There is no significance between naïve control and all EAE groups. (* = $p < 0.05$; ** = $p < 0.01$; *** = $p < 0.005$; ns = not significant, ANOVA followed by Tukey's posthoc test).

5.6.5 CX3CR1 GENE EXPRESSION ANALYSIS IN THE DRG

Total CX3CR1 mRNA expression in the DRG is significantly altered at different times in the disease progression in correlation with the onset and peak of neurological disability (Figure 3C). Results are shown as a ratio of CX3CR1 mRNA to the housekeeping gene GAPDH. Naïve control animals (white bars) show CX3CR1 mRNA expression at 0.01897 ± 0.001914 . Active control animals (grey bars) showed a similar mRNA expression of CX3CR1 to naïve control at days 3, 6, 9 and 12 (AC3 = 0.02083 ± 0.002316 ; AC6 = 0.02537 ± 0.009212 ; AC9 = 0.02497 ± 0.006014 ; AC12 = 0.0287 ± 0.007300) and with significant change at day 15 (AC15 = 0.03497 ± 0.003150 , $P < 0.01$). In comparison, active EAE animals (black bars) show a significant increase of CX3CR1 expression in DRG over Naïve control at days 9 and 12 (EAE9 = 0.03793 ± 0.002801 , $p < 0.005$ and EAE12 = 0.03273 ± 0.02517 , $P < 0.01$). However, there is no significant change of CX3CR1 expression between active EAE and naïve control at days 3, 6 and 12 (EAE3 = 0.0228 ± 0.002621 and EAE6 = 0.02477 ± 0.004092). Furthermore, Active EAE animals show significant increase in mRNA expression over active control group at days 9 and 15 ($p < 0.05$ and

p<0.05). (* = p<0.05; ** = p<0.01; *** = p<0.005; ns= Not Significant; ANOVA followed by Tukey's posthoc test) shown in Figure 3C.

5.6.6 CX3CR1 PROTEIN EXPRESSION ANALYSIS IN THE DRG BY ELISA

Total CX3CR1 protein expression in the DRG is altered at different times in the disease progression in correlation with peak neurological disability (Figure 3D). Results are given as ng CX3CR1 per 10 µg total protein for each sample. Naïve control (white bars) animals show a baseline level of CX3CR1 in the DRG of 2.24 ± 0.24 ng/10 µg total protein. Active control (grey bars) animals show a similar expression level of CX3CR1 to naïve control across all time points assessed (AC3 = 2.08 ± 0.15 ng/10 µg total protein; AC6 = 2.90 ± 0.85 ng/10 µg total protein; AC9 = 2.21 ± 0.22 ng/10 µg total protein; AC12 = 2.15 ± 0.13 ng/10 µg total protein and AC15 = 2.34 ± 0.29 ng/10 µg total protein) In comparison, the active EAE (black bars) spinal cord levels of CX3CR1 protein are significantly increased over naïve control and active control at day 12 (EAE12 = 3.10 ± 0.54 ng/10 µg total protein, p<0.05 and p<0.01), however, days 3, 6, 9 and 15 do not show an increase over baseline (EAE3 = 2.20 ± 0.22 ng/10 µg total protein; EAE6 = 2.42 ± 0.17 ng/10 µg total protein; EAE9 = 2.65 ± 0.26 ng/10 µg total protein and EAE 15 = 2.62 ± 0.49 ng/10 µg total protein). (* = p<0.05; ** = p<0.01; *** = p<0.005; ns= not Significant, ANOVA followed by Tukey's posthoc test). See Figure 3D.

5.6.7 CX3CL1 GENE EXPRESSION ANALYSIS IN THE SPINAL CORD

CX3CL1 mRNA expression in the spinal cord at different times in the disease progression is shown in Figure 4A. Results are shown as ratio of CX3CL1 mRNA to GAPDH mRNA. Naïve

control animals (white bars) show CX3CL1 mRNA expression at 0.1054 ± 0.01314 . Active control animals (grey bars) showed a similar mRNA expression of CX3CL1 to naïve control at all-time points (AC3 = 0.1111 ± 0.01530 ; AC6 = 0.1301 ± 0.02640 ; AC9 = 0.1768 ± 0.009242 ; AC12 = 0.1160 ± 0.005810 ; AC15 = 0.1270 ± 0.0209). In comparison, active EAE animals (black bars) show a significant increase of CX3CL1 expression in spinal cord over naïve control at day 9, 12 and 15 (EAE9 = 0.1727 ± 0.02617 , $p < 0.01$; EAE12 = 0.2067 ± 0.02101 , $p < 0.005$ and EAE15 = 0.1783 ± 0.005294 , $P < 0.005$). However, there is no significant change of CX3CL1 expression between active EAE and naïve control at days 3 and 6 (EAE3 = 0.1253 ± 0.005880 and EAE6 = 0.1083 ± 0.005248). In addition, active EAE animals show significant increase in mRNA expression over active control group at days 12 and 15 ($p < 0.005$ and $p < 0.05$). (* = $p < 0.05$; ** = $p < 0.01$; *** = $p < 0.005$; ns = not Significant, ANOVA followed by Tukey's posthoc test) (Figure 4A).

5.6.8 CX3CL1 PROTEIN EXPRESSION ANALYSIS IN THE SPINAL CORD BY ELISA

Total CX3CL1 protein expression in the spinal cord is significantly altered at different times in the disease progression (Figure 4B). Results are given as ng CX3CL1 per 10 μ g total protein for each sample. Naïve control (white bars) animals show a baseline level of CX3CL1 in the spinal cord of 40.05 ± 6.09 ng/10 μ g total protein. Active control (grey bars) animals show a similar expression level of CX3CL1 to naïve control across all time points assessed (AC3 = 47.59 ± 8.33 ng/10 μ g total protein; AC6 = 51.45 ± 7.30 ng/10 μ g total protein; AC9 = 59.55 ± 8.97 ng/10 μ g total protein; AC12 = 57.79 ± 2.62 ng/10 μ g total protein and AC15 = 62.67 ± 9.61 ng/10 μ g total protein) In comparison, the active EAE (black bars) spinal cord levels of CX3CL1 are significantly increased over baseline levels at days 6, 9 and 12 (EAE6 = 68.4 ± 9.16 ng/10 μ g

total protein, $p < 0.01$; EAE9 = 65.06 ± 7.29 ng/10 μ g total protein, $p < 0.05$ and EAE12 = 93.61 ± 29.61 ng/10 μ g total protein, $p < 0.005$), however, days 3 and 15 do not show an increase over baseline (EAE3 = 64.74 ± 2.11 ng/10 μ g total protein and EAE 15 = 63.20 ± 14.76 ng/10 μ g total protein). (* = $p < 0.05$; ** = $p < 0.01$; *** = $p < 0.005$; ns = not Significant, ANOVA followed by Tukey's posthoc test). See Figure 4B.

5.6.9 CX3CR1 GENE EXPRESSION ANALYSIS IN THE SPINAL CORD

The qRT-PCR results show that CX3CR1 mRNA expression in the spinal cord is not significantly altered at different times in the disease progression (Figure 4C). The levels of CX3CR1 are significantly increased at day 12 in the EAE rats only ($p < 0.001$). Naïve control animals (white bars) show CX3CR1 mRNA expression at 0.03977 ± 0.006133 . Active control animals (grey bars) showed a similar mRNA expression of CX3CR1 to naïve control at days 3, 6, 9 and 12 (AC3 = 0.04237 ± 0.003614 ; AC6 = 0.0450 ± 0.002265 ; AC9 = 0.04427 ± 0.004143 ; AC12 = 0.04683 ± 0.003894 and AC15 = 0.03767 ± 0.005393). In comparison, active EAE animals (black bars) show a significant increase of CX3CR1 expression in DRG over Naïve control at days 9, 12 and 15 (EAE9 = 0.05417 ± 0.002969 , $p < 0.05$, EAE12 = 0.0630 ± 0.079 , $p < 0.005$ and EAE15 = 0.0536 ± 1153). However, there is no significant change of CX3CR1 expression between active EAE and Naïve control at days 3, 6 and 9 (EAE3 = 0.0433 ± 0.004124 , EAE6 = 0.04623 ± 0.01201 and EAE9 = 0.05417 ± 0.002969). Furthermore, Active EAE animals show significant increase in mRNA expression over active control group at days 12 and 15 ($p < 0.05$ and $p < 0.05$). (* = $p < 0.05$; ** = $p < 0.01$; *** = $p < 0.005$; ns = Not Significant, ANOVA followed by Tukey's posthoc test). See Figure 4C.

5.6.10 CX3CR1 PROTEIN EXPRESSION ANALYSIS IN THE SPINAL CORD BY ELISA

Total CX3CR1 protein expression in the spinal cord, at different times in the disease progression is shown in Figure 4D. Results are given as ng CX3CL1 per 10 µg total protein for each sample. Naïve control (white bars) animals show a baseline level of CX3CR1 in the spinal cord of 2.20 ± 0.54 ng/10 µg total protein. Active control (grey bars) animals show a similar expression level of CX3CR1 to naïve control across all time points assessed (AC3 = 2.03 ± 0.12 ng/ml; AC6 = 2.19 ± 0.38 ng/10 µg total protein; AC9 = 1.82 ± 0.36 ng/10 µg total protein; AC12 = 1.94 ± 0.26 ng/10 µg total protein and AC15 = 2.50 ± 0.53 ng/10 µg total protein). In comparison, the active EAE (black bars) spinal cord levels of CX3CR1 protein are significantly increased over Naïve control and active control at day 12 (EAE12 = 3.56 ± 1.29 ng/1 µg total protein, $p < 0.05$ and $p < 0.005$), however, days 3, 6, 9 and 15 do not show an increase over baseline (EAE3 = 2.13 ± 0.21 ng/10 µg total protein; EAE6 = 2.02 ± 0.19 ng/10 µg total protein; EAE9 = 2.01 ± 0.36 ng/10 µg total protein and EAE15 = 2.41 ± 0.53 ng/10 µg total protein). (* = $p < 0.05$; ** = $p < 0.01$; *** = $p < 0.005$; ns = not Significant, ANOVA followed by Tukey's posthoc test). See Figure 4D.

5.6.11 IMMUNOHISTOCHEMICAL ANALYSIS OF CX3CL1 PROTEIN EXPRESSION IN THE SPINAL CORD

The IHC double staining results (CX3CL1 labeling red and Neuron labeling green) showed CX3CL1 co-localized with neurons (labeling yellow) (Figure 5A) and (CX3CL1 labeling red and

GFAP labeling green) CX3CL1 co-localized with astrocytes (labeling yellow) (Figure 5B). Images were taken at a total magnification of 100X and 400X from active EAE 12 group.

5.6.12 IMMUNOHISTOCHEMICAL ANALYSIS OF CX3CR1 PROTEIN EXPRESSION IN THE SPINAL CORD

The IHC double staining results (CX3CR1 labeling red and Neuron labeling green) showed CX3CR1 co-localized with neurons (labeling yellow) (Figure 6A) and (CX3CR1 labeling red and CD68 labeling green) CX3CR1 co-localized with microglia (labeling yellow) (Figure 6B). Images were taken at a total magnification of 100X and 400X from active EAE 12 group.

5.7 SUMMARY

We demonstrate significantly increased CX3CL1 gene and protein levels in the DRG and spinal cord correlating with peak neurological disability and sensory thermal hypoalgesia in an EAE animal model of MS.

We demonstrate significantly increased CX3CR1 gene and protein levels in the DRG and spinal cord correlating with peak neurological disability and sensory thermal hypoalgesia in an EAE animal model of MS.

We identify that neurons and astrocytes are expressing CX3CL1 in the spinal cord in an EAE animal model of MS.

We identify that neurons and microglia are expressed CX3CR1 in the spinal cord in an EAE animal model of MS.

5.8 DISCUSSION

In this study, we demonstrated significant changes in CX3CL1 and its receptor CX3CR1 in the EAE rat model of MS. MS is an autoimmune disease with biphasic progression, with an initial inflammatory phase followed by a second demyelinating phase [15]. Thus the EAE rat model is an ideal model to identify the molecular mechanisms underlying the inflammatory phase of the disease process [15]. Neuropathic pain has been reported as the secondary worst disease induced symptoms in patients [20]. Interestingly, neuropathic pain is also reported to be present in MS patients prior to the time of diagnosis and therefore, may be a promising prediagnostic indicator to facilitate the early diagnosis of MS. Previous studies have shown that EAE animals also experience neuropathic pain as part of their disease progression [17]. Further, we have previously shown that levels of pain mediators are significantly increased in the DRG and spinal cord of EAE [15]. CX3CL1 and CX3CR1 are established factors in the modulation of pain perception via a central pro-algesic mechanism [21] Our study demonstrates increased CX3CL1 expression during the inflammatory phase of disease, which correlates with the onset of neurological disability and neuropathic pain in the EAE rat.

CX3CL1 is the only member of the fourth group of chemokines with the CX3C motif. It exists in two forms; membrane-bound, tethered to the cell membrane by a mucin-like stalk and as a soluble protein following cleavage. CX3CL1 is constitutively expressed by neurons in the brain, spinal cord and DRG [11]. Under normal physiological conditions, membrane-bound CX3CL1 is cleaved by ADAM17 (a matrix metalloproteinase formerly known as TNF converting enzyme [TACE]) to release soluble CX3CL1 [22]. In inflammatory states, increased expression of

CX3CL1 occurs in neurons, and also in astrocytes in the dorsal horn of the spinal cord [23]. Interestingly, peripheral nerve injury results in a decrease in membrane bound CX3CL1 DRG neurons [24], but not in the dorsal horn of the spinal cord [11]. The CX3CL1 receptor, CX3CR1, is constitutively expressed in microglia of the brain and spinal cord (Nishiyori, Minami et al. 1998; Lindia, McGowan et al. 2005), and is significantly increased as a result of microglial activation [11]. CX3CR1 is known to be critical for the generation of neuropathic pain, as mice lacking CX3CR1 do not develop allodynia following peripheral nerve injury [25].

Injured neurons release ATP, which binds to the P2X7 receptor on microglia, which results in the release of the protease Cathepsin S [26]. CX3CL1 is bound to the neuronal membrane, and is cleaved by the Cathepsin S. Soluble CX3CL1 binds to the CX3CR1 on microglia resulting in the increased synthesis and release of pro-nociceptive mediators such as IL-6 and nitric oxide [27]. These bind to receptors on dorsal horn neurons, resulting in the hypersensitivity and spontaneous firing that characterises central pain [27]. In addition, these nociceptive factors activate further microglia in a feedback loop that maintains the CX3CL1/CX3CR1 signalling pathway. Early studies have shown that CX3CL1 and CX3CR1 play important roles in neuron-glia communication. In our previous study, we showed significantly up-regulation of the pro-inflammatory cytokine TNF at the gene and protein levels within the DRG and spinal cord in the EAE model [15]. Recent research has shown that TNF induces CX3CL1 expression in endothelial cells [28]. Further, TNF also has functional implications in the post-transcriptional regulation of CX3CL1 [29]. These findings indicate that TNF is a factor inducing CX3CL1 production. Thus, our studies indicate that up-regulation of TNF in the DRG and spinal cord might regulate pain induction via CX3CL1 in MS. Further studies are required to confirm this hypothesis.

Our data show significant changes in CX3CL1 and its receptor CX3CR1 at both gene and protein levels in the DRG and spinal cord. These changes only occurred after onset of neurological disability and the onset of neuropathic pain, and were not detected in active control and naïve groups. Thus, we can conclude that changes in CX3CL1 and CX3CR1 expression levels are the direct result of activation of the immune response by CNS-myelin-specific antigens. Changes in the expression of CX3CL1 and CX3CR1 correlate with the onset of hypoalgesia confirmed by the behavioral studies conducted in our EAE model of MS. Based on the experimental findings of our research, we propose that CX3CL1 plays a role in MS induced neuropathic pain based on the signaling crosstalk between neurons and microglia in the spinal cord. In our study, the up-regulated expression of CX3CL1 and CX3CR1 correlated with the hypoalgesic phase of neuropathic pain. Neuropathic pain is characteristic of the EAE models of MS [17]. The current study, added to our previous studies, provide evidence that TNF may be a critical regulatory protein involved in the induction of neuropathic pain. However, it is still unclear how the synthesis and secretion of CX3CL1 are regulated and what the pathways of CX3CL1 signaling in glia cells. Further studies are required to study the effect of TNF on production of CX3CL1 in spinal cord neurons, astrocytes and microglia.

Our study demonstrated that in an inflammatory state, CX3CL1 is expressed in neurons and astrocytes, and its receptor CX3CR1 is expressed predominantly in microglia. A remarkable finding of our study is that in the EAE model, CX3CL1 and its receptor show significant changes in expression pattern that correlates with the onset of pain, indicating that the activation of glial cells by an inflammatory response leads to increase pain signaling between neurons and microglia. Our finding that CX3CR1 immunoreactivity is localized on microglia and neurons in the rat spinal cord is interesting because CX3CR1 is usually expressed on microglia in the CNS

[21]. Thus our findings indicate that neuronal expression of CX3CR1 occurs as a direct result of CNS inflammation. This expression change may be a critical mechanism involved in MS induced neuropathic pain. Further, our study demonstrated that CX3CL1 is expressed in neurons, but its receptor CX3CR1 is expressed predominately in microglia. This finding is in concordance with previously published studies showing that CX3CL1 works as a molecule signaling from neuron to microglia to induce glia activation. Spinal cord microglia and astrocytes have been shown to be involved in various types of neuropathic pain such as peripheral nerve injury, bone cancer and spinal root constriction [29, 30]. The activation of glia is directly involved in inflammatory and neuropathic pain. Recent research has shown that administration of glial inhibitors exerts anti-allodynic function [31]. In addition, we found that astrocytes also express CX3CL1 in the EAE spinal cord, indicating that activated astrocytes is also involved in the EAE rat model of MS.

Our data strongly suggests that in the early inflammatory stage of MS prior to demyelination, CX3CL1 signaling in dorsal horn neurons in the spinal cord activates the ascending pathways involved in pain transmission. Interestingly, increased serum levels of CX3CL1 are seen in MS patients, without significant changes in CX3CL1 levels in the cerebral spinal fluid (CSF) [32]. Studies are ongoing, to investigate the correlation between serum levels of CX3CL1 in patients with relapsing remitting MS, at different stages of their disease (relapse vs. stable remission phase). Our studies suggest that CX3CL1 may be an easily assessed marker of MS induced neuropathic pain that will serve as a diagnostic marker to assist in the treatment regime for MS patients.

5.8.1 ACKNOWLEDGEMENTS

We would like to thank our funding & supporting agencies: Biogen Idec Canada Inc (MN & EEF), Manitoba Medical Services Foundation (EEF & MN), Manitoba Institute of Child Health (MN & EEF), Manitoba Health Research Council (EEF), Pfizer UK Global (MN & EEF), Pfizer Canada (MN & EEF), and Purdue Pharma (MN & EEF). WZ was the recipient of a Canada Millennium Scholarship Foundation award.

Statement of interest

The authors confirm that there are no conflicts of interest.

5.9 REFERENCES

1. Namaka, M.P., Ethans, K., Jensen, B., Esfahani, F. & Frost, E.E. (2011) Multiple Sclerosis *Therapeutic Choices/e-Therapeutic*. Canadian Pharmacists Association Publishers, Inc, pp. 309-319.
2. Zhu, W., Le Dorze, J.A., Prout, M., Frost, E.E. & Namaka, M.P. (2010) An Overview of Relapsing Remitting Multiple Sclerosis (RRMS) and Current Treatment Options. *Pharmacy Practice* 9.
3. Ransohoff, R.M. (2009) Chemokines and chemokine receptors: standing at the crossroads of immunobiology and neurobiology. *Immunity* 31, 711-721.

4. Karpus, W.J. (2001) Chemokines and central nervous system disorders. *J Neurovirol* 7, 493-500.
5. Bazan, J.F., Bacon, K.B., Hardiman, G., Wang, W., Soo, K., Rossi, D., Greaves, D.R., Zlotnik, A. & Schall, T.J. (1997) A new class of membrane-bound chemokine with a CX3C motif. *Nature* 385, 640-644.
6. Chapman, G.A., Moores, K., Harrison, D., Campbell, C.A., Stewart, B.R. & Strijbos, P.J. (2000) Fractalkine cleavage from neuronal membranes represents an acute event in the inflammatory response to excitotoxic brain damage. *J Neurosci* 20, RC87.
7. Harrison, J.K., Jiang, Y., Chen, S., Xia, Y., Maciejewski, D., McNamara, R.K., Streit, W.J., Salafranca, M.N., Adhikari, S., Thompson, D.A., Botti, P., Bacon, K.B. & Feng, L. (1998) Role for neuronally derived fractalkine in mediating interactions between neurons and CX3CR1-expressing microglia. *Proceedings of the National Academy of Sciences of the United States of America* 95, 10896-10901.
8. Haskell, C.A., Hancock, W.W., Salant, D.J., Gao, W., Csizmadia, V., Peters, W., Faia, K., Fituri, O., Rottman, J.B. & Charo, I.F. (2001) Targeted deletion of CX(3)CR1 reveals a role for fractalkine in cardiac allograft rejection. *J Clin Invest* 108, 679-688.
9. Lamb, B. (2012) The roles of fractalkine signaling in neurodegenerative disease. *Mol Neurodegener* 7 Suppl 1, L21.
10. Nishiyori, A., Minami, M., Ohtani, Y., Takami, S., Yamamoto, J., Kawaguchi, N., Kume, T., Akaike, A. & Satoh, M. (1998) Localization of fractalkine and CX3CR1 mRNAs in rat brain: does fractalkine play a role in signaling from neuron to microglia? *FEBS Letters* 429, 167-172.
11. Verge, G.M., Milligan, E.D., Maier, S.F., Watkins, L.R., Naeve, G.S. & Foster, A.C. (2004) Fractalkine (CX3CL1) and fractalkine receptor (CX3CR1) distribution in spinal cord and dorsal

12. Hu, P., Bembrick, A.L., Keay, K.A. & McLachlan, E.M. (2007) Immune cell involvement in dorsal root ganglia and spinal cord after chronic constriction or transection of the rat sciatic nerve. *Brain Behav Immun* 21, 599-616.
13. Holmes, F.E., Arnott, N., Vanderplank, P., Kerr, N.C., Longbrake, E.E., Popovich, P.G., Imai, T., Combadiere, C., Murphy, P.M. & Wynick, D. (2008) Intra-neural administration of fractalkine attenuates neuropathic pain-related behaviour. *J Neurochem* 106, 640-649.
14. Johnston, I.N., Milligan, E.D., Wieseler-Frank, J., Frank, M.G., Zapata, V., Campisi, J., Langer, S., Martin, D., Green, P., Fleshner, M., Leinwand, L., Maier, S.F. & Watkins, L.R. (2004) A role for proinflammatory cytokines and fractalkine in analgesia, tolerance, and subsequent pain facilitation induced by chronic intrathecal morphine. *J Neurosci* 24, 7353-7365.
15. Zhu, W., Frost, E., Begum, F., Vora, P., Au, K., Gong, Y., Macneil, B., Pillai, P. & Namaka, M. (2011) The role of dorsal root ganglia activation and brain derived neurotrophic factor in multiple sclerosis. *J Cell Mol Med*.
16. Hargreaves, K., Dubner, R., Brown, F., Flores, C. & Joris, J. (1988) A new and sensitive method for measuring thermal nociception in cutaneous hyperalgesia. *Pain* 32, 77-88.
17. Aicher, S.A., Silverman, M.B., Winkler, C.W. & Bebo Jr, B.F. (2004) Hyperalgesia in an animal model of multiple sclerosis. *Pain* 110, 560-570.
18. Sporkel, O., Uschkureit, T., Bussow, H. & Stoffel, W. (2002) Oligodendrocytes expressing exclusively the DM20 isoform of the proteolipid protein gene: myelination and development. *Glia* 37, 19-30.
19. Bradford, M.M. (1976) A rapid and sensitive method for the quantitation of microgram quantities of protein utilizing the principle of protein-dye binding. *Anal Biochem* 72, 248-254.

20. Namaka, M., Turcotte, D., Leong, C., Grossberndt, A. & Klassen, D. (2008) Multiple sclerosis: etiology and treatment strategies. *Consult Pharm* 23, 886-896.
21. D'Haese, J.G., Demir, I.E., Friess, H. & Ceyhan, G.O. (2010) Fractalkine/CX3CR1: why a single chemokine-receptor duo bears a major and unique therapeutic potential. *Expert Opin Ther Targets* 14, 207-219.
22. Ludwig, A., Hundhausen, C., Lambert, M.H., Broadway, N., Andrews, R.C., Bickett, D.M., Leesnitzer, M.A. & Becherer, J.D. (2005) Metalloproteinase inhibitors for the disintegrin-like metalloproteinases ADAM10 and ADAM17 that differentially block constitutive and phorbol ester-inducible shedding of cell surface molecules. *Comb Chem High Throughput Screen* 8, 161-171.
23. Lindia, J.A., McGowan, E., Jochnowitz, N. & Abbadie, C. (2005) Induction of CX3CL1 expression in astrocytes and CX3CR1 in microglia in the spinal cord of a rat model of neuropathic pain. *J Pain* 6, 434-438.
24. Zhuang, Z.Y., Kawasaki, Y., Tan, P.H., Wen, Y.R., Huang, J. & Ji, R.R. (2007) Role of the CX3CR1/p38 MAPK pathway in spinal microglia for the development of neuropathic pain following nerve injury-induced cleavage of fractalkine. *Brain Behav Immun* 21, 642-651.
25. Staniland, A.A., Clark, A.K., Wodarski, R., Sasso, O., Maione, F., D'Acquisto, F. & Malcangio, M. (2010) Reduced inflammatory and neuropathic pain and decreased spinal microglial response in fractalkine receptor (CX3CR1) knockout mice. *J Neurochem* 114, 1143-1157.
26. Coddou, C., Stojilkovic, S.S. & Huidobro-Toro, J.P. (2011) Allosteric modulation of ATP-gated P2X receptor channels. *Rev Neurosci* 22, 335-354.

27. Milligan, E.D., Sloane, E.M. & Watkins, L.R. (2008) Glia in pathological pain: A role for fractalkine. *Journal of Neuroimmunology* 198, 113-120.
28. Melanson, M., Miao, P., Eisenstat, D., Gong, Y., Gu, X., Au, K., Zhu, W., Begum, F., Frost, E. & Namaka, M. (2009) Experimental autoimmune encephalomyelitis-induced upregulation of tumor necrosis factor-alpha in the dorsal root ganglia. *Mult Scler* 15, 1135-1145.
29. Sung, M.J., Kim, D.H., Davaatseren, M., Hur, H.J., Kim, W., Jung, Y.J., Park, S.K. & Kwon, D.Y. (2010) Genistein suppression of TNF-alpha-induced fractalkine expression in endothelial cells. *Cell Physiol Biochem* 26, 431-440.
30. Watkins, L.R. & Maier, S.F. (2003) Glia: a novel drug discovery target for clinical pain. *Nat Rev Drug Discov* 2, 973-985.
31. Sweitzer, S., Martin, D. & DeLeo, J.A. (2001a) Intrathecal interleukin-1 receptor antagonist in combination with soluble tumor necrosis factor receptor exhibits an anti-allodynic action in a rat model of neuropathic pain. *Neuroscience* 103, 529-539.
31. Sweitzer, S., Martin, D. & DeLeo, J.A. (2001b) Interleukin-1 receptor antagonist in combination with soluble tumor necrosis factor receptor exhibits an anti-allodynic action in a rat model of neuropathic pain. *Neuroscience* 103, 541-550.
32. Kastenbauer, S., Koedel, U., Wick, M., Kieseier, B.C., Hartung, H.P. & Pfister, H.W. (2003) CSF and serum levels of soluble fractalkine (CX3CL1) in inflammatory diseases of the nervous system. *J Neuroimmunol* 137, 210-217.

5.10 FIGURES

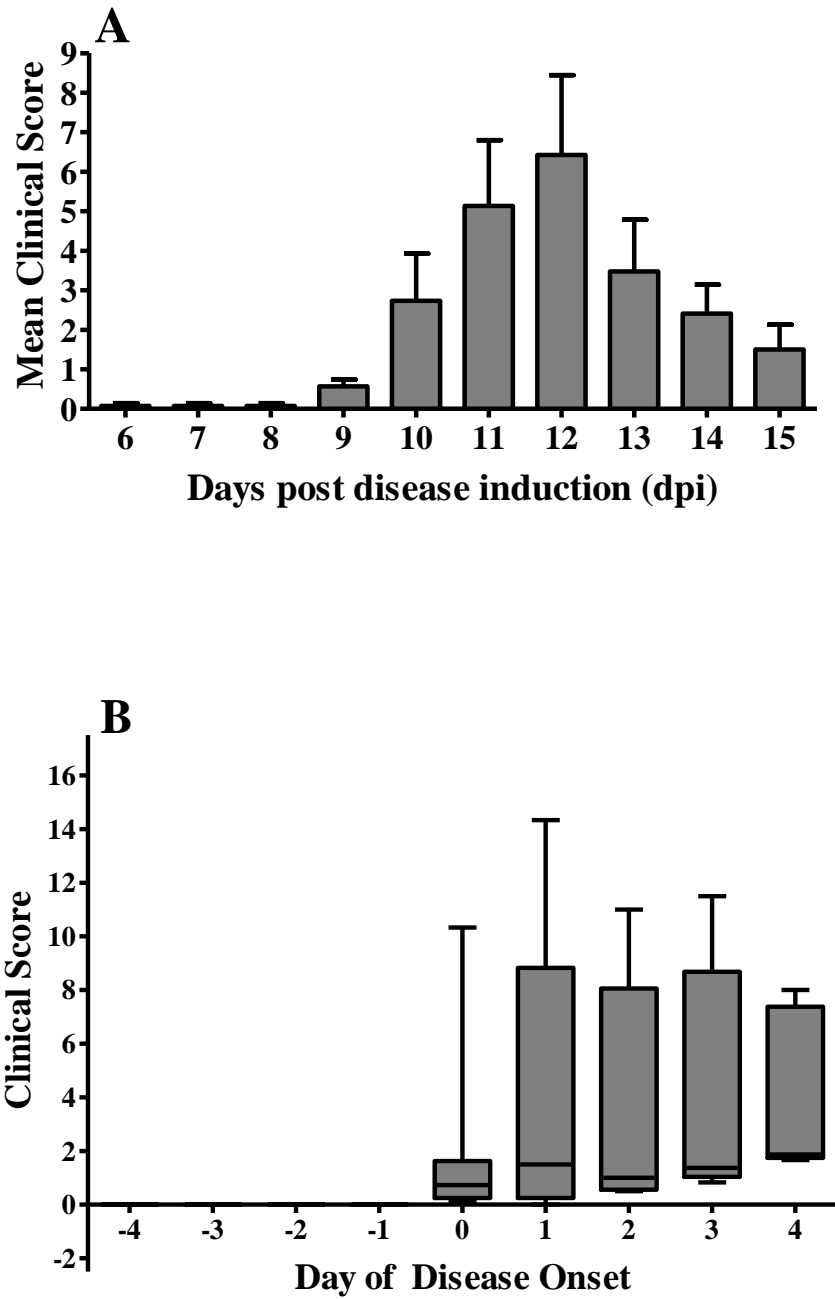
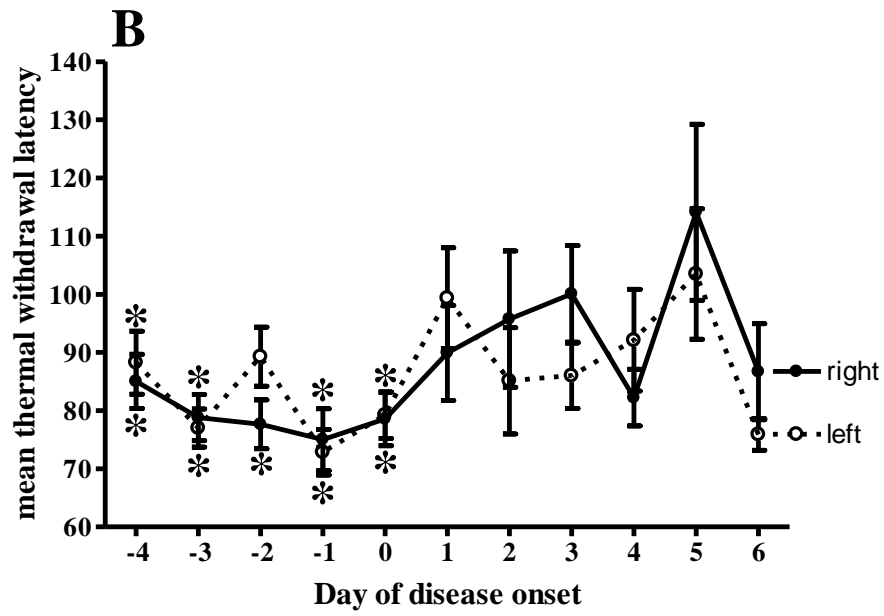
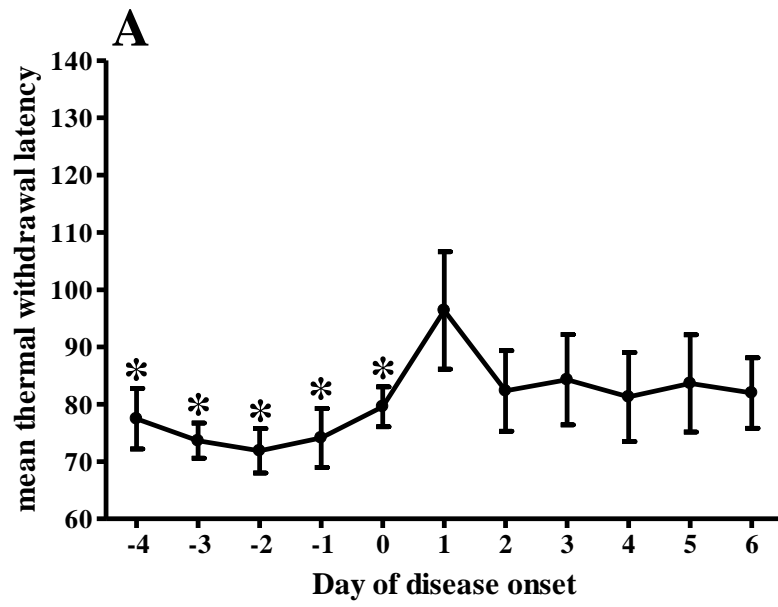


Figure 1 – Neurological disability scores



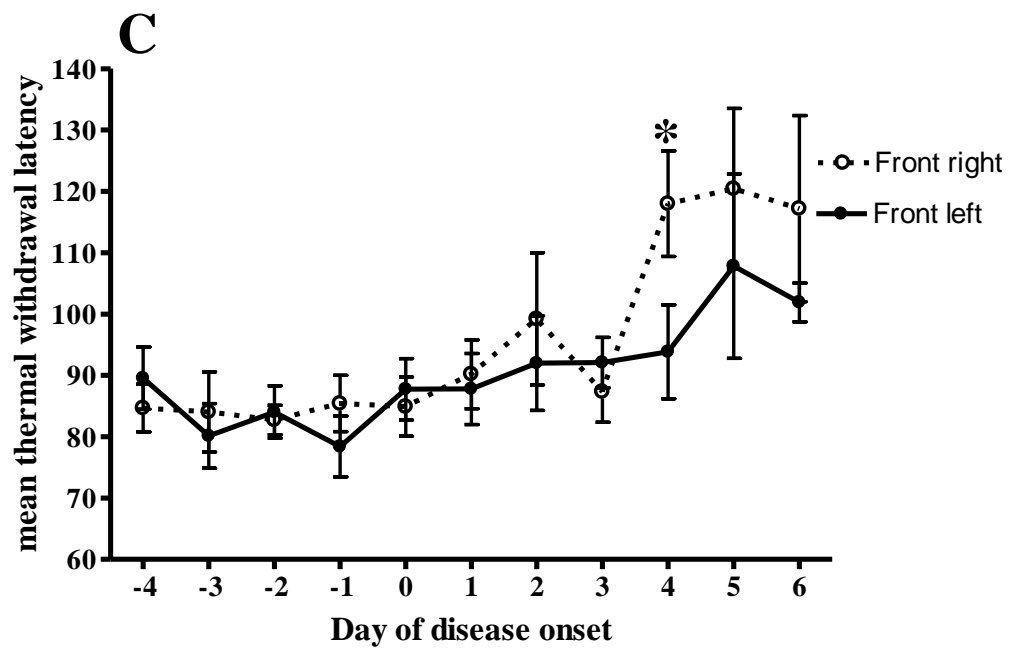
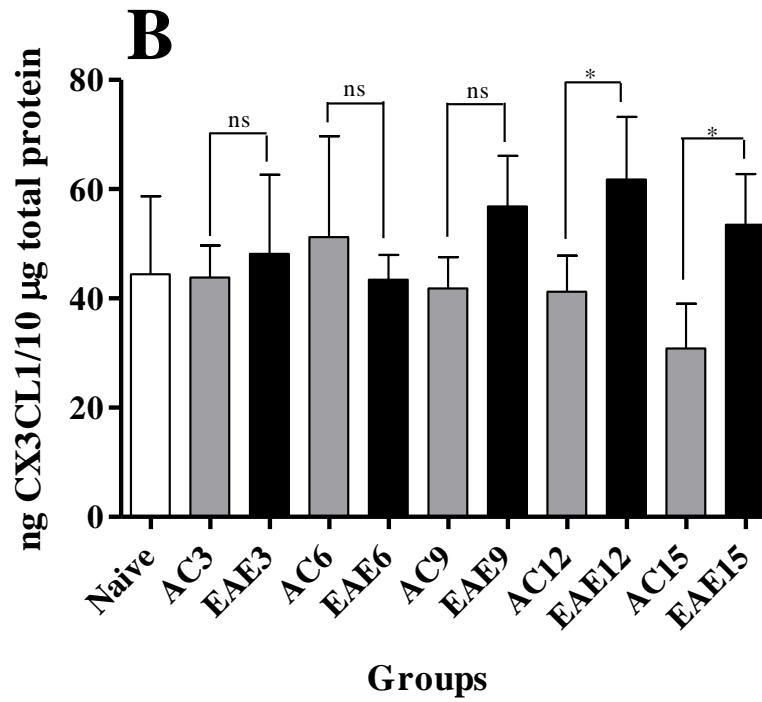
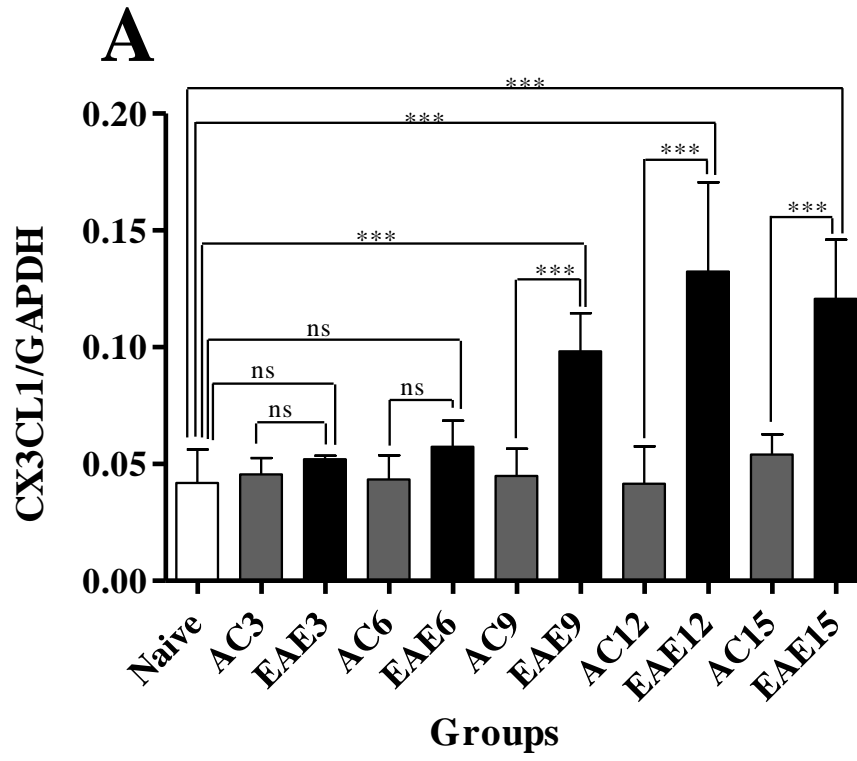


Figure 2- EAE animals thermal sensory testing in the limbs



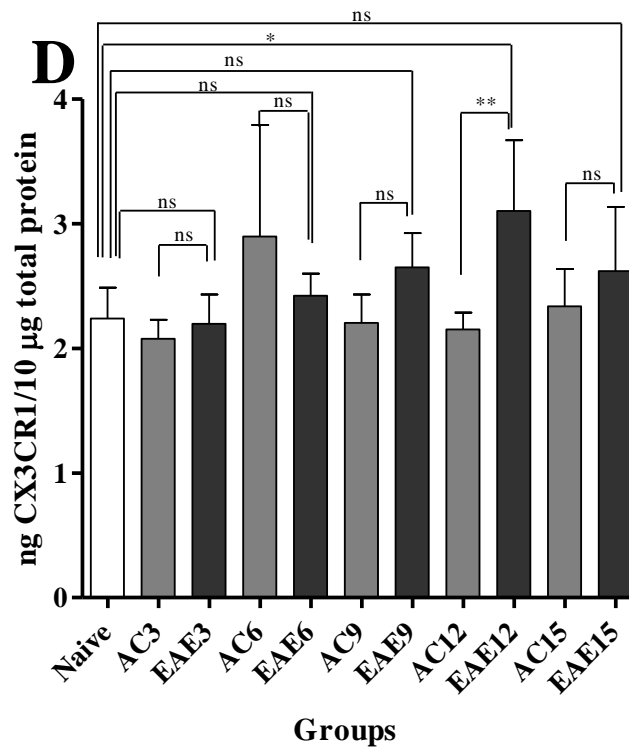
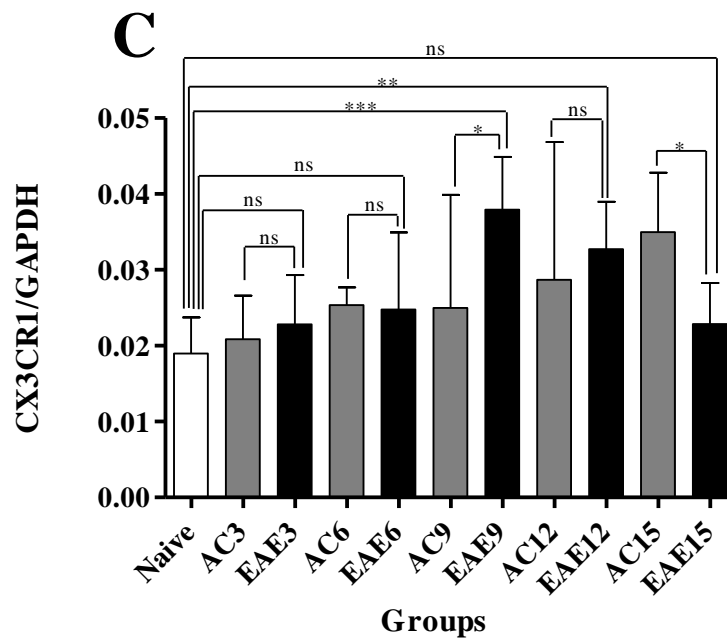
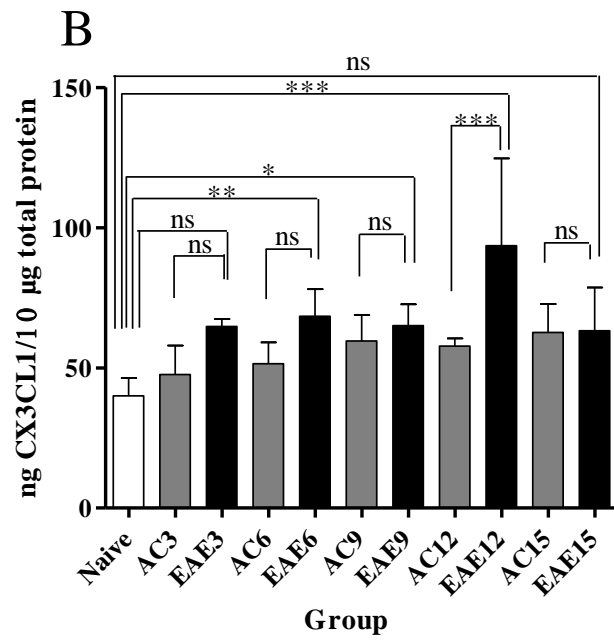
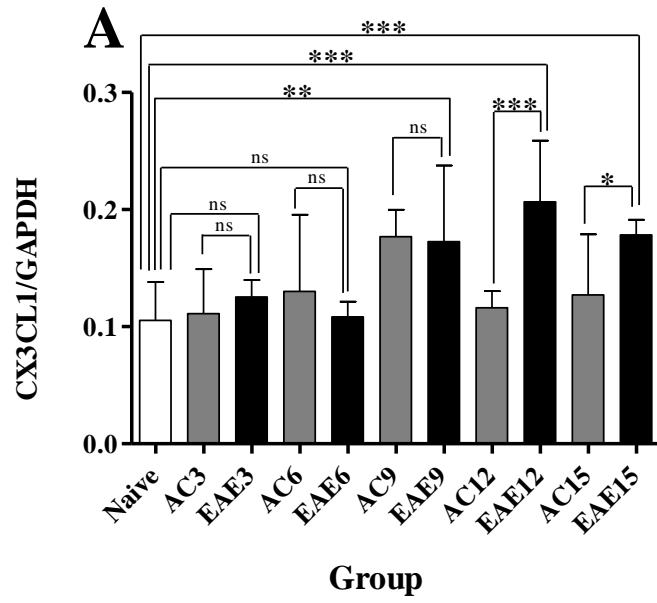


Figure 3- DRG expression of CX3CL1 and its receptor CX3CR1 mRNA and protein in EAE



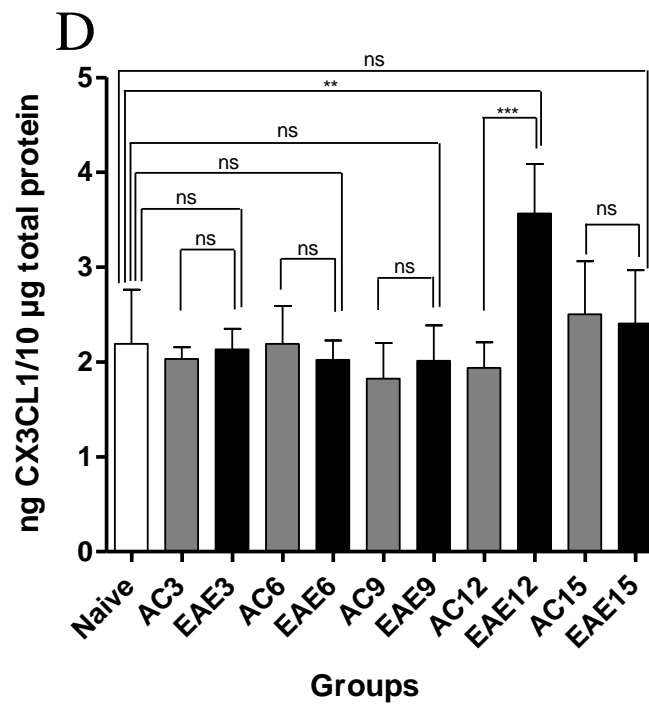
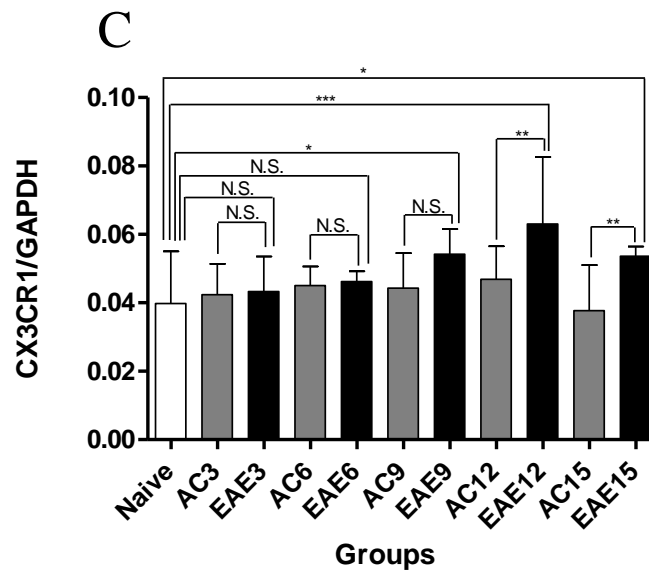


Figure 4- Spinal cord expression of CX3CL1 and its receptor CX3CR1 mRNA and protein in EAE

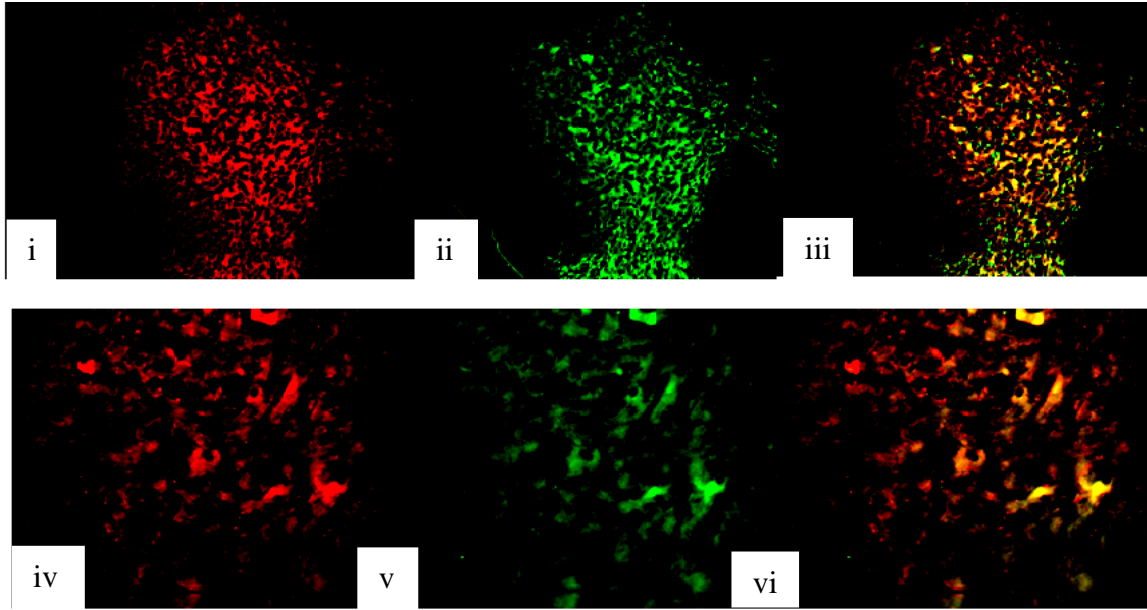


Figure 5A – CX3CL1 and NeuN double staining in spinal cord

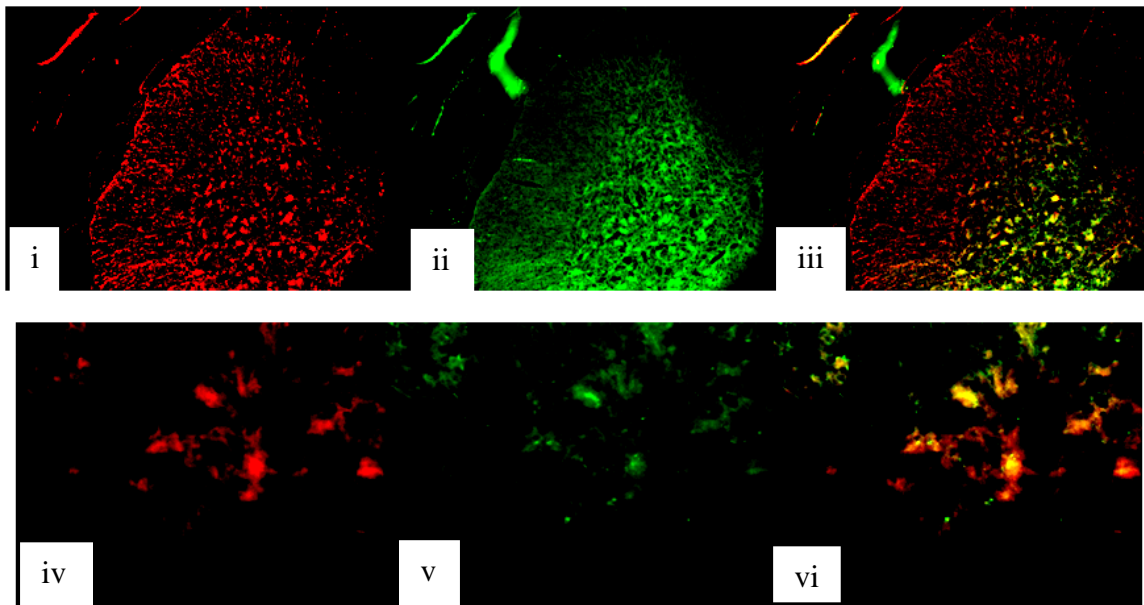


Figure 5B – CX3CL1 and GFAP double staining in spinal cord

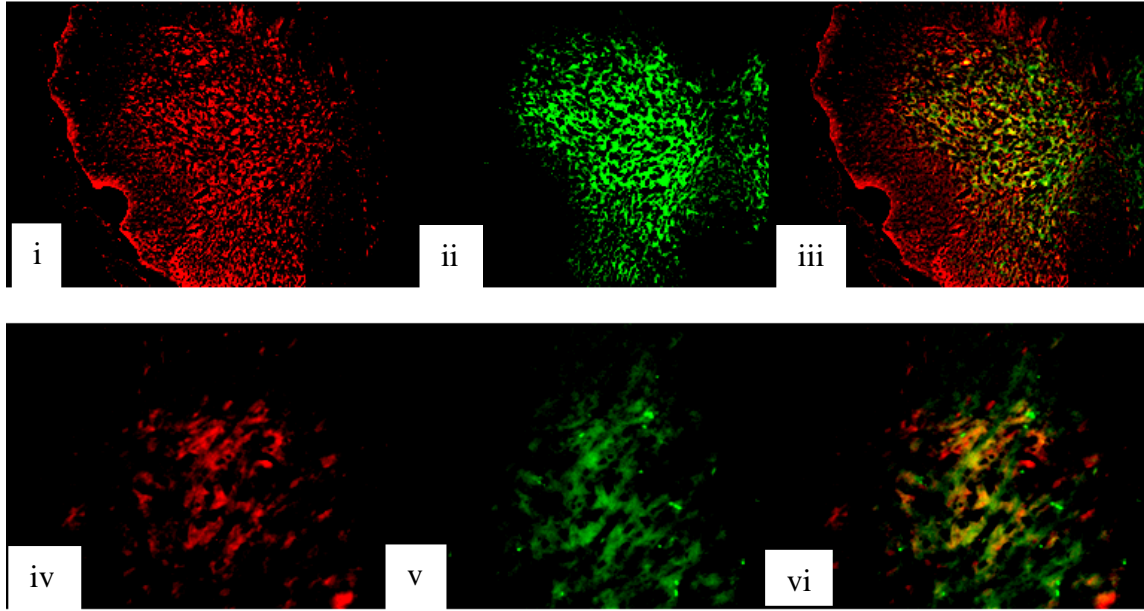


Figure 6A– CX3CR1 and CD68 double staining in spinal cord

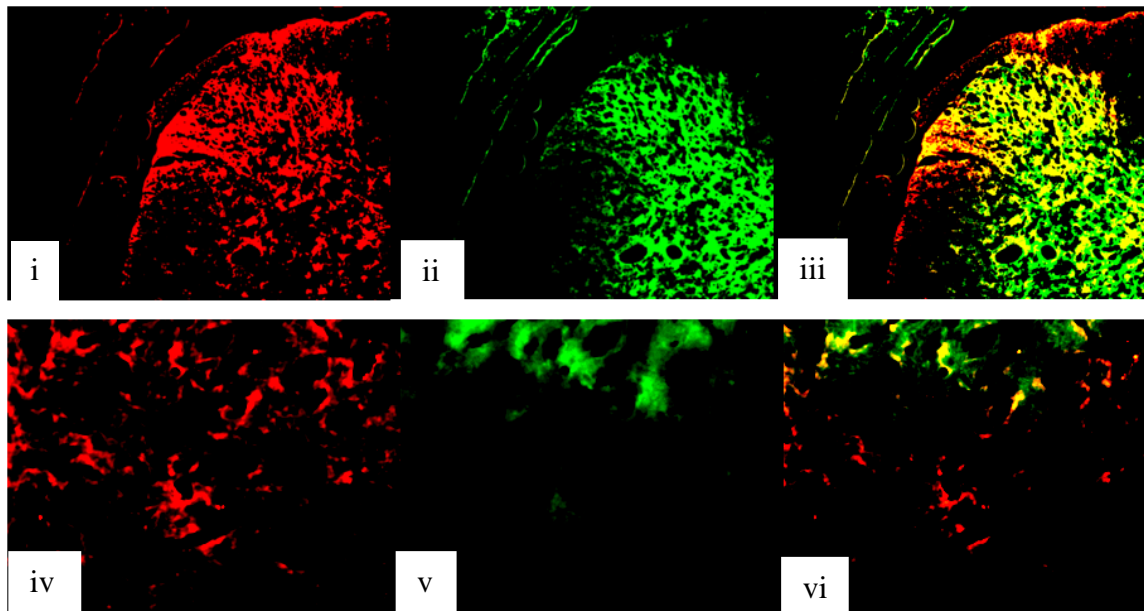


Figure 6B– CX3CR1 and NeuN double staining in spinal cord

5.11 FIGURE LEGENDS

Figure 1- EAE animals Neurological Disability Clinical Score

Panel A - All animals in the EAE groups were assessed for neurological disability according to a previously described global neurological disability assessment tool (Melanson, Miao et al. 2009; Zhu, Frost et al. 2011). Clinical neurological deficits appear at 6 days post induction (dpi). By 9 dpi all animals started to display clinical signs of neurological disability (mean 0.57 ± 0.45). Neurological disability progressively worsened upon daily assessment until 12 dpi (peak disability; mean 6.42 ± 5.35), then subsided by 15 dpi (mean 1.5 ± 1.41) as the animals entered the remission phase of disease induction, well characterized for this animal model (Figure 1).

Panel B – Box and whisker plot of the mean neurological disability score plotted by day of disease onset shows the variation of clinical symptoms seen in this model. On the first day of disease onset the mean NDS is 1.98 ± 3.2 with a range of 0 to 10, on the second day the mean NDS is 4.01 ± 4.90 with a range of 0 to 14.

Figure 2- EAE animals thermal sensory testing

Panel A - This figure illustrates thermal sensory testing results in the tails from EAE animals, at different times in the disease progression. Normalized thermal withdrawal latencies in EAE15 rats for tail relative to time of disease onset (Day 0 is the first day of clinical symptoms/signs for each individual animal). Values are normalized to average baseline responses prior to disease induction and displayed as means \pm standard deviations. Withdrawal latencies were significantly elevated at day 1 compared to the previous 5 days ($*=p=0.023$ using a one sample t-test assuming a theoretical mean of 100%).

Panel B - This figure illustrates thermal sensory testing results in the limbs from EAE animals, at different times in the disease progression. Data are aligned to day of onset of clinical disease; Day 0 is the first day of clinical symptoms/signs for each individual animal. Withdrawal latencies were significantly elevated at day 4 compared to all days before except Day 3 (Repeated measures ANOVA, $p > 0.05$, Tukey's posthoc test). ANOVA by SITE for DAY effect is significant for front right, front left and rear left.

Figure 3- DRG expression of CX3CL1 and its receptor CX3CR1 mRNA and protein in EAE

Panel A - This figure illustrates CX3CL1 mRNA expression in the DRG, at different times in the disease progression. Naïve control (white bars) levels are significantly lower than CX3CL1 levels in the EAE rat spinal cord (black bars) at days 9, 12 and 15. In addition, at days 9, 12 and 15, EAE levels of CX3CL1 mRNA are significantly higher than in active control tissue (grey bars) from the same time points. (* = $P < 0.05$; ** = $P < 0.01$; *** = $P < 0.005$; ns = Not Significant, ANOVA followed by Tukey's posthoc test).

Panel B - This figure illustrates total CX3CL1 protein expression in the DRG, at different times in the disease progression. At days 12 and 15, EAE tissue (black bars) has significantly higher levels of CX3CL1 protein compared to active control tissue on the same day (grey bars). (* = $P < 0.05$; ns = Not Significant, ANOVA followed by Tukey's posthoc test).

Panel C - This figure illustrates total CX3CR1 mRNA expression in DRG at different times in the disease progression. At days 9 and 12, EAE DRG (black bars) has significantly higher CX3CR1 mRNA levels than naïve control (white bars) and active control tissue (grey bars).

There is a significant difference between active control and EAE DRG mRNA levels. (* = $P < 0.05$; ** = $P < 0.01$; *** = $P < 0.005$; ns = Not Significant, ANOVA followed by Tukey's posthoc test).

Panel D - This figure illustrates total CX3CR1 protein expression in the DRG at different times in the disease progression. Protein levels of CX3CR1 are significantly higher in DRG at day 12 in EAE animals (black bars) compared to both naïve control (white bars) and active control (grey bars). There are no other significant differences in the expression levels of CX3CR1 in the DRG at different times during the disease progression. (* = $P < 0.05$; ** = $P < 0.01$; ns = Not Significant, ANOVA followed by Tukey's posthoc test).

Figure 4 - Spinal cord expression of CX3CL1 and its receptor CX3CR1 mRNA and protein in EAE

Panel A - This figure illustrates CX3CL1 mRNA expression in the spinal cord at different times in the disease progression. Naïve control (white bars) levels are significantly lower than CX3CL1 levels in the EAE rat spinal cord (black bars) at days 9, 12 and 15. In addition, at days 12 and 15, EAE levels of CX3CL1 mRNA are significantly higher than in active control tissue (grey bars) from the same time points. (* = $P < 0.05$; ** = $P < 0.01$; *** = $P < 0.005$; ns = Not Significant, ANOVA followed by Tukey's posthoc test).

Panel B - This figure illustrates total CX3CL1 protein expression in the spinal cord, at different times in the disease progression. Naïve control (white bars) levels are significantly lower than CX3CL1 levels in the EAE rat spinal cord (black bars) at days 6, 9, and 12. In addition, at day 12 EAE levels of CX3CL1 protein are significantly higher than in active control tissue (grey bars) at

the same time point. (* = $P < 0.05$; ** = $P < 0.01$; *** = $P < 0.005$; ns = Not Significant, ANOVA followed by Tukey's posthoc test).

Panel C - This figure illustrates CX3CR1 mRNA expression in the spinal cord, at different times in the disease progression. Naïve control (white bars) levels are significantly lower than CX3CR1 levels in the EAE rat spinal cord (black bars) at days 9, 12 and 15. In addition, at days 12 and 15, EAE levels of CX3CR1 mRNA are significantly higher than in active control tissue (grey bars) from the same time points. (* = $P < 0.05$; ** = $P < 0.01$; *** = $P < 0.005$; ns = Not Significant, ANOVA followed by Tukey's posthoc test).

Panel D - This figure illustrates total CX3CR1 protein expression in the spinal cord, at different times in the disease progression. Levels of CX3CR1 protein in the spinal cord are significantly increased in the EAE tissue (black bars) relative to both naïve control (white bars) and active controls (grey bars). There are no other significant differences. (** = $P < 0.01$; ns = Not Significant, ANOVA followed by Tukey's posthoc test).

Figure 5 – CX3CR1 expression in the spinal cord of EAE rats at day 12 post disease induction.

Panel A - This figure shows significantly increased immunoreactivity to CX3CR1 (panes i & iv: red) in neurons (NeuN: panes ii & v: green). CX3CR1 co-localizes with neurons (pane iii & vi: yellow). Images were taken at a total magnification of 100X (panes i-iii) and 400X (panes iv-vi) from active EAE 12 group.

Panel B - This figure illustrates significantly increased immunoreactivity to CX3CL1 (panes i & iv: red) in astrocytes (GFAP: panes ii & v: green). CX3CL1 co-localized with astrocytes (panes iii & vi: yellow). Images were taken at a total magnification of 100X (panes i-iii) and 400X (panes iv-vi) from active EAE 12 group.

Figure 6 – CX3CR1 expression in the spinal cord of EAE rats at 12 days post disease induction.

Panel A - This figure shows significantly increased immunoreactivity to CX3CR1 (panes i & iv: red) in microglia (CD68: panes ii & v: green). CX3CR1 co-localizes with microglia (pane iii & vi: yellow). Images were taken at a total magnification of 100X (panes i-iii) and 400X (panes iv-vi) from active EAE 12 group.

Panel B - This figure illustrates increased immunoreactivity to CX3CR1 (panes i & iv: red) in neurons (NeuN: panes ii & v: green). CX3CR1 co-localized with neurons (panes iii & vi: yellow). Images were taken at a total magnification of 100X (panes i-iii) and 400X (panes iv-vi) from active EAE 12 group.

CHAPTER 6 - A NOVEL DECALCIFICATION METHOD FOR ADULT RODENT BONE FOR HISTOLOGICAL ANALYSIS OF PERIPHERAL-CENTRAL NERVOUS SYSTEM CONNECTIONS.

Authors and addresses- Farhana Begum, Wenjun Zhu, Michael P. Namaka, Emma E. Frost

Faculty of Pharmacy, University of Manitoba, Apotex Center, 750 McDermot Avenue, Winnipeg, Manitoba, Canada

This paper was published in Journal of Neuroscience Methods, 2010 Mar 15; 187(1):59-66. Epub 2009 Dec 28.

6.1 STATEMENT OF CONTRIBUTION

This technique was developed in order to allow the complete cryosectioning of bone encased CNS tissue that was critical for the success of my thesis work. I worked closely with another Masters student (Farhana Begum) in order to devise, troubleshoot and validate the novel technique for decalcifying bone without disrupting the structural integrity of the myelin of the CNS. I was specifically responsible for inducing EAE in the rats, harvesting the tissue, and dissecting out the spinal column segments. In addition I assisted with the calcium analysis, and immunohistochemical staining of the sections.

6.2 ABSTRACT

Histological analysis of bone-encased tissue is severely hampered by technical difficulties associated with sectioning calcified tissue. Cryosectioning of bone is possible but requires significant technical adaptation and expensive materials and is often time-consuming. Some decalcifying reagents in common use result in successful cryosectioning in less time but the integrity of the soft tissue of the spinal column is often compromised during processing. This can result in significant loss of cellular detail. In order to find a method that would allow cryosectioning of the bone without loss of structural integrity of the underlying soft tissue we assessed the efficacy of four different decalcifying reagents with respect to their effects on the cellular structure of the myelin of the grey and white matter of the spinal cord. The antigenic integrity of the spinal cord white matter was evaluated using tissue structural integrity and quality of myelin basic protein immunostaining. The result of this research shows that 6% TCA not only decalcifies intact spinal column suitably for cryosectioning but does so without compromising the antigenic integrity of the tissue. The ease of application, speed of processing and a favorable cost-effective profile were secondary benefits noted with the use of the 6% TCA decalcifying solution. The ability to utilize a decalcifying solution that allows for both histomorphometry and immunohistochemistry in the same spinal column segment represents a novel technique that will provide new insights into pathophysiological aspects and therapeutic approaches in spinal cord damage or disease.

6.3 KEYWORDS

Decalcification; 6% TCA; Immunohistochemistry; Cryosectioning; Spinal cord; Myelin basic protein; Antigenic integrity

6.4 INTRODUCTION

There are numerous animal models of central nervous system (CNS) disorders used by researchers worldwide [1-8]. A common feature of these animal models is the examination of the cellular and molecular signaling events underlying CNS disorders. Immunohistochemical examination of protein expression is frequently used for the analysis of spinal cord and brain tissue from animals of varying maturity. One of the greatest challenges to the successful completion of these studies is the ability to analyze the soft CNS tissue contained within the spinal column or cranium. In particular, the ability to analyze changes in myelin represents a critical aspect of many studies examining nervous tissue disease and damage. Myelin is a dynamic structure that wraps neuronal axons, facilitating normal nerve signal conduction, as well as maintaining the homeostasis of the periaxonal space [9-11]. The structural integrity of the myelin sheath is critical for normal neuronal function and can be used as a marker of neuronal damage [12,13]. In addition to myelin analysis, the ability to examine cell signaling from the peripheral to the central nervous systems via intact connections between dorsal and ventral root systems offers a distinct advantage to explore mRNA and protein transport.

Removal of brain and spinal cord tissue from the spinal column or cranium may cause damage that compromises the accurate analysis of tissue damage resulting from the injury or disease model. In addition, removal of the tissue from the bone breaks the delicate physical connections between the peripheral and central nervous systems in the region of the spinal roots and the dorsal root ganglia connections. Maintaining the integrity of the intact connections between the peripheral and central nervous systems is essential to the advanced understanding of the bi-directional cell signaling mechanisms that are involved in the development of disorders such as

MS and neuropathic pain [14-16]. Consequently, it is preferable to cryosection the tissue while it is still contained within the bone.

Investigation of the literature revealed several different techniques available for cryosectioning of bone tissue [17-19]. These techniques involve expensive tungsten carbide cryoblades, labor-intensive techniques using special tapes and glues to obtain usable sections [20], or expensive modifications of a standard cryostat [21]. Alternative techniques have used plastic embedding material such as methyl methacrylate (MMA) [22]. However, the extremely high temperatures required for plastic embedding of tissue frequently destroys the antigenicity of the very proteins under investigation [22]. As a result, many researchers have preferred to decalcify the bone prior to sectioning the tissue.

The calcium in bone is mainly in the form of insoluble salts. In order to successfully cryosection the bone, the insoluble calcium-phosphate crystals need to be solubilized. This can be achieved relatively easily using dilute strong acids (such as nitric or hydrochloric), chelating agents (such as EDTA), or weak acids (such as formic, acetic or picric acids). Removal of the calcium salts leaves a fibrous collagenous structure, which is easily sectioned. At present, there are several reagents available for use to decalcify bone to facilitate sectioning using a regular cryoblade. Commercial reagents include RDO-Gold and Krajian's Solution. RDO-Gold is a buffered solution of hydrochloric acid (<10%), which was formulated to facilitate rapid decalcification of bone tissue for histological analysis. Krajian's Solution, a modification of a decalcification technique first described in 1953, is a solution of formic acid and sodium citrate dihydrate. Other widely used decalcification solutions include EDTA-Glycerol solution [23-24] or trichloroacetic acid [25-27].

Most solutions used for decalcification allow accurate histological analysis of the neuronal tissue. However, nuclear antigens including Ki-67 that are commonly used in the analysis of CNS tissue are markedly reduced after acid decalcification protocols [27]. Further, decalcification often destroys tissue antigenicity [28], preventing accurate analysis of molecular expression in the CNS tissue. In our study, the structure of the myelin was significantly damaged by the commercially available decalcifying reagent RDO-Gold. Therefore, we set out to determine which of the available decalcification techniques was the most suitable for the analysis of CNS tissue. We used tissue obtained from a rodent experimental autoimmune encephalomyelitis (EAE) model of MS.

After decalcification, the spinal columns were cryosectioned at 10 μm and stained using hematoxylin and eosin for gross tissue morphology, and immunostained for MBP to assess the integrity of the myelin. In addition, we performed *in situ hybridization* on the tissue to ensure the mRNA was not damaged during processing. Further, we compared the time and cost of each reagent, in order to maximize resources. We found that of the four solutions tested, decalcification with trichloroacetic acid resulted in the best spinal cord integrity as judged by histological analysis of myelin structure and stability of the mRNA. In addition, the manpower and resources used for this method are the most cost-effective of the four solutions assessed.

6.5 MATERIALS AND METHODS

6.5.1. TISSUE PREPARATION

Female Sprague Dawley rats were deeply anaesthetized using an I.P. injection of Ketamine (Biospacific Emeryville, CA: cat. #: A52310) 30 mg/100 g and xylazine (Bayer Health Care,

Toronto, Ontario) 3 mg/100 g body weight diluted in saline. Full body perfusion was performed via intra-cardiac canulation using a pre-fixative solution containing 1U/ml heparin (LEO Pharma Inc., Thornhill, Ontario: DIN 00453811) and 1% sodium nitrate (ThermoFisher Scientific, Ottawa, Ontario: cat. # S343) in 0.9% sodium chloride (Sigma–Aldrich, Oakville, Ontario: cat. #S9625) at a volume equal to 1/3 of the animal's body weight. The animals were then perfused with a 4% paraformaldehyde (Sigma–Aldrich: cat. # 158127) in 0.1% NaPO₄ (ThermoFisher Scientific: cat. # S373) fixative buffer at a volume equal to 2× body weight of the animal. The whole vertebral column was removed, dissected free of surrounding soft tissue, and fixed in 4% paraformaldehyde for 24 h at 4 °C. All animal experiments were conducted in accordance with the University of Manitoba Animal Users and Protocol Management Review Committee protocols, which comply with the Canadian Council on Animal Care guidelines.

6.5.2. DECALCIFICATION

6.5.2.1. RDO-Gold (RDO-G) (less than 10% HCL)

After fixation, the vertebral column was washed in distilled water and divided into segments (<1 cm in each piece), according to the manufacturer's supplied specifications. This is to ensure that there is adequate perfusion of the solution throughout the specimen. The specimen was then placed into 6 ml RDO-Gold solution (Apex Engineering Products Corporation, Plainfield, IL). The progression of decalcification was checked with insertion of a sharp needle, as well as by chemical testing of the RDO-G solution every 30 min after the first 2.5 h (see below). The RDO-G solution was replaced each time. After decalcification in RDO-G, the specimen was rinsed in distilled water to remove excess RDO.

6.5.2.2. Krajian Decalcifying Solution

100 g/l sodium citrate, dihydrate, and 250 ml/l formic acid (88%) in water.

After fixation, the specimen was washed in PBS for 20 min. The whole vertebral column was then decalcified in Krajian solution (Mallinckrodt Baker, Phillipsburg New Jersey: cat. # G161-02) for 4 days at 4 °C. Incubation time was assessed at several time points using insertion of a sharp needle into the bone, and chemical testing of the Krajian solution, to determine the end-point of decalcification. After decalcification, the specimen was washed in PBS for 20 min prior to processing for sectioning.

6.5.2.3. EDTA–Glycerol Solution (EDTA-G)

After fixation, the spinal column was washed for 12 h at 4 °C in each of the following series of solutions: 0.01 M PBS containing 5% glycerol, 0.01 M PBS containing 10% glycerol (Mallinckrodt Baker Chemicals: cat. # 5092), and 0.01 M PBS containing 15% glycerol [29]. The specimen was then decalcified in EDTA-G solution (14.5 g EDTA (Sigma–Aldrich cat. # ED2P), 1.25 g NaOH (ThermoFisher Scientific: cat. # S318), and 15% glycerol in 100 ml distilled pH 7.3. The EDTA-G solution was replaced every 5 days as previously described [29]. The progression of decalcification was checked at several time points using insertion of a sharp needle into the bone and chemical testing. After decalcification in EDTA-G, the specimen was washed at 4 °C for 12 h in successive washes of 15% sucrose and 15% glycerol in PBS, 20% sucrose and 10% glycerol in PBS, 20% sucrose and 5% glycerol in PBS, 20% sucrose in PBS, 10% sucrose in PBS, 5% sucrose in PBS, and 100% PBS.

6.5.2.4. 6% Trichloroacetic Acid (TCA)

There are several published techniques using TCA to make a weak acid solution, mostly using a 5, 6 or 10% solution in distilled water. Previous studies have shown that 6% TCA decalcification preserves the immunoreactivity of laminin in bone [25] and [26]. Therefore, we assessed a 6% solution of TCA in distilled water. After fixation, the specimen was washed in PBS for 20 min. The whole vertebral column was then decalcified in 6% TCA (Sigma–Aldrich: cat. # T6399) in distilled water (this needs to be defined somewhere), for 5 days at 4 °C. Incubation time was assessed at several time points using insertion of a sharp needle into the bone and chemical testing, to determine the end-point of decalcification. After decalcification in 6% TCA, the vertebral column was washed in PBS for 20 min.

6.5.3. CHEMICAL TESTING OF CALCIUM EXTRACTION

To test for the presence of calcium in the decalcifying solution, 5 ml of the decalcifying solution was added to 1 ml of 5% ammonium oxalate, and left to stand for 5 min to check for the formation of a precipitate of calcium oxalate. If a precipitate formed, the decalcification was deemed incomplete. If a clear solution was obtained, indicating that no further calcium was being extracted from the sample, the decalcification process was deemed complete.

6.5.4. TISSUE PROCESSING FOR CRYOSECTIONING

After decalcification, the specimens were cryopreserved in 20% sucrose (MP Biomedicals, LLC, Solon, OH: cat. # 904713) in PBS for 24 h and 30% sucrose in PBS for another 24 h at 4 °C.

Vertebral columns were divided into segments (<1 cm), then placed in Tissue-Tek O.C.T. (Sakura Finetek, Torrance, CA: cat. # 4583) overnight at 4 °C. The pieces were then embedded in OCT and stored at -80 °C until cryosectioned.

Serial sections were cut at 10 µm using a Thermo Shandon CME cryostat, air dried onto SuperFrost microscope slides (ThermoFisher) and stored at -80 °C.

6.5.5. EVALUATION

The morphologic features of both hematoxylin and eosin (H&E) - and antibody-stained sections were evaluated for each decalcifying solution, and results obtained for each decalcifying solution were compared. The morphologic changes were subjectively evaluated by two of the authors (FB and EEF). MBP immunoreactivity was used to show preservation of myelin structure.

6.5.6. IMMUNOHISTOCHEMISTRY FOR MYELIN BASIC PROTEIN (MBP)

MBP IHC was performed as previously described [30]. Briefly, sections were thawed, washed with PBS, and then incubated in 100% methanol (ThermoFisher: cat. # A433P-4) for 10 min at room temperature. Non-specific binding of antibodies was blocked with normal donkey serum (NDS) (Sigma-Aldrich: cat. # D 9663) (20% in PBS) for 15 min. Sections were then incubated in goat anti-MBP (Santa Cruz, CA: cat. # 13914) at 1:50 dilution of stock in PBS + 5% NDS, for 60 min at room temperature. Sections were incubated in secondary antibody (TRITC conjugated Affinipure Donkey Anti-Goat IgG (Jackson ImmunoResearch, West Grove, Philadelphia: cat. # 705 025 147)) at 1:100 dilution in PBS, for 30 min at room temperature. Nuclei were

counterstained with DAPI (1 µg/ml; Sigma–Aldrich: cat. # D9542) and sections mounted on aqueous mounting medium (R&D Systems, Burlington, Ontario: cat. # CTS011).

6.5.7. IN SITU HYBRIDIZATION

In situ hybridization (ISH) was performed as previously described [31] and [2]. The probe sequence used was 5'-[AminoC6 + Dig]-GGA GGA GTC TTC CAG CTG GAG AAG GGG GAC-3', which detects chloride intracellular channel 1 (CLIC1). The probe was labeled with digoxigenin (DIG) post synthesis by EurofinOPERON (Huntsville, Alabama). Digoxigenin was detected with an alkaline phosphatase conjugated sheep anti-digoxigenin antibody (Roche Applied Science, Laval, Quebec, cat. # 11093274910), followed by reaction with NBT/BCIP substrate (DAKO, Carpinteria, CA, cat. # K0598).

6.5.8. IMAGING

Imaging was performed using an inverted Olympus IX51 microscope with EXFO X-CITE 120 W metal halide fluorescent light source. Images were captured in Image Pro 7 via a c-mounted RETIGA 2000RV monochrome camera. Confocal imaging was performed using an Olympus BX51 configured with FV5000 Confocal laser scanning capability. Images were captured in Fluoview Version 4.3.

6.6 RESULTS

6.1. MORPHOLOGICAL ASSESSMENT

We found that treatment with all four decalcifying solutions resulted in sufficient decalcification to allow for easy cryosectioning of the spinal column at 10 μm . Further, all four treatments resulted in preservation of the peripheral–central nervous system connections within the spinal column. Using H&E staining to assess the morphology of the spinal cord tissue, we found that none of the treatments significantly affected the gross cellular structure of the spinal column. All sections assessed showed clear definition of the gross tissue structure (Fig. 1).

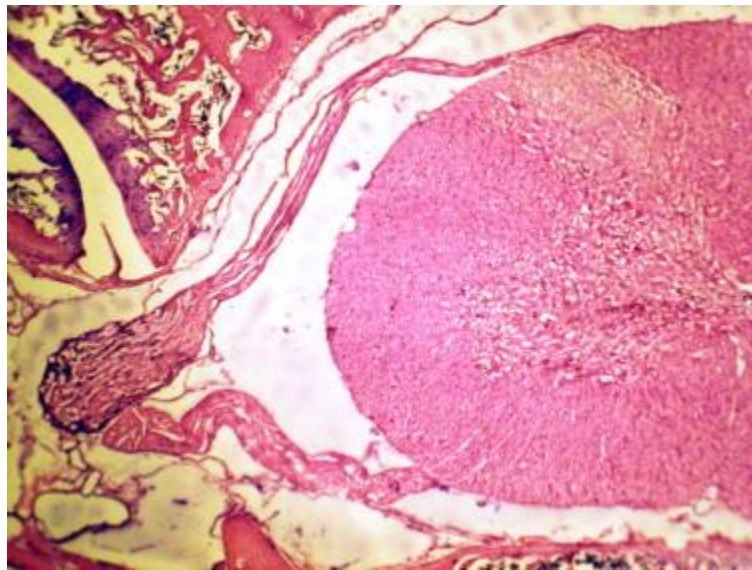


Fig.1. Cross section of the 6% TCA decalcified spinal cord stained with hematoxylin and eosin (H&E) stain. Gross tissue morphology is unaffected by the decalcification process. The peripheral–central nervous system connections are shown, with the dorsal root connecting the spinal cord to the dorsal root ganglion (DRG). The ventral root is shown connected to the ventral

horn and runs adjacent to the DRG towards the point of connection with the sensory root distal to the DRG. Brightfield image at 4× magnification.

6.2. RDO-G

RDO-Gold decalcification was fairly rapid in terms of reagent and sample preparation, and time taken to decalcify (see Table 1). Following the manufacturer's protocols, we found that at 2.5 h the bone specimen was soft and that chemical testing showed there was no calcium precipitation in the decalcifying solution, indicating complete decalcification of the spinal column. Cryosectioning of the tissue produced intact spinal column sections at 10 µm that maintained the integrity of the peripheral–central connections. However, upon IHC analysis of MBP expression, we observed that the myelin structure was severely compromised. The immunoreactivity was disorganized and much of the detail of myelin sheaths was lost (Fig. 2). The myelin sheaths appeared blurry, with little definition, in both the white and grey matter of the spinal cord. In addition, the MBP immunoreactivity in the spinal roots was also blurred with no definition of the individual myelin sheaths.

Table 1. Cost breakdown of the different decalcifying reagents tested.

Reagent	Source	Cost/volume	Approximate time for making up solutions and preparing tissue prior to embedding in OCT	Time taken to decalcify	Reagent cost
RDO-	Apex	58.99/1 l	Ready to use	2.5 h	\$ 4.25/cord

Reagent	Source	Cost/volume	Approximate time for making up solutions and preparing tissue prior to embedding in OCT	Time taken to decalcify	Reagent cost
Gold	Engineering Products Corporation		solution		
		6 ml per sample	Washing and chemical testing during decalcification		
		12 samples per cord	Total: 2 man hours		
		4.5 cords per bottle			
Krajian	J.T. Baker	86.80/1 l	Ready to use solution	4 days	\$ 8.68/cord
		100 ml/column	Washing before and after decalcification		
			Total: 1 man hour		
EDTA-G	ED2P (Sigma-Aldrich)	232.00/500 g	Making glycerol pretreatments, and EDTA-G solution, and washing before and after decalcification	7 days	\$ 19.84/cord
	Glycerol (Mallinckrodt Baker Chemicals)	53.34/500 ml	Total: 4.5 man hours		

Reagent	Source	Cost/volume	Approximate time for making up solutions and preparing tissue prior to embedding in OCT	Time taken to decalcify	Reagent cost
		100 ml/column			
TCA	Sigma–Aldrich	130.00/500 g	Making TCA solution and washing before and after decalcification	5 days	\$ 1.63/cord
		100 ml/column	Total: 1 man hour		

For each reagent used, the approximate time commitment was calculated based on the preparation of reagents and number of steps involved in the entire process. The cost per spinal column was calculated on the commercial price (at date of publication) of the reagents used, divided by the number of samples that can be processed by the commercially available volumes and does not include manpower costs. For example, the RDO-Gold reagent requires the spinal column to be divided into smaller segments, thus more reagents are required per column than other reagents that can decalcify an entire column at once.

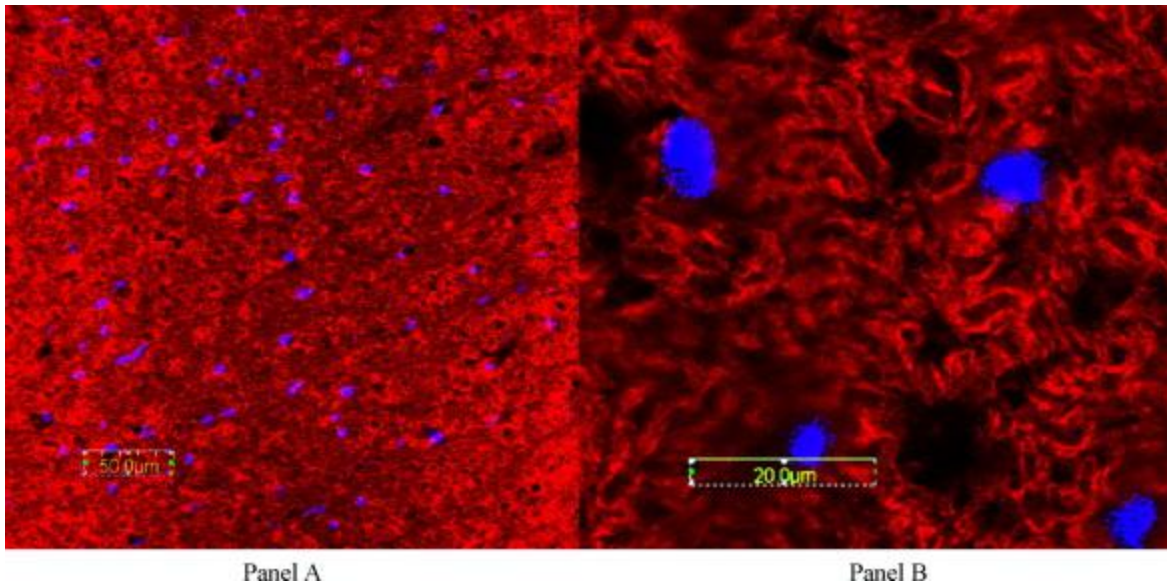


Fig.2. Rat spinal cord myelin structure after RDO-G decalcification of the vertebral column. Serial sections were cut at 10 μm thickness and stained with myelin basic protein (MBP). Nuclei were counterstained with DAPI (blue). Panel A—low power (40 \times) MBP immunoreactivity (red) shows disruption of the myelin ring structure in the white matter of the spinal cord. Total magnification was 400 \times , taken at 598 PMT. Panel B—High magnification (100 \times) of the same region of spinal cord white matter showing the lack of definition in the myelin surrounding the axons. Total magnification was 1000 \times , taken at 743 PMT. (For interpretation of the references to color in this figure legend, the reader is referred to the web version of the article.).

6.3. KRAJIAN SOLUTION

Krajian solution decalcification preparation was fairly rapid (1 man hour). However, decalcification took considerably longer than RDO-Gold; 4 days compared to 2.5 h (see Table 1). In addition, Krajian solution was almost twice as expensive as RDO-G (see Table 1). Cryosectioning of the tissue produced intact spinal column sections at 10 μm that preserved the

tissue morphology, similar to that seen with the RDO compound. However, immunohistochemical staining for MBP expression, showed the myelin structure to be disrupted and disorganized, similar to that seen after RDO-G decalcification (Fig. 3). The myelin sheaths of the white and grey matter of the spinal cord were disorganized, and appeared blurred. There was no definition of the individual myelin sheaths, even in the spinal roots. Further, the myelin immunoreactivity was inconsistent across the section, with incomplete MBP positive rings surrounding the large axons of the white matter.

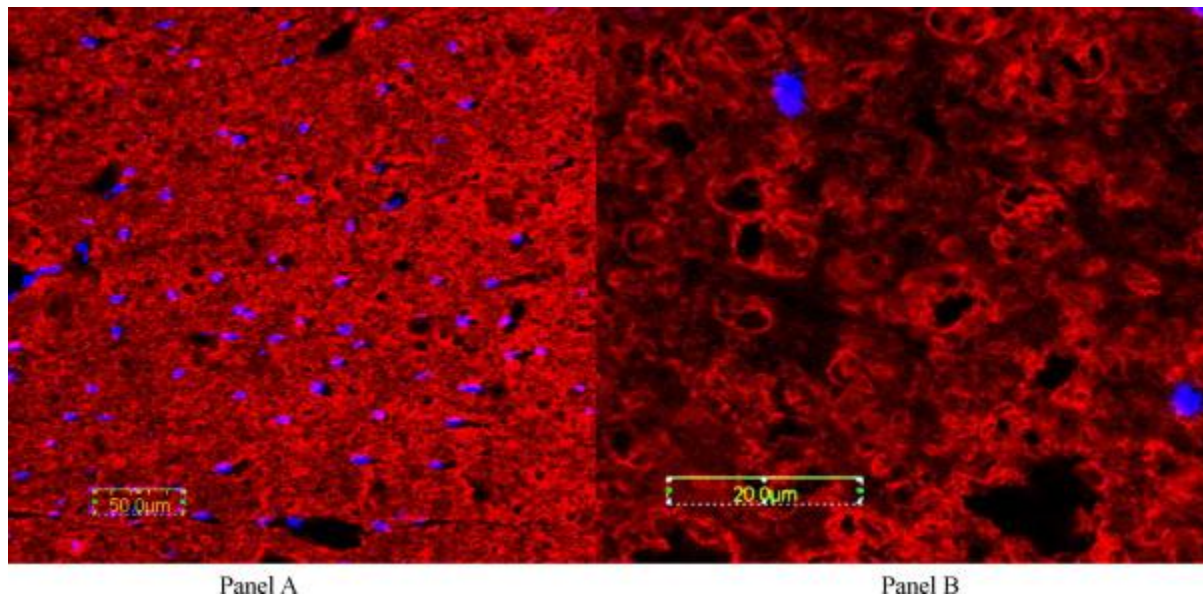
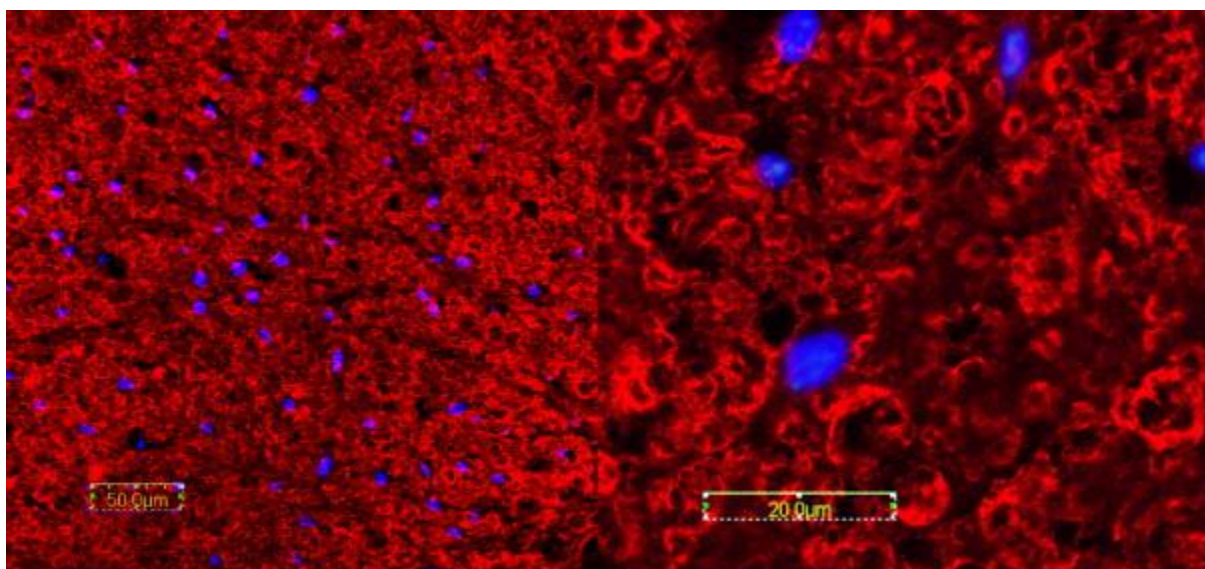


Fig.3. Rat spinal cord myelin structure after Krajan solution decalcification of the vertebral column. Serial sections, cut at 10 μm thickness, are stained for myelin basic protein (MBP). Nuclei were counterstained with DAPI (blue). Panel a—low power (40×) MBP immunoreactivity (red) shows disruption of the myelin ring structure in the white matter of the spinal cord. Total magnification was 400× and picture was taken at 598 PMT. Panel B—high magnification (100×) of the same region of spinal cord white matter showing the lack of

definition in the myelin surrounding the axons of the white matter. (For interpretation of the references to color in this figure legend, the reader is referred to the web version of the article.).

6.4. EDTA-G

Decalcification of spinal column using EDTA-glycerol solution was the most time-consuming of the four solutions tested. Tissue and solution preparation required 4.5 man-hours, and the decalcification took 7-day incubation, before needle stick and chemical testing determined that decalcification was complete. Cryosectioning of the tissue at 10 μm produced intact sections with preservation of the peripheral–central nervous system connection as assessed by H&E staining. Further, the structure of the myelin was preserved after EDTA-G decalcification with clear myelin ring structures observed around the axons of the grey and white matter of the spinal cord. However, there was still some disorganization of the MBP immunoreactivity, and some fine detail of the nerve root myelin structure was disorganized (Fig. 4).



Panel A

Panel B

Fig. 4. Rat spinal cord myelin structure after EDTA-G solution decalcification of the vertebral column. 10 μm thick sections of spinal cord are immunostained for myelin basic protein (MBP). Nuclei are counterstained with DAPI (blue). Panel A: low power (40 \times) MBP immunoreactivity (red) shows clear myelin ring structures in the white matter of the spinal cord. Total magnification was 400 \times and picture was taken at 598 PMT. Panel B: high magnification (100 \times) of the same region of spinal cord white matter showing the lack of definition in the myelin surrounding the axons. Total magnification was 1000 \times and picture was taken at 743 PMT. (For interpretation of the references to color in this figure legend, the reader is referred to the web version of the article.).

6.5. 6% TCA

Decalcification using 6% TCA was one of the easiest techniques for tissue and solution preparation, requiring 1 man-hour of work. Decalcification was longer than the commercially available reagents, but shorter than the EDTA-G solution, at 5 days (see Table 1) After 5 days of incubation, the spinal column bone decalcification was determined to be complete as the bone was soft upon needle stick and chemical testing revealed no calcium precipitation. Cryosectioning of the tissue at 10 μm produced intact sections with preservation of the peripheral–central nervous systems connection as assessed by H&E staining. The structure of the myelin, as assessed by MBP immunoreactivity, was clear and distinct. The myelin rings around the nerve axons were sharp and well defined in the white matter of the spinal cord. Further, myelin structure was clear in the grey matter of the spinal column with Nodes of Ranvier apparent when compared to EDTA-G decalcification (Fig. 5). In addition, the fine detail of the nerve root myelin was well maintained (Panel C, Fig. 5).

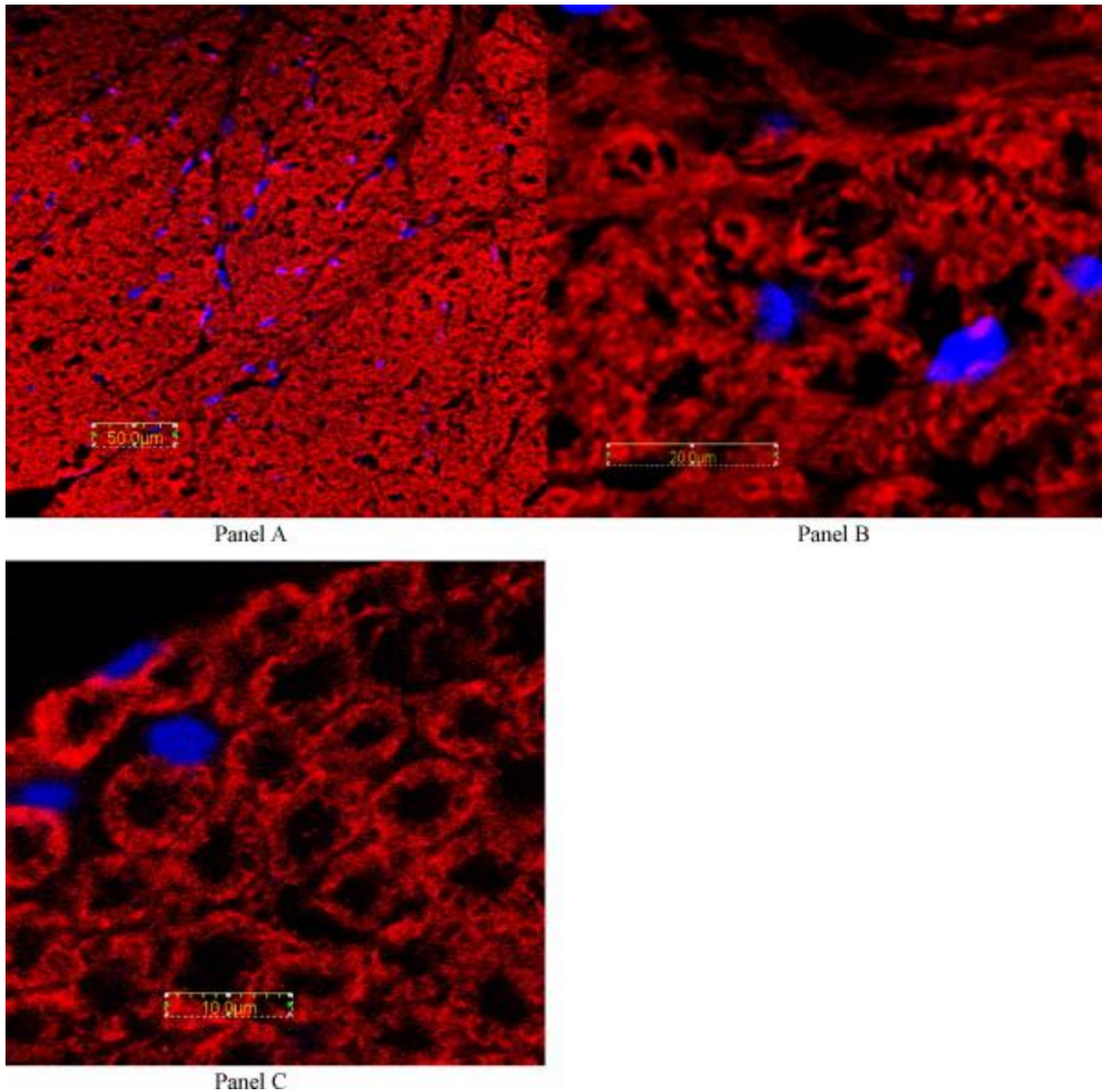


Fig.5. Rat spinal cord myelin structure after 6% TCA solution decalcification of the vertebral column. 10 µm sections of spinal cord are immunostained for myelin basic protein (MBP). Nuclei were counterstained with DAPI (blue). Panel A: low power (40×) MBP immunoreactivity (red) shows clean and distinct myelin ring structures in the white matter of the spinal cord. Total magnification was 400× and picture was taken at 598 PMT. Panel B: high magnification (100×) shows distinct myelin ring structure as well as nodes of Ranvier in the grey matter of the spinal

cord. Total magnification was 1000× and picture was taken at 743 PMT. Panel C: high magnification (100×) MBP immunoreactivity (red) shows distinct morphology of the nerve root myelin sheaths in a transverse section of sensory nerve root. Picture was taken at 743 PMT. (For interpretation of the references to color in this figure legend, the reader is referred to the web version of the article.).

6.6. IN SITU HYBRIDIZATION

ISH was performed on the 6% TCA decalcified tissue to ensure that the processing did not disrupt RNA integrity. We used a non-specific chloride channel primer sequence and showed that RNA signal is not disrupted in the decalcified spinal cord when compared to untreated spinal cord sample (Fig. 6).

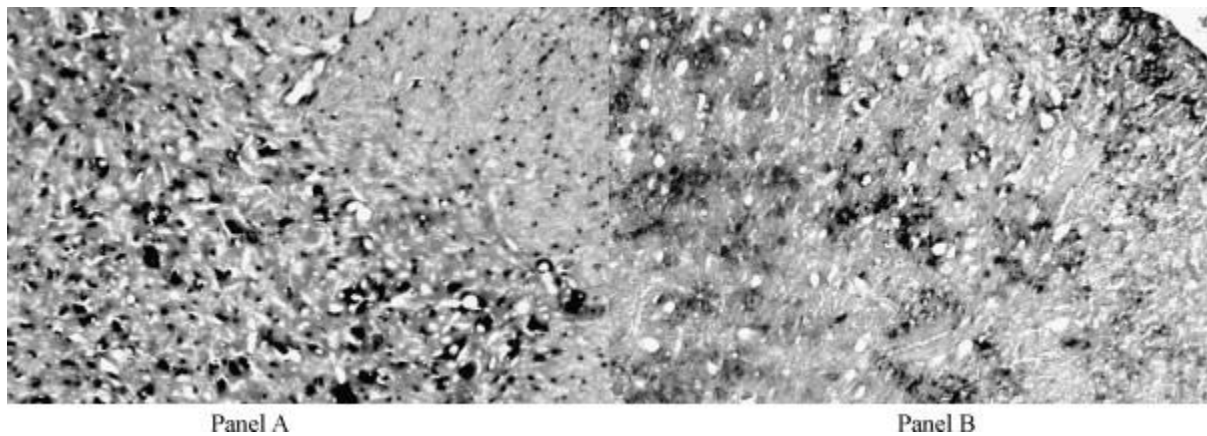


Fig. 6. *In situ* hybridization in decalcified and non-decalcified spinal cord. *In situ* hybridization was performed on 10 µm sections of rat spinal cord. Signal was detected in cells throughout the grey and white matter. Decalcification did not markedly affect the probe hybridization in cells of

the spinal cord. Panel A: low power (10×) bright field photomicrograph showing a non-specific antisense riboprobe signal throughout the spinal cord of non-decalcified spinal column. Panel B: low power (10×) bright field photomicrograph showing a non-specific antisense riboprobe signal throughout the spinal cord of 6% TCA decalcified spinal column.

6.7 DISCUSSION

Many studies of animal models of nervous tissue damage, such as inflammatory models of MS or traumatic spinal cord injury, require the sectioning of rodent spinal column without disrupting the spinal root connections or DRG. Expression of proteins involved in the processes of tissue damage and repair are frequently analyzed using IHC or ISH techniques to identify changes in expression patterns and levels. Preservation of the intricate cellular interactions is required for the correct interpretation of the results. Protein and gene expression analysis is best accomplished in frozen sections, as the heat involved in paraffin or plastic embedding can disrupt the molecular structures required for successful immunoreactivity or ISH. Several early studies have shown that decalcification techniques can be easily employed to facilitate the cryosectioning of bone [32-34], and there are numerous commercially available solutions for decalcification of bone samples. However, more recent studies have identified problems associated with the subsequent analysis of decalcified tissue at the molecular level [35-37].

For our study of the molecular events surrounding inflammation in the spinal cord, we need to cryosection the entire spinal cord, maintaining the peripheral–central nervous system connections and analyse myelin structure alongside inflammatory regulatory protein expression [19]. We initially used a popular, commercially available decalcification solution, RDO-Gold.

However, the samples were difficult to analyze due to the significant disruption of myelin structure. Specifically, the myelin immunoreactivity was disrupted and it was not possible to distinguish individual myelin sheaths. Therefore, we set out to identify a decalcification technique that would allow cryosectioning at 10 μm while still maintaining the integrity of the myelin sheath.

We compared the effect of four different decalcification agents (RDO-Gold, Krajian's Solution, EDTA-Glycerol and 6% TCA) on the quality of myelin structure as assessed by MBP immunoreactivity. The results clearly show that 6% TCA decalcification is superior to the other treatments when investigating the fine structure of myelin sheaths in the grey and white matter of the spinal column. In addition, this decalcification technique did not disrupt RNA signals within the tissue, as revealed by *in situ* hybridization (ISH).

All of the four reagents for decalcification of adult rat spinal cord resulted in easy cryosectioning of the entire vertebral column, which included not only the bone but also associated muscle and enclosed nervous tissue. Further, H&E analysis of spinal cord morphology after decalcification showed that all four decalcification solutions produced well-defined structures, without loss of tissue morphology. In addition, a basic comparative cost analysis revealed a considerable cost savings per unit for TCA.

We found that the commercially available solutions, Krajian's Solution and RDO-Gold, both resulted in significant loss of structure of the myelin as assessed using MBP immunohistochemistry, in the grey and white matter of the spinal cord and in the roots. In contrast, we found that EDTA-G and 6% TCA solutions preserved the myelin structure of the spinal cord with clear immunostaining in both grey and white matter. However, 6% TCA

solution preserved the structure more clearly with distinct rings of myelin visible in both the DRG and the grey and white matter of the spinal cord. In addition, nodes of Ranvier are clearly seen in the grey matter of the spinal cord in 6% TCA treated spinal columns.

Our findings are in agreement with previous studies of decalcification techniques, looking at the effects of different reagents on immunoreactivity, ISH and Comparative Genomic Hybridization (CGH) [25-27], [35-36].

6.8 CONCLUSION

The present study shows that the 6% TCA decalcification technique is the optimum decalcification method that can be routinely used for easy and effective IHC analysis of myelin structure and nodal integrity, as well as ISH analysis of gene expression. Thus, this technical tool serves as a critical step in advancing investigative research into the pathogenic mechanisms of various CNS/PNS diseases. In addition, the ability to maintain the intact connections of the peripheral and central nervous system tissue with connective dorsal and ventral nerve roots facilitates the understanding of translocation of proteins and mRNA between the DRG and spinal cord. As a result, this technique may have significant implications for advancing understanding of neurological disorders such as MS.

6.9 REFERENCES

1. Ma M, Basso DM, et al. Behavioral and histological outcomes following graded spinal cord contusion injury in the C57Bl/6 mouse. *Exp Neurol* 2001; 169 (2):239–54.
2. Frost EE, Nielsen JA, et al. PDGF and FGF2 regulate oligodendrocyte progenitor responses to demyelination. *J Neurobiol* 2003; 54 (3):457–72.
3. Hallam TM, Floyd CL, et al. Comparison of behavioral deficits and acute neuronal degeneration in rat lateral fluid percussion and weight-drop brain injury models. *J Neurotrauma* 2004;21(5):521–39.
4. Moon L, Bunge MB. From animal models to humans: strategies for promoting CNS axon regeneration and recovery of limb function after spinal cord injury. *J Neurol Phys Ther* 2005;29(2):55–69.
5. Neal CJ, Lee EY, et al. Effect of penetrating brain injury on aquaporin-4 expression using a rat model. *J Neurotrauma* 2007; 24 (10):1609–17.
6. Durukan A, Strbian D, et al. Rodent models of ischemic stroke: a useful tool for stroke drug development. *Curr Pharm Des* 2008;14(4):359–70.
7. Strbian D, Durukan A, et al. Rodent models of hemorrhagic stroke. *Curr Pharm Des* 2008;14(4):352–8.
8. Mannie M, Swanborg RH, et al. Experimental autoimmune encephalomyelitis in the rat. *Curr Protoc Immunol* 2009;Apr.(15.2):15.2.

9. Mikoshiba K, Okano H, et al. Structure and function of myelin protein genes. *Annu Rev Neurosci* 1991; 14:201–17.
10. McLaurin JA, Yong VW. Oligodendrocytes and myelin. *Neurol Clin* 1995;13(1): 23–49.
11. Dyer CA. The structure and function of myelin: from inert membrane to perfusion pump. *Neurochem Res* 2002; 27 (11):1279–92.
12. Kurz A, Riemenschneider M, et al. Potential biological markers for cerebrovascular disease. *Int Psychogeriatr* 2003; 15 (Suppl. 1):89–97.
13. Vercellino MMDP, Masera SMD, et al. Demyelination, inflammation, and neurodegeneration in multiple sclerosis deep gray matter. *J Neuropathol Exp Neurol* 2009; 68 (5):489–502.
14. Altar CA, DiStefano PS. Neurotrophin trafficking by anterograde transport. *Trends Neurosci* 1998; 21 (10):433–7.
15. Shubayev VI, Myers RR. Anterograde TNF[alpha] transport from rat dorsal root ganglion to spinal cord and injured sciatic nerve. *Neurosci Lett* 2002;320(1–2):99–101.
16. Ng BK, Chen L, et al. Anterograde transport and secretion of brain-derived neurotrophic factor along sensory axons promote schwann cell myelination. *J Neurosci* 2007; 27 (28):7597–603.
17. McElroy HH, Shih MS, et al. Producing frozen sections of calcified bone. *Biotech Histochem* 1993;68(1):50–5.

18. Kawamoto T. Use of a new adhesive film for the preparation of multi-purpose freshfrozen sections from hard tissues, whole-animals, insects and plants. *Arch Histol Cytol* 2003;66(2):123–43.
19. Melanson M, Miao P, et al. Experimental autoimmune encephalomyelitis-induced upregulation of tumor necrosis factor-alpha in the dorsal root ganglia. *Mult Scler* 2009;15(10):1135–45.
20. Tadokoro M, Hattori K, et al. Rapid preparation of fresh frozen tissue-engineered bone sections for histological, histomorphological and histochemical analyses. *Biomed Mater Eng* 2006; 16 (6):405–13.
21. Salie R, Li H, et al. A rapid, nonradioactive in situ hybridization technique for use on cryosectioned adult mouse bone. *Calcif Tissue Int* 2008;83(3):212–21.
22. Gomes SA, dos Reis LM, et al. Usefulness of a quick decalcification of bone sections embedded in methyl methacrylate [corrected]: an improved method for immunohistochemistry. *J Bone Miner Metab* 2008; 26 (1):110–3.
23. Mori S, Sawai T, et al. Anewdecalcifying technique for immunohistochemical studies of calcified tissue, especially applicable to cell surface marker demonstration. *J Histochem Cytochem* 1988; 36 (1):111–4.
24. Bourque WT, Gross M, et al. A histological processing technique that preserves the integrity of calcified tissues (bone, enamel), yolky amphibian embryos, and growth factor antigens in skeletal tissue. *J Histochem Cytochem* 1993;41(9):1429–34.

25. Graner E, Line SR, et al. Use of TCA as a decalcifying agent for laminin immunohistochemistry. *Calcif Tissue Int* 1995a;57(4):306.
26. Graner E, Line SR, et al. Laminin and collagen IV distribution and ultrastructure of the basement membrane of the gingiva of the rat incisor. *J Peridont Res* 1995b;30:349–54.
27. Yamamoto-Fukuda T, Shibata Y, et al. Effects of various decalcification protocols on detection of DNA strand breaks by terminal dUTP nick end labelling. *Histochem J* 2000; 32(11):697–702.
28. Bianco P, Silvestrini G, et al. Immunohistochemical localization of osteonectin in developing human and calf bone using monoclonal antibodies. *Calcif Tissue Int* 1988;43(3):155–61.
29. Miao D, Scutt A. Histochemical localization of alkaline phosphatase activity in decalcified bone and cartilage. *J Histochem Cytochem* 2002;50(3):333–40.
30. Blaschuk K, Frost E, et al. The regulation of proliferation and differentiation in oligodendrocyte progenitor cells by alphaV integrins. *Development* 2000;127(9):1961–9.
31. Messersmith DJ, Murtie JC, et al. Fibroblast growth factor 2 (FGF2) and FGF receptorexpression in an experimental demyelinating disease with extensive remyelination. *J Neurosci Res* 2000; 62(2):241–56.
32. Plank J, Rychlo A. A method for quick decalcification. *Zentralbl Allg Pathol* 1952; 89 (8):252–4.
33. Case NM. The use of a cation exchange resin in decalcification. *Stain Technol* 1953; 28 (3):155-8.

34. Verdenius HH, Alma L. A quantitative study of decalcification methods in histology. *J Clin Pathol* 1958;11(3):229–36.
35. Arber JM, Weiss LM, et al. The effect of decalcification on in situ hybridization. *Mod Pathol* 1997; 10 (10):1009–14.
36. Alers JC, Krijtenburg P-J, et al. Effect of bone decalcification procedures on DNA in situ hybridization and comparative genomic hybridization: EDTA is highly preferable to a routinely used acid decalcifier. *J Histochem Cytochem* 1999;47(5):703–10.
37. Moore JL, Aros M, et al. Fixation and decalcification of adult zebrafish for histological, immunocytochemical, and genotypic analysis. *Biotechniques* 2002;32(2):296–8.

CHAPTER 7 - OVERALL DISCUSSION AND CONCLUSIONS

7.1 OVERVIEW

MS is a complex condition that affects individuals across their lifespan. Every day, research is being conducted to advance our understanding and knowledge of the etiology of this disease, as well as treatment and potential cures. It is widely accepted that MS has an autoimmune origin [1]. The disease course has an initial inflammatory phase, followed by a second demyelinating phase [2]. Our working model of MS induction describes activation of immune cells in the periphery by CNS myelin-like antigens [see Figure 1]. Our global hypothesis is that the pro-inflammatory cytokine TNF and the neurotrophins BDNF and NGF form a triad of critical signaling proteins that underlie the pathophysiology of MS [Figure 2].

We have previously shown activation of DRG neurons in the inflammatory stage of EAE, with increased expression of the proinflammatory cytokine TNF [3]. Other studies have shown that TNF induces BDNF expression in cells of the nervous system [4]. In addition, TNF induces NGF expression and regulates NGF signalling [5]. Interestingly, NGF also induces TNF expression in neurons and immune cells [6]. Further, BDNF acts as a chemo-attractant directional cue for NGF which subsequently promotes preferential TNF signaling via TNFR2.

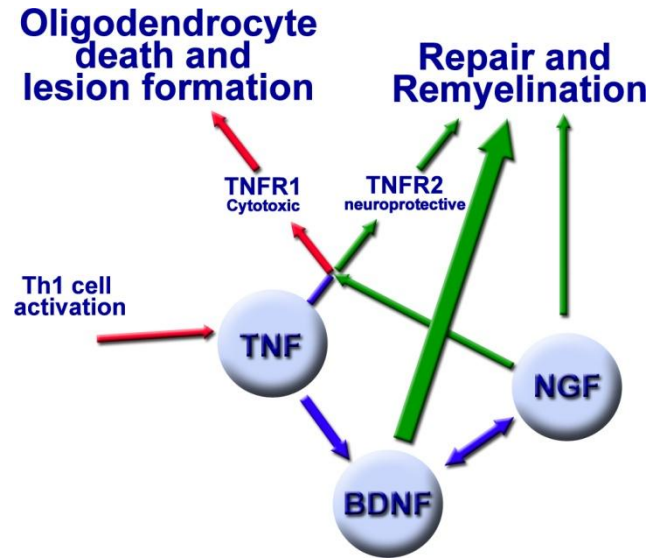


Figure 2: Triad model of cytokine neurotrophin interactions in the molecular regulation of MS disease process.

(Permission from Dr Emma Frost, Faculty of Pharmacy, University of Manitoba)

According to our published model [7], DRG neurons are a primary source of inflammatory mediators in the very early stages of neuroinflammatory disorders such as MS [7]. The current study was designed to test our hypothesis that BDNF expression is up-regulated in the DRG and spinal cord in the EAE model of MS. In order to determine the role of BDNF in MS pathology, we identified the cellular source of BDNF both in the DRG and in the spinal cord, in rats induced to a state of EAE, during the onset, peak disability, and recovery phases of the disease progression. To further determine the role of BDNF in MS pathology, we identified the cells that express the BDNF receptor TrkB, in the spinal cord.

The second worst disease induced symptom of MS is reported by patients to be neuropathic pain [8]. Several studies have shown that BDNF is an important regulator of pain in the CNS [9]. Thus, we conducted a study using a known molecular marker of pain, fractalkine, to characterize the onset of neuropathic pain in the Lewis rat model of EAE.

7.2 BDNF

Neurotrophins and cytokines interact to co-regulate their expression in inflammatory states [4]. For example, TNF α induces the expression of BDNF expression in astrocytes and neurons [4]. Based on our established model [7], we hypothesize that BDNF works in concert with cytokines such as TNF α and other neurotrophins, such as NGF, to regulate cellular effects on myelin [4]. The current study, in conjunction with our previously published studies [7], provides support for the importance of cytokine - neurotrophin interactions in the induction of neuroinflammatory disorders.

Although the exact molecular events underlying the pathophysiology of MS remain unclear, immunomodulatory therapies have proven effective for some MS patients [10]. One such therapy is glatiramer acetate (GA) [11]. While the mechanism of action of GA is unknown, studies have shown that GA-active T-cells produce a significantly increased level of BDNF, which is directly neuroprotective and/or neuroregenerative [12]. Although GA-specific Th1, Th2 and Th0 cells are all involved in BDNF production, larger *in vitro* studies have suggested that Th2 cells play a predominant role in GA modulation of RRMS [12]. Further evidence of a role for BDNF in MS comes from a study showing that BDNF treatment has a beneficial effect on disease progression in EAE [13]. Thus BDNF may play a significant role in the induction and progression of neuronal and oligodendrocyte damage.

In order to characterize the specific cellular source of the BDNF protein, we used cell size to identify the sensory neuron subtypes present in the DRG. Our results show that medium diameter (30-50 μm : A δ) sensory neurons appear to be the predominant source of BDNF in the EAE DRG.

Further, it appears that the specific location of the BDNF positive cells indicates that the cellular source of BDNF in the EAE DRG is changing from the small C fibers, to the medium A δ fibers. Based on Aoki's paper in 2004, the neurons on the outer edge of the DRG are the small NGF dependent (substance P and calcitonin gene related peptide expressing) nociceptive neurons, which are critical for inflammatory hyperalgesia [5]. This cellular source differs from the source of TNF α in the EAE DRG, which is predominantly produced by small diameter (<30 μ m: C) neurons [7]. Interestingly, BDNF enhances the excitability of small diameter neurons, and potentiates their action potential firing, via p75^{NTR} signalling [14]. A study using CFA injection into the rat paw to initiate a pain response showed TrkB, the high affinity BDNF receptor, expression in medium to large sensory neurons of the lumbar DRG, and expression of the low affinity BDNF receptor, p75^{NTR} in the small diameter neurons [13]. Further, microglia activated by peripheral nerve injury secrete high levels of BDNF, which subsequently results in the development of neuropathic pain [9].

Anterograde and retrograde transport of neurotrophins are known to occur between the DRG and spinal cord [1]. We show evidence for the active transport of BDNF from the DRG to the dorsal root entry zone, via kinesin mediated anterograde transport. Kinesin is a dimeric molecule that attaches to protein filled vesicles, and walks towards the plus end of a microtubule, transporting the proteins to the synapse. This form of transport is known as anterograde transport. Vesicular transport is the fastest mechanism of transporting proteins at 50-400 mm/day compared to the slower transport of proteins, at less than 8 mm/day. This provides a plausible explanation for the increase in BDNF protein seen in the dorsal horn, even though levels of *BDNF* mRNA are not increased. This corroborates previous studies showing anterograde transport of BDNF along

microtubules via transport vesicles [2]. Our results are also consistent with other studies that have shown transport of TNF and BDNF in rodent models of nerve injury [1].

Since BDNF is known to affect myelin function [15], it is possible that DRG derived BDNF contributes to the recovery of the inflammatory damage to myelin that has been shown in previous studies [16]. This potential mechanism of disease induction expands the potential for targeted strategies aimed at attenuating white matter disorders such as MS. One caveat to this therapeutic strategy is the potential for the development of pain, as previous studies have shown that elevated BDNF in the dorsal horn correlates with the development of pain [17]. In addition, we have shown the induction of pain in this model of neuroinflammation, associated with the peak neurological disability (see further discussion below).

Our study provides evidence that BDNF expression is upregulated in the early inflammatory stage of neuroinflammation. In addition, we show that BDNF levels are maintained in the spinal cord after amelioration of neurological symptoms, suggesting a role for BDNF in the prevention of immediate cell damage resulting from the initial inflammation. Further longitudinal studies are required to clarify the role of BDNF in neuroprotection in the later, demyelinating stages of disease progression.

7.3 TRKB

Several recent studies identified BDNF as a critical component in the molecular pathology of MS. Yet there is little understanding of the role of BDNF in MS. BDNF has been shown to promote neuronal survival and to support oligodendrocyte proliferation and axon remyelination [18] [15]. As discussed above, we have shown significantly increased expression of BDNF at the mRNA

and protein levels in the EAE spinal cord. Thus, in order to determine the exact role of BDNF, we focused on the expression changes of TrkB, which is the high-affinity receptor for BDNF in the spinal cord. TrkB is the high-affinity receptor of mature BDNF. The TrkB receptor contains an extracellular domain with three leucine-rich motifs and two immunoglobulin-like C2 type domains (Ig-C2), an intracytoplasmic domain with kinase activity and a transmembrane domain [19]. When BDNF binds to TrkB, several intracellular signaling pathways are triggered including Ras/Raf-MAPK, PI3K-Akt and PLC γ -PKC cascades. These pathways promote neuronal survival and differentiation [19].

Our Western blot analysis clearly shows that the protein levels of TrkB are significantly increased in EAE spinal cord induced by MBP compared to naïve and active control rats. However, qRT-PCR data show that there is no significant change in TrkB mRNA expression between active EAE and naïve/active control groups. There are three possibilities to explain why there is protein up regulation without mRNA change. One is that increased protein may be stored in local neurons and released from cells in this time. Another reason is that TrkB protein might be transported from DRG to dorsal horn of spinal cord and released from axonal terminals. The third explanation for these results is an increase in translation of the protein.

Our immunohistochemical analysis shows that TrkB protein is expressed on the axonal terminals in EAE spinal cord. However, it is not possible to specifically state that there is increased storage of protein in the EAE spinal cord compared to naïve or active control tissue. We did not assess TrkB anterograde along the dorsal transport directly using kinesin co-localization. However, there did not appear to be any TrkB immunoreactivity in the dorsal roots of the EAE animals. In order to assess the influence of translational changes on the increased protein levels of TrkB seen

in the spinal cord, precise molecular analysis would need to be performed. For example, a luciferase reporter assay could be used to measure protein synthesis.

Our study shows that spinal cord neuronal cell bodies and axons express TrkB in the EAE rat. Thus, it is conceivable that BDNF exerts its effects on neurons through its neuroprotective function. On the other hand, BDNF may work on neurons to provide a guidance cue for myelin events in the spinal cord. Using IHC analysis, we also found TrkB immunoreactivity is localized on CD4⁺ T and Th17 cells. These data suggest that BDNF may exert its effects on immune cells thereby regulating their immunomodulatory effects. Inflammatory responses can provide regenerative and protective effects during CNS damage [20]. TrkB⁺ T-cells could play an important role in MS immunopathogenesis by modulating autoreactive T-cells survival and behavior. Further, through IHC analysis, we found that TrkB protein is not expressed on mature oligodendrocytes or oligodendrocyte precursors. These results further suggest that in the early inflammatory stage of EAE, BDNF is not working on oligodendrocytes or oligodendrocyte precursors through the TrkB receptor. This has two implications. One, that BDNF may not exert a function in myelin repair because there is no demyelination in the early inflammatory stage of EAE spinal cord. Two, that BDNF regulates oligodendrocytes through a different receptor (i.e. p75^{NTR}). Further, our IHC data show that TrkB is not expressed on spinal cord astrocytes or microglia. This result indicates that BDNF is not involved in microglial or astrocytic activation in the early inflammatory stage of EAE.

Our study provides novel information relating to the cellular source of TrkB expression in an EAE rat model of MS. Further, by determining the direct role of BDNF on TrkB expressing spinal cord cells; we provide novel information that may have the diverse applicability to other diseases the CNS such as non-traumatic spinal cord injury.

Further studies are required to study the expression of p75^{NTR} receptor in EAE spinal cord to determine the effect of TrkB independent BDNF activity. Activation of p75^{NTR} has been associated with multiple cell-specific functions including cell survival, proliferation and apoptosis [19] and myelination [21]. Furthermore, p75^{NTR} can modulate the affinity of BDNF / TrkB interactions [22]. The determination of p75^{NTR} expression in the EAE spinal cord will provide more information underlying BDNF role in MS. Although our study shows that BDNF may not exert its function of myelin repair via TrkB receptor in the early inflammatory stage of MS, it may promote myelination via p75^{NTR} with TrkB- independent pathway.

7.4 FRACTALKINE

We believe that MS and neuropathic pain share similar cellular mechanisms, and that neuropathic pain is initiated earlier in the cascade of molecular events than is MS. We hypothesize that NPP may be a pre-diagnostic marker for the early stages of MS. Neuropathic pain has been reported as the secondary worst disease induced symptoms in patients [8]. Interestingly, neuropathic pain is also reported to be present in MS patients prior to the time of diagnosis and therefore, may be a promising prediagnostic indicator to facilitate the early diagnosis of MS. Previous studies have shown that EAE animals also experience neuropathic pain as part of their disease progression [23] Further, we have previously shown that levels of pain mediators are significantly increased in the DRG and spinal cord of EAE rats [7]. CX3CL1 and CX3CR1 are established factors in the modulation of pain perception via a central pro-algesic mechanism [24]. Increased serum levels of CX3CL1 are seen in MS patients, without significant changes in CX3CL1 levels in the cerebral spinal fluid (CSF). Thus, a proposed role for the chemokine CX3CL1 and its receptor CX3CR1 in the control of microglia activation and

leukocyte infiltration places this chemokine in a potentially strategic position in regard to the pathological events of MS-induced neuropathic pain.

Our data show significant changes in CX3CL1 and its receptor CX3CR1 at both gene and protein levels in the DRG and spinal cord. These changes only occurred after onset of neurological disability and were not detected in active control and naïve groups. Thus, we can conclude that changes in CX3CL1 and CX3CR1 expression levels are the direct result of activation of the immune response by CNS-myelin-specific antigens. Changes in the expression of CX3CL1 and CX3CR1 correlate with the onset of hypoalgesia confirmed by the behavioral studies conducted in our EAE model of MS.

Our study demonstrated that CX3CL1 is constitutively expressed in neurons, but its receptor CX3CR1 is expressed dominantly in microglia. So, it is conceivable that CX3CL1 works as a molecule signaling from neuron to microglia to induce glia activation. A remarkable finding of our study is that in EAE model, CX3CL1 and its receptor significant changes show the glial cells activation based on the signaling from neuron to microglia. This processing may be a critical mechanism involved in MS induced neuropathic pain.

Our study shows that CX3CR1 immunoreactivity is localized on microglia and neurons in the rat spinal cord. This finding is interesting because CX3CR1 is usually mainly expressed on microglia in the central nervous system [24]. Specifically, our study demonstrated that CX3CL1 is constitutively expressed in neurons, but its receptor CX3CR1 is expressed predominately in microglia. So, it is conceivable that CX3CL1 works as a molecule signaling from neuron to microglia to induce glia activation. Spinal cord microglia and astrocytes have been shown to be involved in various types of neuropathic pain such as peripheral nerve injury, bone cancer and

spinal root constriction [25]. The activation of glia is directly involved in inflammatory and neuropathic pain because recent research has shown that administration of glial inhibitors exerts anti-allodynic function [26]. A remarkable finding of our study is significant changes of CX3CL1 and its receptor CX3CR1 show the glial cells activation in the EAE model of MS. This processing may be a critical mechanism involved in MS induced neuropathic pain. The expression of CX3CR1 by spinal neurons indicates these receptors may also be a target for CX3CL1 produced by astrocytes and microglia cells or other neurons. The findings by Meucci *et al.*, 2000 have shown CX3CR1 was expressed on hippocampal neurons, which support neurons as possible targets of CX3CL1.

Early studies have shown that CX3CL1 and CX3CR1 are thought to play important roles in neuron-glia communication. Upon stimulation, the membrane-bound CX3CL1 can be cleaved by TNF converting enzyme (TACE) to release soluble CX3CL1. This soluble CX3CL1 elicits its adhesive and migratory functions by interacting with the highly selective G-protein-coupled receptor CX3CR1 which is expressed on microglia, T-cells, and neurons [24].

Our data strongly suggests that in the early inflammatory stage of MS prior to demyelination, CX3CL1 signaling in neurons in the spinal cord to activate the ascending pathways involved in pain transmission. In addition, we found that in the EAE spinal cord, astrocytes also express CX3CL1. This production of CX3CL1 means that activated astrocytes is also involved in the EAE rat model of MS.

In our previous study, we show significantly up-regulation of the pro-inflammatory cytokine TNF at gene and protein levels within the DRG and spinal cord in the EAE model [7]. Recent researches have shown that TNF induces CX3CL1 expression in endothelial cells [24]. Further,

TNF also has functional implications in the post-transcriptional regulation of CX3CL1 [27]. These findings demonstrate that TNF is a factor inducing CX3CL1 production. Thus, our study shows that significantly increased CX3CL1 gene and protein levels in the DRG and spinal cord in an EAE model of MS. TNF might be one of possible factors to induce neuron or astrocytes to produce CX3CL1 thereby promoting microglia activation involved in pain signaling.

Based on the experimental findings of our research, we propose that CX3CL1 plays a role in MS induced neuropathic pain based on the signaling crosstalk between neurons and microglia in the spinal cord. The up-regulated expression of CX3CL1 and CX3CR1 correlates with hypoalgesic phase of neuropathic pain well documented in EAE rat models of MS [23]. CX3CL1 may work on microglia and neurons in spinal cord to facilitate pain signaling. However, it is still unclear how the synthesis and secretion of CX3CL1 are regulated and what the pathways of CX3CL1 signaling in glia cells. Further studies are required to study the effect of TNF on production of CX3CL1 in spinal cord neurons, astrocytes and microglia.

7.5 SUMMARY

Our study offers new insights into the molecular pathology underlying the onset of immunomodulation in the early stages of MS. Specifically, we identify a role for DRG derived BDNF in the inflammatory response preceding myelin damage in the early stages of MS. We demonstrate significantly increased BDNF mRNA and protein levels in the DRG correlating with peak neurological disability. In addition, we show increased BDNF protein levels in the dorsal horn without an increase in mRNA levels, which suggests that BDNF is transported into, rather than synthesized in, the dorsal horn. We show that medium diameter DRG sensory

neurons are an important source of BDNF, which is anterogradely transported to the spinal cord during the early stage of autoimmune induced neuroinflammation. Further, our findings provide support for the immune activation of the DRG as a critical step in the development of myelin disorders of the CNS. This is the first study to identify changes in BDNF expression and transport in the early inflammatory stages of neuroimmune induction.

In addition, we have found that significantly increased protein expression of BDNF receptor TrkB in EAE spinal cord without increase in its mRNA. We identified BDNF responsive cells (neurons, CD4+ T-cells and Th17 cells) in the EAE spinal cord. However, the glial cells including oligodendrocytes, microglial cells and astrocytes do not express BDNF receptor TrkB. Our findings provide novel information relating to the direct role of BDNF signaling via TrkB (neuroprotection and immunomodulation) in the early inflammatory stage of neuroimmune activation. However, BDNF may exert its effects via p75^{NTR} with TrkB independent pathway for myelin repair.

Finally, we show that the onset of neuropathic pain, which correlates with peak BDNF expression in the spinal cord, is paralleled by increased expression of the pain mediator, Fractalkine. Previous studies have shown that Fractalkine levels are markedly increased in the serum of MS patients. The onset of neuropathic pain in the EAE rat model occurs at the same time as the onset of neurological disability, and thus may be a pre-diagnostic marker for patients presenting with a clinically isolated incident. Further studies are required to fully characterise the expression profile of Fractalkine in MS, and to determine its potential as a diagnostic tool for clinical use.

7.6 FUTURE RESEARCH DIRECTION

Based on our global hypothesis that the pro-inflammatory cytokine TNF and the neurotrophins BDNF and NGF form a triad of critical signaling proteins that underlie the pathophysiology of MS [Figure 2], we have previously studied the changes in expression of TNF and BDNF. We have shown activation of DRG neurons in the inflammatory stage of EAE, with increased expression of the proinflammatory cytokine TNF and BDNF. Thus, further study will be directed to determine expression of NGF in the EAE animal model of MS. In order to determine the role of NGF in the pathology of MS we will also need to determine the NGF responsive cells via TrkA signalling. In addition, we have identified the expression profile of one of the BDNF receptors, TrkB. Therefore we need look into p75^{NTR} receptor expression on cells. Since p75^{NTR} also acts as an NGF receptor, this study is critical to validate our model. We will specifically investigate oligodendrocyte expression of receptors in order to determine a potential role in remyelination. As the rat MBP model does not undergo demyelination, we will also need to switch to the mouse model of EAE. The MOG mouse model shows a biphasic disease process, with the initial inflammatory phase, which is followed by demyelination. There is also some limited remyelination in this model, which we can target with TNF, BDNF and NGF specific agonists and antagonists.

Further, we have shown increased expression of fractalkine and its receptor (CX3CR1) at gene and protein levels in the EAE spinal cord. In future studies, we need to look at their expression in the DRG and serum to correlate with neurological disability and onset of neuropathic pain.

All of our current studies are conducted in animal models. Therefore, in order to accurately extrapolate our data to the human condition, we need to analyse the expression patterns of our triad of proteins in human MS patients. We have initiated a human study, and will be assessing

the serum levels of BDNF, TNF, NGF and fractalkine in different stages of the disease progression.

7.7 REFERENCES

1. Zweifel LS, Kuruvilla R, Ginty DD. (2005). Functions and mechanisms of retrograde neurotrophin signalling. *Nat Rev Neurosci.* 6: 615-25.
2. Altar CA, Di Stefano PS. Neurotrophin trafficking by anterograde transport. (1998). *Trends Neurosci.* 21: 433-37.
3. Melanson M, Miao P, Eisenstat D, *et al.*(2009). Experimental autoimmune encephalomyelitis induced upregulation of tumor necrosis factor-alpha in the dorsal root ganglia. *Mult Scler* 15: 1135-45.
4. Aloe L, Properzi F, Probert L, *et al.* (1999). Learning abilities, NGF and BDNF brain levels in twolines of TNF-alpha transgenic mice, one characterized by neurological disorders, the other phenotypically normal. *Brain Res.* 840: 125-37.
5. Woolf C J, Allchorne A, Safieh-Garabedian B, Poole S. (1997). Cytokines, nerve growth factor and inflammatory hyperalgesia: the contribution of tumour necrosis factor alpha. *Br J Pharmacol.* 121: 417-24.
6. Takei Y, Laskey R. Tumor Necrosis Factor alpha Regulates Responses to Nerve Growth Factor, Promoting Neural Cell Survival but Suppressing Differentiation of Neuroblastoma Cells. *Mol Biol Cell.* 2008; 19: 855-64.
7. Melanson M, Miao P, *et al.* Experimental autoimmune encephalomyelitis-induced upregulation of tumor necrosis factor-alpha in the dorsal root ganglia. *Mult Scler* 2009;15(10):1135–45.
8. Namaka, M.P., Ethans, K., Jensen, B., Esfahani, F. & Frost, E.E. (2011) Multiple Sclerosis *Therapeutic Choices/e-Therapeutic.* Canadian Pharmacists Association Publishers, Inc, pp. 309-319.

9. Coull JAM, Beggs S, Boudreau D, *et al.* (2005). BDNF from microglia causes the shift in neuronal anion gradient underlying neuropathic pain. *Nature*. 438: 1017-21.
10. Namaka M, Leong C, Prout M, *et al.* (2010). Emerging Therapies for the Management of Multiple Sclerosis. *Clinical Medicine Insights: Therapeutics*. 2: 1-13.
11. Skihar V, Silva C, Chojnacki A, *et al.* (2009). Promoting oligodendrogenesis and myelin repair using the multiple sclerosis medication glatiramer acetate. *Proc Natl Acad Sci U S A*. 106: 17992-97.
12. Ziemssen T, Kumpfel T, Klinkert WE, *et al.* (2002). Glatiramer acetate-specific T-helper 1- and 2-type cell lines produce BDNF: implications for multiple sclerosis therapy. Brain-derived neurotrophic factor. *Brain*. 125: 2381-91.
13. Makar T K, Bever C T, Singh I S, *et al.* (2009). Brain-derived neurotrophic factor gene delivery in an animal model of multiple sclerosis using bone marrow stem cells as a vehicle. *J Neuroimmunol*. 210: 40-51.
14. Zhang YH, Chi XX, Nicol GD. (2008). Brain-derived neurotrophic factor enhances the excitability of rat sensory neurons through activation of the p75 neurotrophin receptor and the sphingomyelin pathway. *J Physiol*. 586: 3113-27.
15. McTigue DM, Horner PJ, Stokes BT, Gage FH. (1998). Neurotrophin-3 and Brain-Derived Neurotrophic Factor Induce Oligodendrocyte Proliferation and Myelination of Regenerating Axons in the Contused Adult Rat Spinal Cord. *J Neurosci*. 18: 5354-65.
16. De Santi L, Annunziata P, Sessa E, Bramanti P. (2009). Brain-derived neurotrophic factor and TrkB receptor in experimental autoimmune encephalomyelitis and multiple sclerosis. *J Neurol Sci*. 287: 17-26.

17. Merighi A, Salio C, Ghirri A, (2008). BDNF as a pain modulator. *Progress in Neurobiology*. 85: 297-317
18. Gravel, C., Götz, R., Lorrain, A., Sendtner, M. (1997). Adenoviral gene transfer of ciliary neurotrophic factor and brain-derived neurotrophic factor leads to long-term survival of axotomized motor neurons. *Nat Med*, 3, 765–70.
19. Arévalo, J.C., Wu, S.H. Neurotrophin signaling: many exciting surprises! *Cell Mol Life Sci* **2006**, 63, 1523–1537.
20. Moalem, G., Leibowitz-Amit, R., Yoles, E., Mor, F., Cohen, I.R., Schwartz, M. (1999). Autoimmune T cells protect neurons from secondary degeneration after central nervous system axotomy. *Nat Med* 5, 49–55.
21. Cosgaya, J.M., Chan, J.R., Shooter, E.M. (2002). The neurotrophin receptor p75NTR as a positive modulator of myelination. *Science*, 298, 1245-1248.
22. Copray, S., Küst, B., Emmer, B., Young, Lin. M., Liem, R., Amor, S., et al. (2004). Deficient p75 low affinity neurotrophin receptor expression exacerbates experimental allergic encephalomyelitis in C57/BL6 mice. *J Neuroimmunol*; 148, 41–53
23. Aicher, S.A., Silverman, M.B., Winkler, C.W. & Bebo Jr, B.F. (2004) Hyperalgesia in an animal model of multiple sclerosis. *Pain* 110, 560-570.
24. D'Haese, J.G., Demir, I.E., Friess, H. & Ceyhan, G.O. (2010) Fractalkine/CX3CR1: why a single chemokine-receptor duo bears a major and unique therapeutic potential. *Expert Opin Ther Targets* 14, 207-219.
25. Johnston, I.N., Milligan, E.D., Wieseler-Frank, J., Frank, M.G., Zapata, V., Campisi, J., Langer, S., Martin, D., Green, P., Fleshner, M., Leinwand, L., Maier, S.F. & Watkins, L.R. (2004)

A role for proinflammatory cytokines and fractalkine in analgesia, tolerance, and subsequent pain facilitation induced by chronic intrathecal morphine. *J Neurosci* 24, 7353-7365.

26. Sweitzer, S., Martin, D. & DeLeo, J.A. (2001a) Intrathecal interleukin-1 receptor antagonist in combination with soluble tumor necrosis factor receptor exhibits an anti-allodynic action in a rat model of neuropathic pain. *Neuroscience* 103, 529-539.

27. Matsumiya, T., Ota, K., Imaizumi, T., Yoshida, H., Kimura, H. & Satoh, K. (2010) Characterization of synergistic induction of CX3CL1/fractalkine by TNF-alpha and IFN-gamma in vascular endothelial cells: an essential role for TNF-alpha in post-transcriptional regulation of CX3CL1. *J Immunol* 184, 4205-4214.